AD NUMBER: AD0822085

LIMITATION CHANGES

TO:

Approved for public release; distribution is unlimited.

FROM:

Distribution authorized to U.S. Gov't. agencies and their contractors; Administrative/Operational Use;10/01/1967. Other requests shall be referred to Air Force Weapons Lab., Kirtland AFB, NM

AUTHORITY

AFWL ltr 30 Nov 1971

AFWL-TR
66-85

SIMULATION OF AIRBLAST-INDUCED GROUND MOTIONS PHASE II A

Jimmie L. Bratton
Lt USAF

Howard R. Pratt
Lt USAF

TECHNICAL REPORT NO. AFWL-TR-66-85

OCTOBER 1967

AIR FORCE WEAPONS LABORATORY
Research and Technology Division
Air Force Systems Command
Kirtland Air Force Base
New Mexico

AFWL-TR-66-85

Research and Technology Division
AIR FORCE WEAPONS LABORATORY
Air Force Systems Command
Kirtland Air Force Base
New Mexico

SIMULATION OF AIRBLAST-INDUCED GROUND MOTIONS

(PHASE IIA)

Jimmie L. Bratton
Lt USAF

Howard R. Pratt
Lt USAF

TECHNICAL REPORT NO. AFWL-TR-66-85

FOREWORD

This research was performed under Program Element 7.60.06.01.D, Project 5710, Subtask 13.144, and was funded by the Defense Atomic Support Agency (DASA).

Inclusive dates of research were March 1965 to July 1966. The report was submitted 2 June 1967 by the Air Force Weapons Laboratory Project Officer, Lt Jimmie L. Bratton (WLDC).

This technical report has been reviewed and is approved.

Jimmie L. Bratton
JIMMIE L. BRATTON
Lt, USAF
Project Officer

Allen F. Dill
ALLEN F. DILL
CDR, CEC, USNR
Chief, Civil Engineering Branch

George C. Darby Jr
GEORGE C. DARBY, JR
Colonel, USAF
Chief, Development Division

ABSTRACT

The results of the Phase IIA, High-Explosive Simulation Technique (HEST) experiment are presented in the form of reduced data. A comprehensive analysis is not presented, although irregularities in the data are discussed. The experiment simulated airblast loading from a nuclear burst by detonating a contained Primacord matrix over a plan area 88 feet by 100 feet. The peak overpressure was 598 psi, the total impulse 19.25 psi-sec, the total duration was 172 msec, and the shock front velocity was 5640 feet per second. Measurements of free field stress, strain, particle velocity, particle acceleration, time of arrival of the wave front, and long span displacement were made. These data are presented as plots of peak values and time histories.

CONTENTS

ILLUSTRATIONS

ILLUSTRATIONS (cont'd)

ILLUSTRATIONS (cont'd)

ILLUSTRATIONS (cont'd)

TABLES

SECTION I

INTRODUCTION

The primary objective of the High-Explosive Simulation Technique (HEST) Phase IIA experiment was to observe the response of a buried structural model in an environment simulating the airblast and airblast-induced ground motions from a surface nuclear explosion. The specific requirements were to produce a traveling airblast wave having a peak overpressure of 600 psi, decaying to one-half peak pressure in 16.5 msec, and having a shock front velocity of 6800 ft/sec. Secondary objectives were to determine both the airblast and ground-shock environments which were made to define the loading input to the structural model and to further verify the theoretical techniques which are utilized to predict the airblast environment. In addition, the airblast and ground-shock data were obtained as a part of a continuing program designed to increase understanding of the basic phenomena associated with airblast-induced ground motions. The test was conducted on 6 May 1965 at Kirtland Air Force Base, New Mexico. The test constituted a reload of the model tested previously at the 300-psi level and reported in references 1 and 2.

The purpose of this report is to present the data measured during HEST Phase IIA. HEST Phase IIA is part of a continuing series of conventional high-explosive experiments conducted by the Air Force Weapons Laboratory. The HEST tests endeavor to simulate a nuclear blast environment by detonating a conventional high explosive* within enclosed pits. Variable parameters include pit size, type of overburden material, overburden mass, overburden density, cavity depth, and detonation cord wrap angle and density. A detailed discussion of the HEST environment is presented in references 1, 3, and 4. A summary of the HEST experiments giving location, date, pit size, overpressure, report number, and primary objective of each test is listed in Table I.

The specifications for HEST Phase IIA are as follows: the pit size was 100 feet by 88 feet with a 3-foot cavity. The Primacord wrap angle (β) was 13.25°, the Primacord density (ρ) was 0.1415 lb/ft^3. This density required

*Primacord is a registered trademark of the Ensign-Bickford Co., Simsbury, Conn., for a detonating cord of PETN.

Table I

SUMMARY OF HEST EXPERIMENTS

Experiment	Location	Date	Pit size (ft)	Overpressure (psi)	Report No.	Primary Objective
			Experimental Tests			
AF Phase I (Phase I Gasbag)	CERF, Kirtland AFB, NMex	4 tests	20 x 40	(325 to 375)	AFWL-TR-65-11	To perfect the HEST environment and to test model structures in this environment.
AF Phase II	Kirtland AFB, NM	15 Dec 64	96 x 150	312	AFWL-TR-65-26	
AF Phase IIa	Kirtland AFB, NM	6 May 65	88 x 100	598	AFWL-TR-66-85	
BSD Antenna Test	CERF, Kirtland AFB	2 Jul 65	40 x 96	Classified	AFWL-TR-66-86	
Parameter Study	CERF, Kirtland AFB	Several tests (22)	Variable	(117 to 1905)	Not published	To study the parameters controlling the HEST Air Pressure-Time History.
HEST-1	CERF, Kirtland AFB	30 Oct 65	32 x 36	---	Not published	
HEST-2	CERF, Kirtland AFB	5 Feb 65	32 x 36	1497	Not published	
HEST-3	CERF, Kirtland AFB	10 Mar 65	40 x 48	870	Not published	
HEST-6	McCormack's Ranch (near Albuquerque, New Mexico)	15 Mar 66	64 x 148	451	Not published	To study free field ground motions.
Project Drillhole (HEST-5)		9 Dec 66	64 x 148	907	Not published	
Project Backfill (HEST-4)		29 Jul 67	56 x 72	650 (Scheduled)	Not published	
			Operational Tests			
HEST Test-1	Cheyenne, Wyo	1 Dec 65	302 x 304	Classified	WLDC 66-043	To test operational Minuteman sites and launch control centers.
HEST Test-2	Kimball, Nebr	22 Jul 66	304 x 352	Classified	Not published	
HEST Test-3	Valley City, ND	14 Sep 66	302 x 304	Classified	AFWL-TR-67-23	
			HEST Improvement Study			
HIP I	CERF, Kirtland AFB	May 66	40 x 60	1150	Not published	To improve the HEST environment.
HIP Ia	CERF, Kirtland AFB	28 Jun 66	40 x 60	730	Not published	

14,500 feet of 175 grain detonation cord. The data recorded on magnetic tape were digitized at a rate of 40,000 bits per second (40 bits/msec) and plotted. Integration of these traces was accomplished using a planimeter.

Section II of this report describes and locates the instrumentation. Section III analyzes the airblast data. Section IV contains the soil response data. Raw data are contained in the Appendix.

A detailed analysis, synthesizing data from the entire HEST series, up to and including HEST Test-3, is planned in the near future. A more detailed analysis of HEST Phase IIA data will be presented in a later report.

SECTION II

INSTRUMENTATION

The Air Force Weapons Laboratory recorded 50 channels of free-field instrumentation during HEST Phase IIA. Figures 1 and 2 show the location of each of these gages and Table II summarizes the pertinent information on each gage.

Gages are identified by a code of the general form hh T cc-dd, where hh is the hole number, T identifies the property being measured, cc is the cable number, and dd is the depth of burial in feet. The abbreviations used for measured properties are P for air pressure, L for soil stress, A for acceleration, - for long-span displacement, and V for velocity. G in the depth location designated a measurement at the ground surface. The instrumentation was the same as that used in the initial test and was not removed between tests. However, three new long-span displacement gages and eight soil-strain gages were installed for this test.

In addition to the soil stress and motion measurements, the time of arrival of the stress wave in the soil was recorded using 100 omnidirectional "ball switches" positioned in a three-dimensional array in the ground.

A complete description of the instrumentation is presented in reference 1.

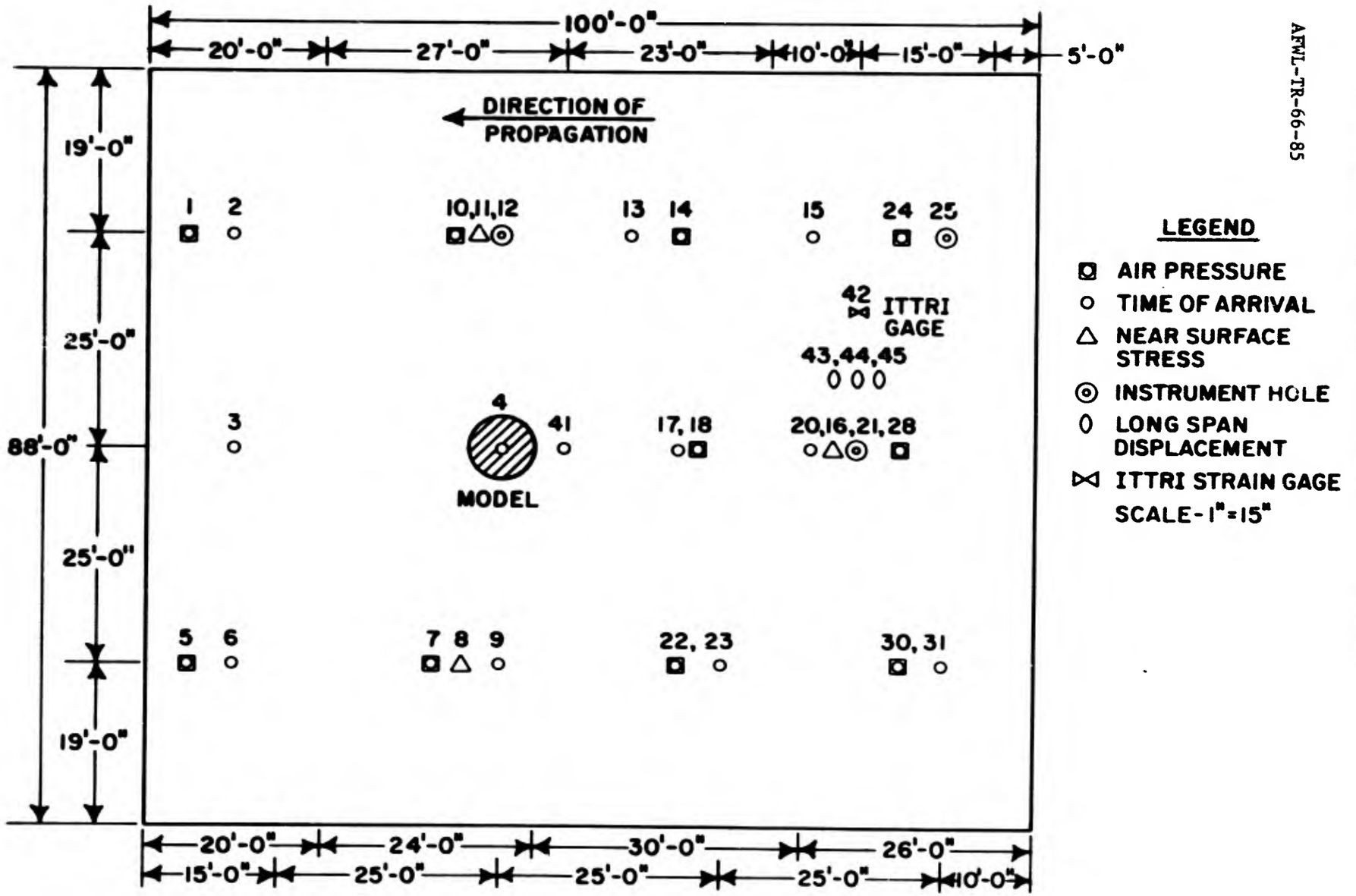

Figure 1. Location of Instrumentation within the Test Pit

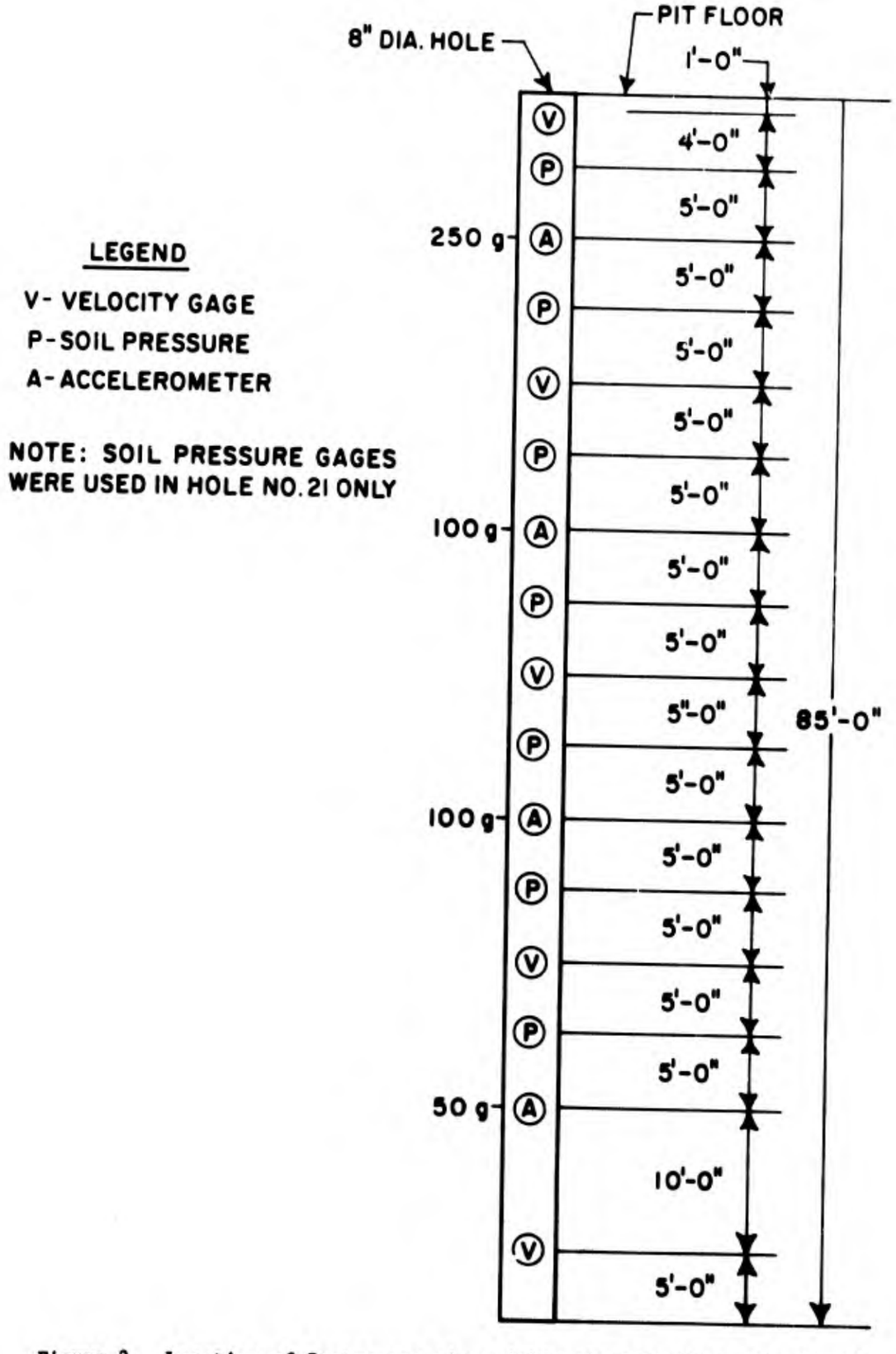

Figure 2. Location of Instrumentation within the Test Holes 12, 21, 25

Table II

INSTRUMENTATION LIST

Gage type	Gage make	Serial number	Hole	Depth (ft)
Velocity	Sandia	0092	12	1
Velocity	Sandia	0027	12	20
Velocity	Sandia	0085	12	40
Velocity	Sandia	0084	12	60
Velocity	Sandia	0089	12	80
Velocity	Sandia	0099	21	1
Velocity	Sandia	0097	21	20
Velocity	Sandia	0090	21	40
Velocity	Sandia	0101	21	60
Velocity	Sandia	0095	21	80
Velocity	Sandia	0062	25	1
Velocity	Sandia	0094	25	20
Velocity	Sandia	0100	25	40
Velocity	Sandia	0093	25	60
Velocity	Sandia	0088	25	80
Acceleration	Statham	10142-250g	21	10
Acceleration	Statham	7617-150g	21	30
Acceleration	Statham	7618-100g	21	50
Acceleration	Statham	10048-100g	21	70
Acceleration	Statham	1018-250g	12	10
Acceleration	Statham	7615-150g	12	30
Acceleration	Statham	10043-100g	12	50
Acceleration	Statham	10139-100g	12	70
Acceleration	Statham	10141-250g	25	10
Acceleration	Statham	10042-100g	25	30
Acceleration	Statham	10041-100g	25	50
Acceleration	Statham	10136-100g	25	70
Soil pressure	Lynch	Lynch 1	21	5
Soil pressure	Lynch	Lynch 2	21	15
Soil pressure	Lynch	Lynch 3	21	25
Soil pressure	Lynch	Lynch 4	21	35
Soil pressure	Lynch	Lynch 5	21	45
Soil pressure	Lynch	Lynch 6	21	55
Soil pressure	Lynch	Lynch 7	21	65
Soil pressure	Lynch	Lynch 8	8	0.5
Soil pressure	Lynch	Lynch 9	11	0.5
Soil pressure	Lynch	Lynch 10	16	0.5
Air pressure	Norwood	7528	4	---
Air pressure	Norwood	7264-1000psi	14	---
Air pressure	Norwood	5290-1000psi	18	---
Air pressure	Bytrex	5288-2000psi	22	---
Air pressure	Norwood	7267-1000psi	24	---
Air pressure	Bytrex	5293-2000psi	28	---
Air pressure	Norwood	7261-1000psi	30	---
Air pressure	Norwood	7257-1000psi	7	---
Air pressure	Bytrex	5294-2000psi	10	---
Air pressure	Bytrex	5293-2000psi	28	---

Table II (cont'd)

Gage type	Gage make	Serial number	Hole	Depth (ft)
Air pressure	Norwood	7260-1000psi	1	---
Air pressure	Norwood	7262-1000psi	5	---
Long span displacement	---	4	43	100
Long span displacement	---	5	44	70
Long span displacement	---	6	45	40

SECTION III

AIR FREE FIELD ENVIRONMENT

Eleven air-pressure gages were used to record the air free field. Their locations within the test pit are shown in figure 1. All gages except 10P9G functioned properly. From these, the composite air pressure curve shown in figure 3 was derived. This curve has a peak pressure of 598 psi, a time to one-half pressure of 15.5 msec, a total duration of 172.2 msec, and a total impulse of 19.25 psi-sec. The impulse-time history is also plotted in figure 3. The composite air pressure curve was found to have the form

$$P = 598(1 - \tau)\left(A + Be^{-\alpha\tau}\right)$$

where

P = overpressure, psi

τ = t/172

t = time after arrival of the shock, sec

A = 0.283

B = 0.717

α = 14.71

This curve satisfied the boundary conditions of a 598 psi peak pressure, a total duration of 172 msec, and a total impulse of 19.25 psi-sec with an r-squared of 0.88 and a standard deviation of 15.04 psi.

Figures 28 through 38 show the individual air pressure curves from which the composite air-pressure curve was computed. The sign of the ordinate (pressure) should be neglected as all air pressures are positive. Impulses were obtained either by numerical integration as a part of the computer data reduction, or by using a planimeter. Figures 4 through 13 are the smoothed air-pressure curves resulting from the analysis of the digitized data.

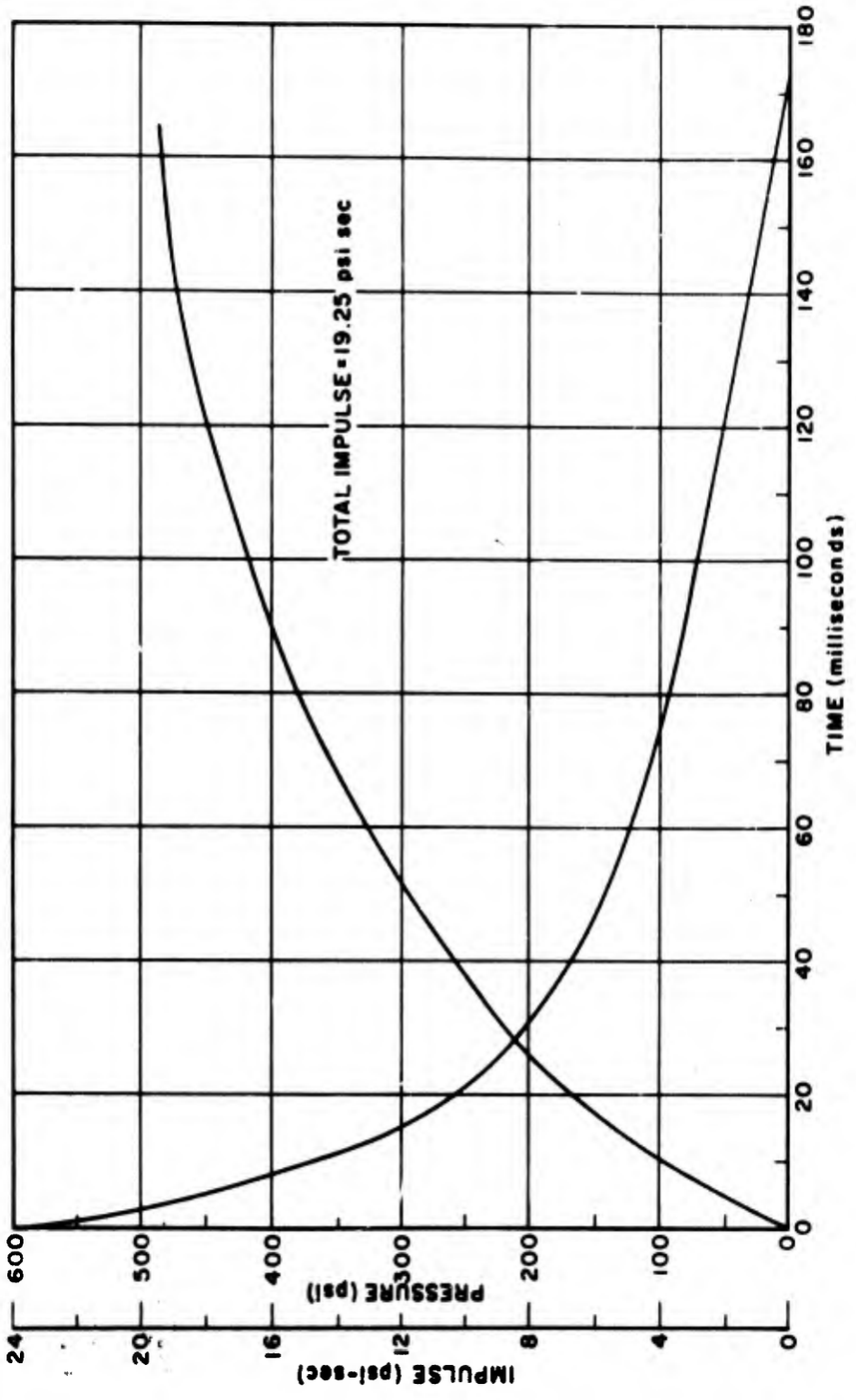

Figure 3. Composite Overpressure-Time History and Total Impulse Curve

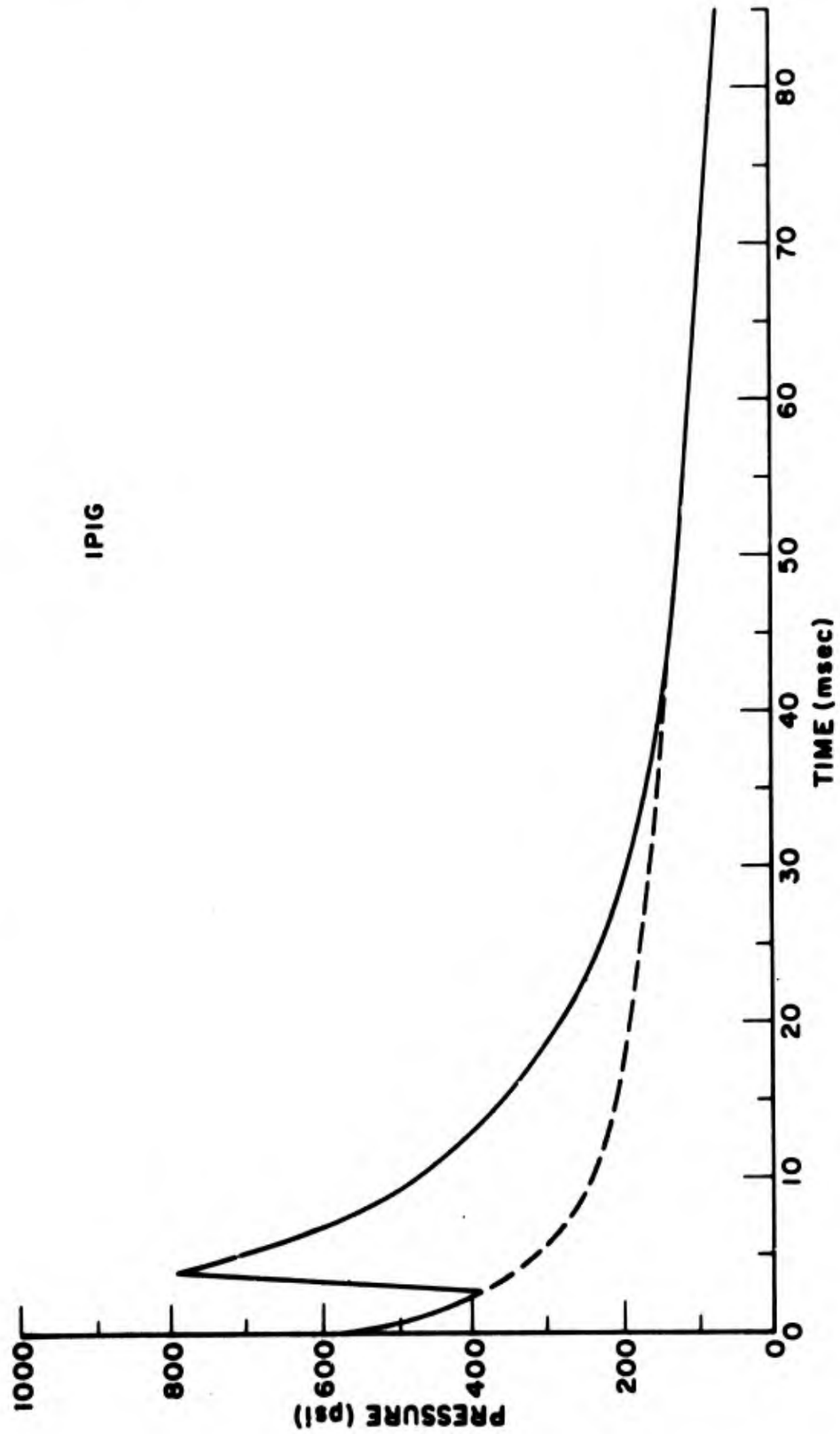

Figure 4. Overpressure-Time History 1P1G

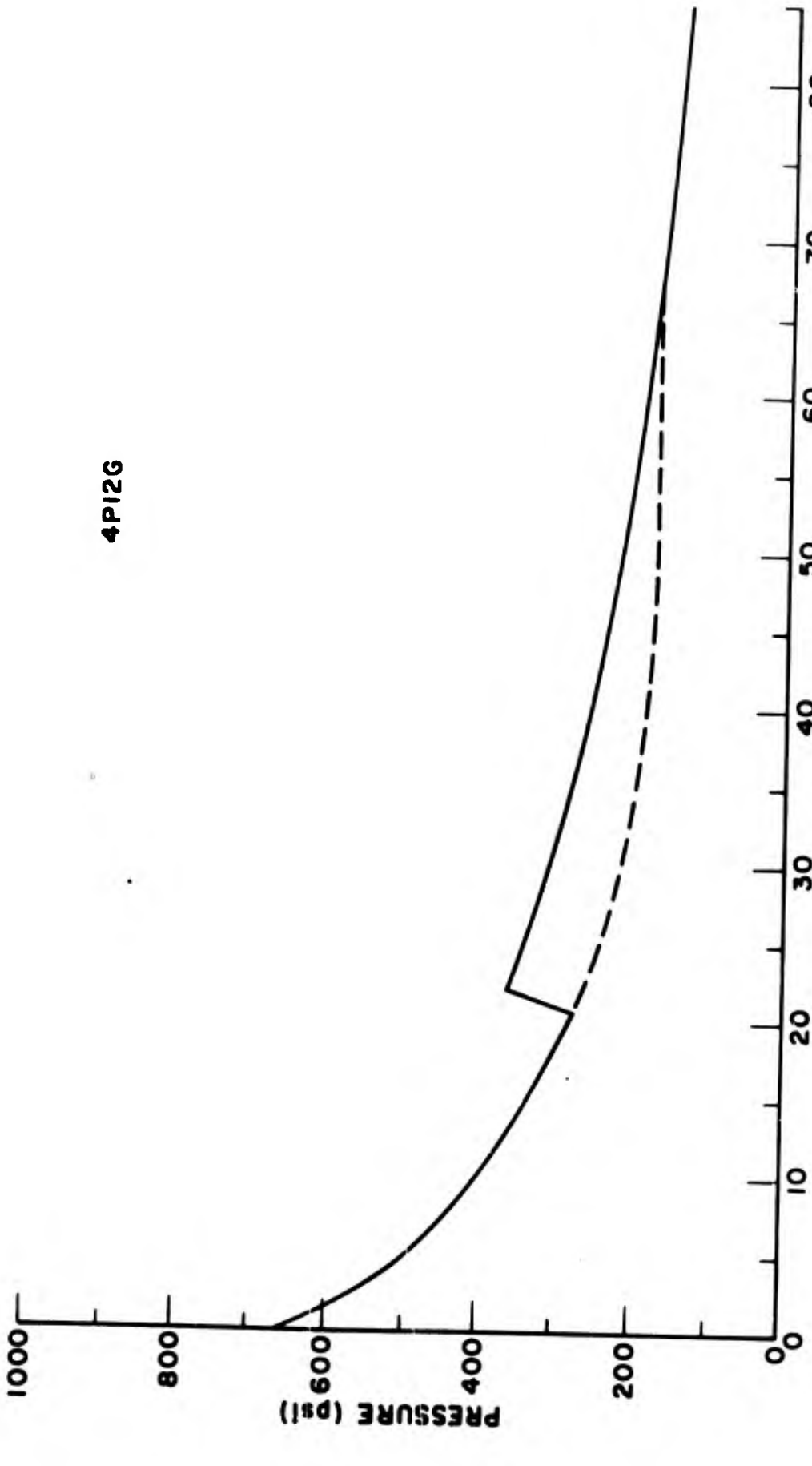

Figure 5. Overpressure-Time History 4P12G

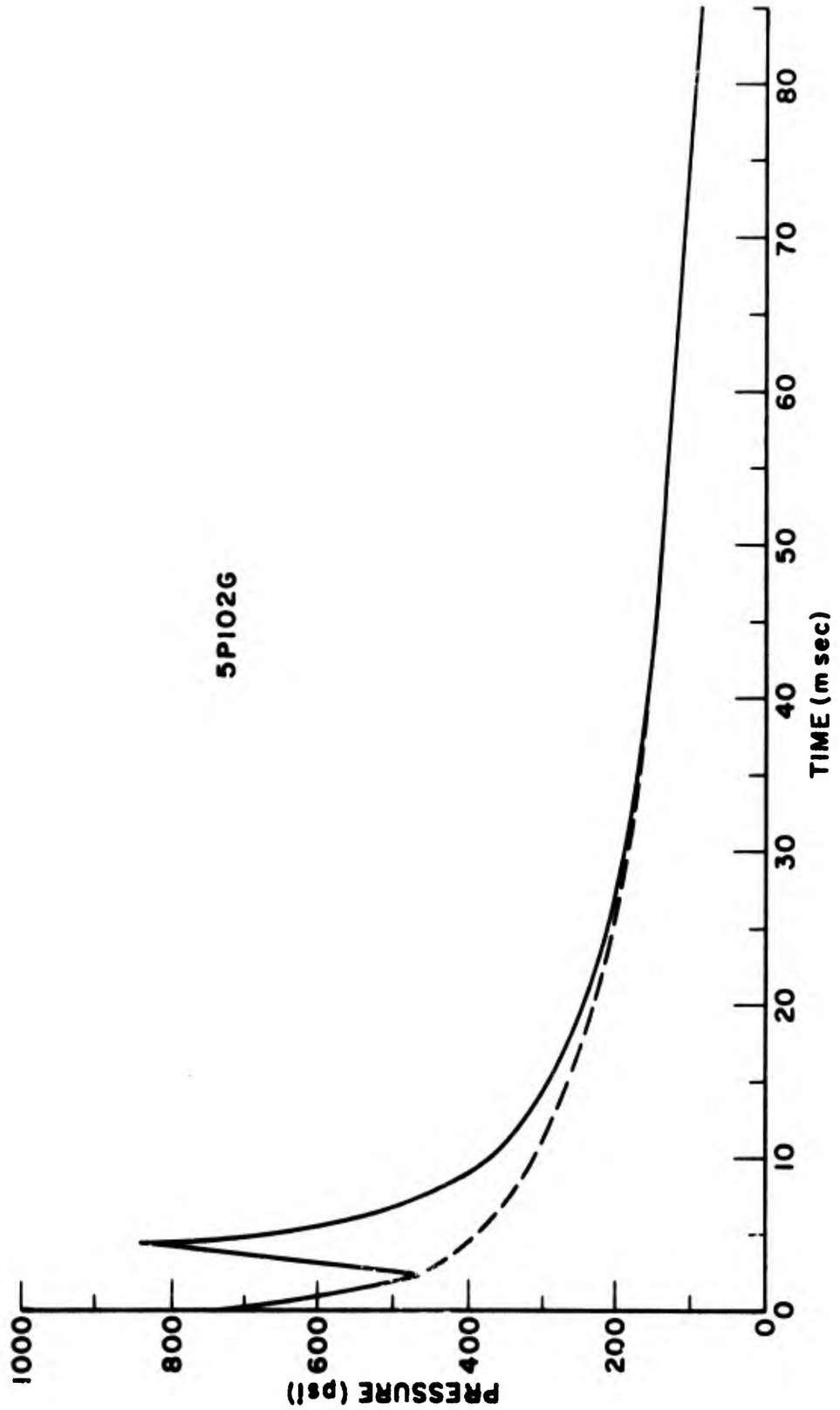

Figure 6. Overpressure-Time History 5P102G

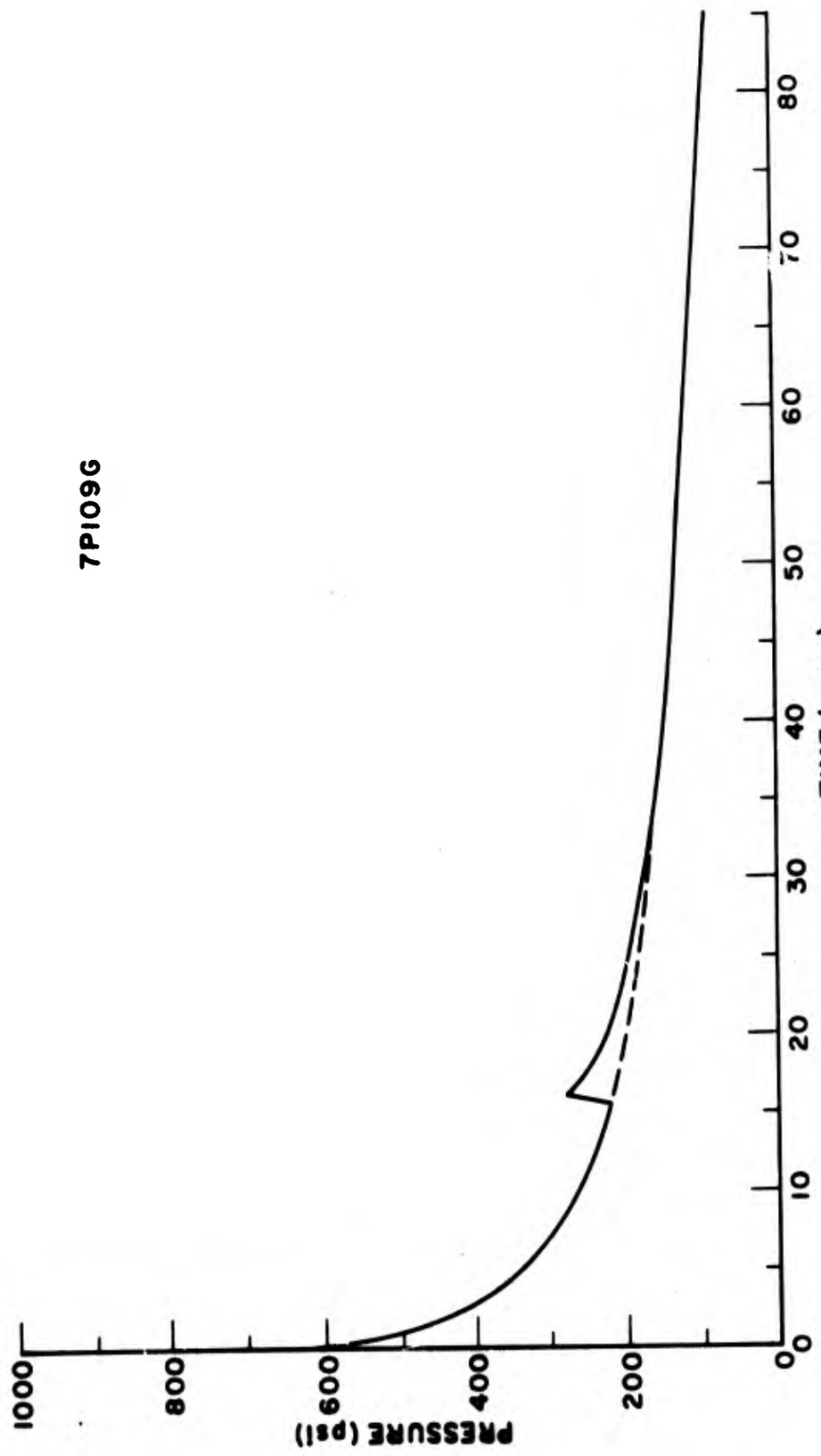

Figure 7. Overpressure-Time History 7P109G

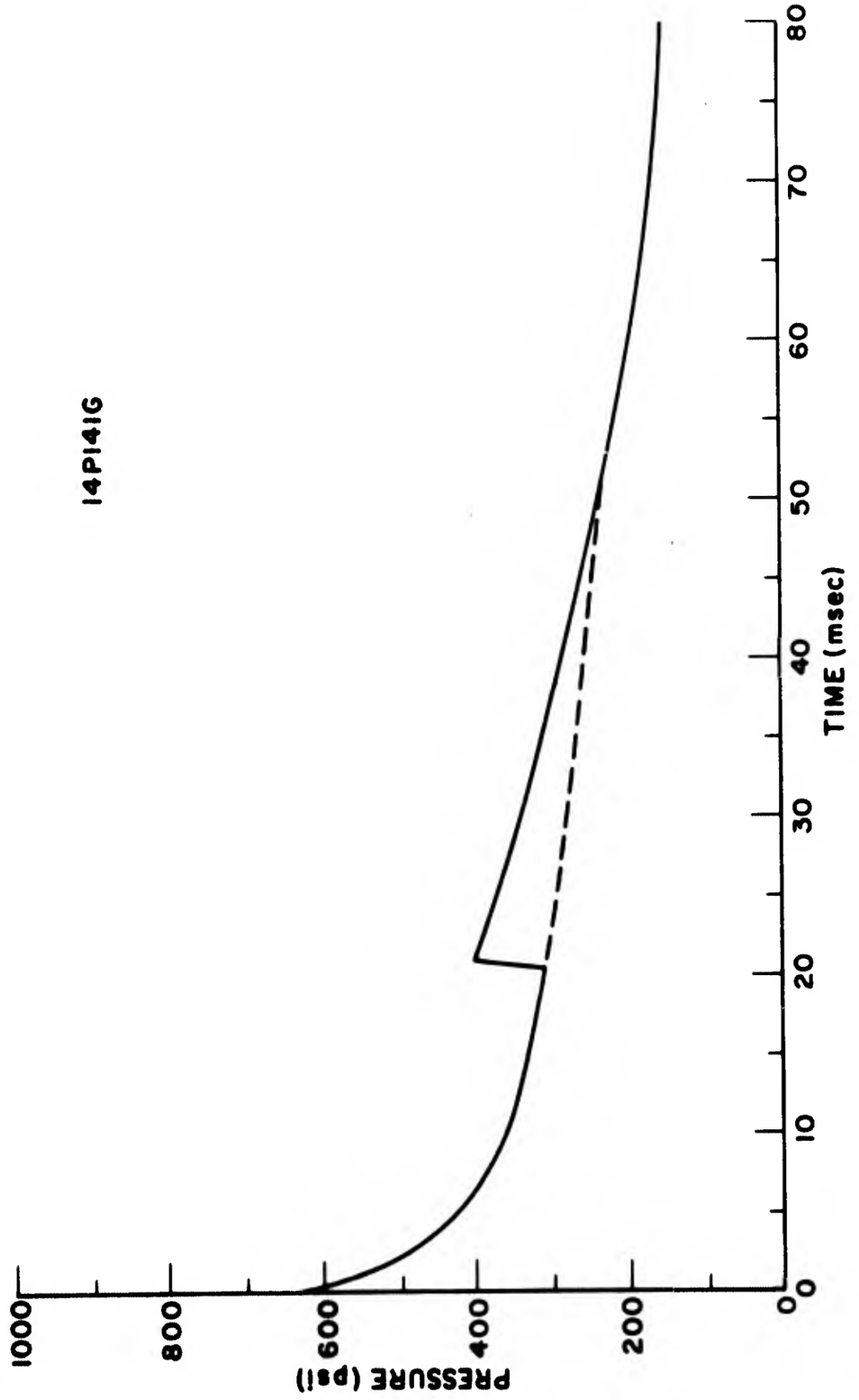

Figure 8. Overpressure-Time History 14P141G

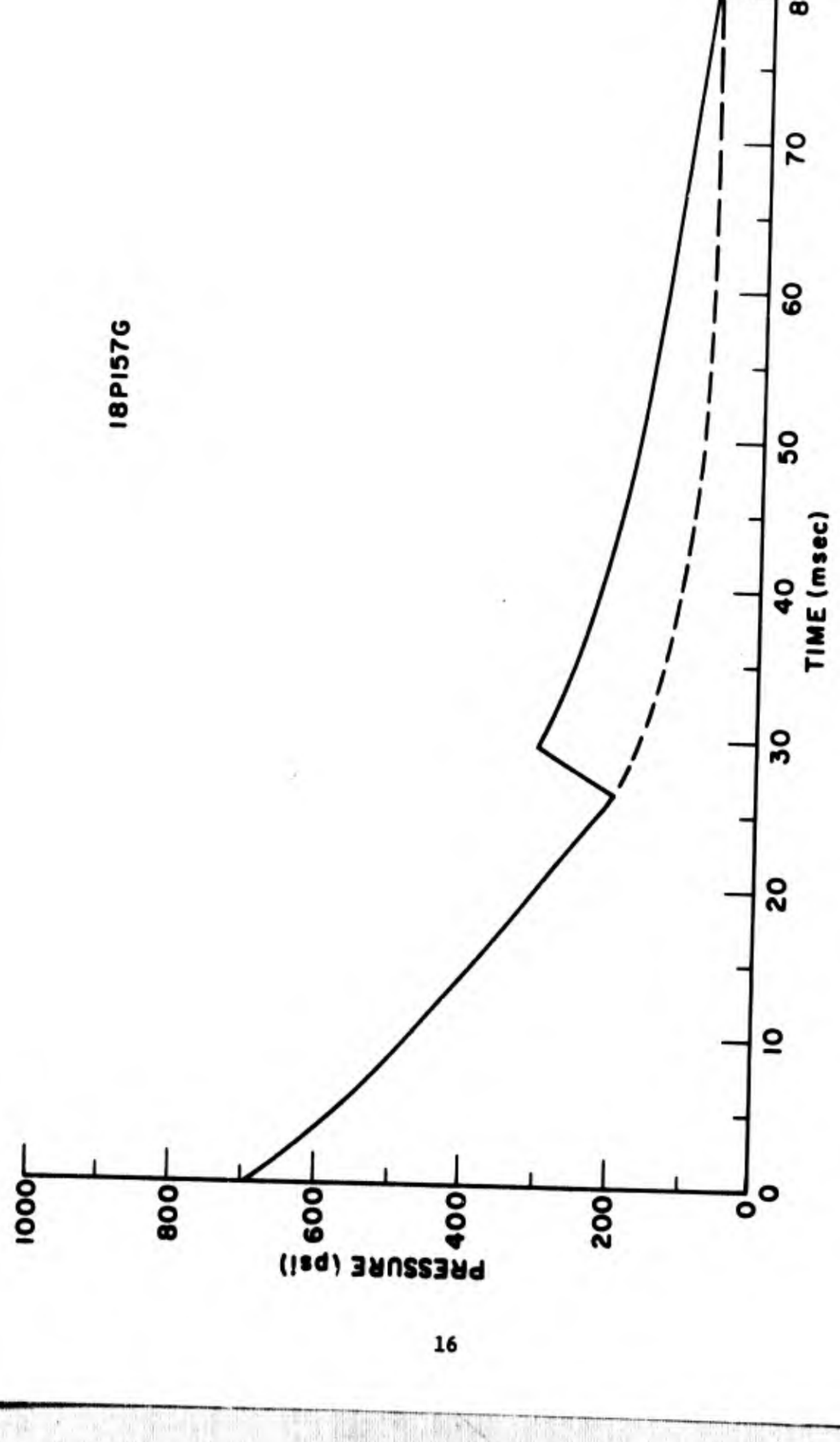

Figure 9. Overpressure-Time History 18P157G

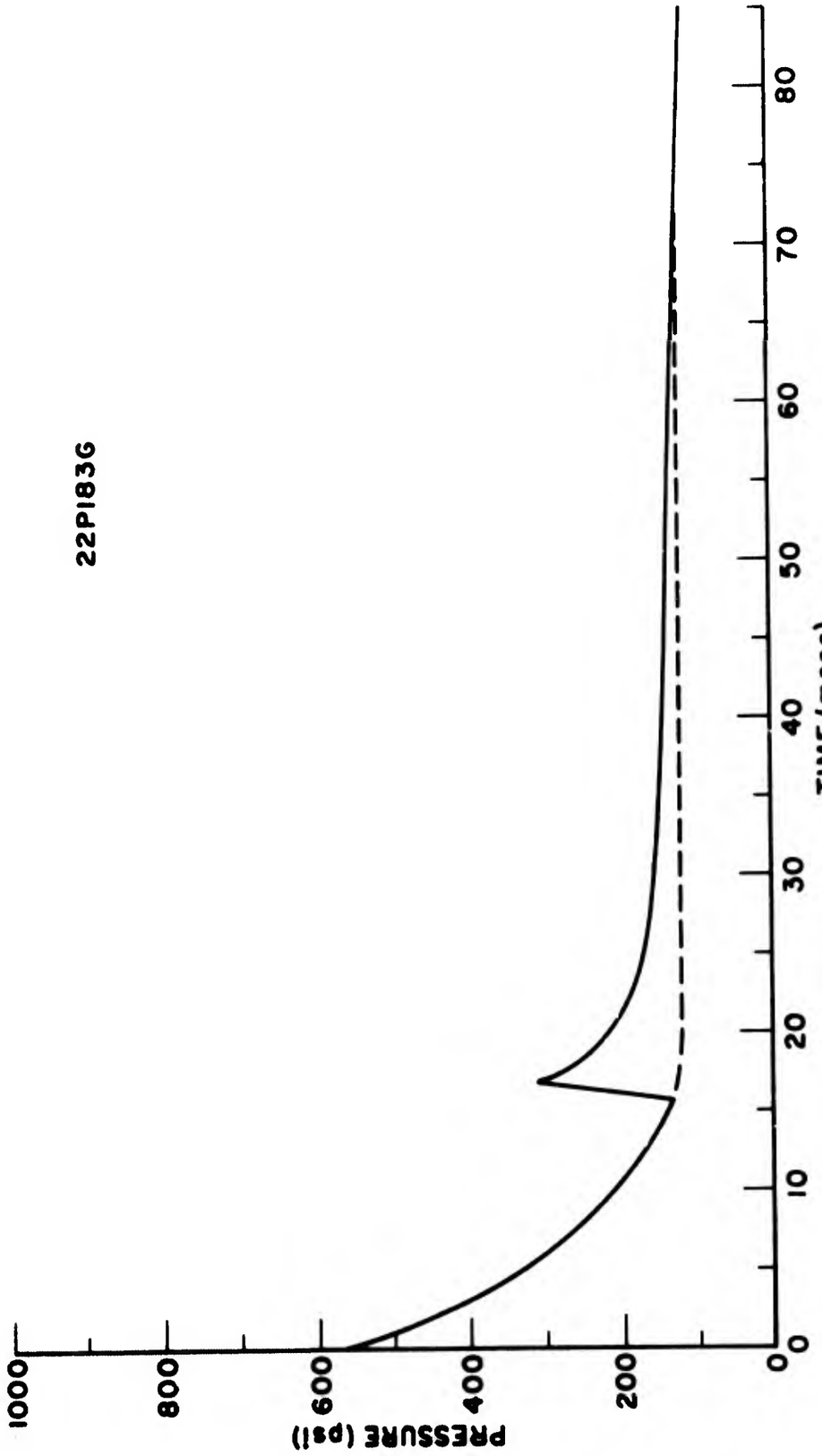

Figure 10. Overpressure-Time History 22P183G

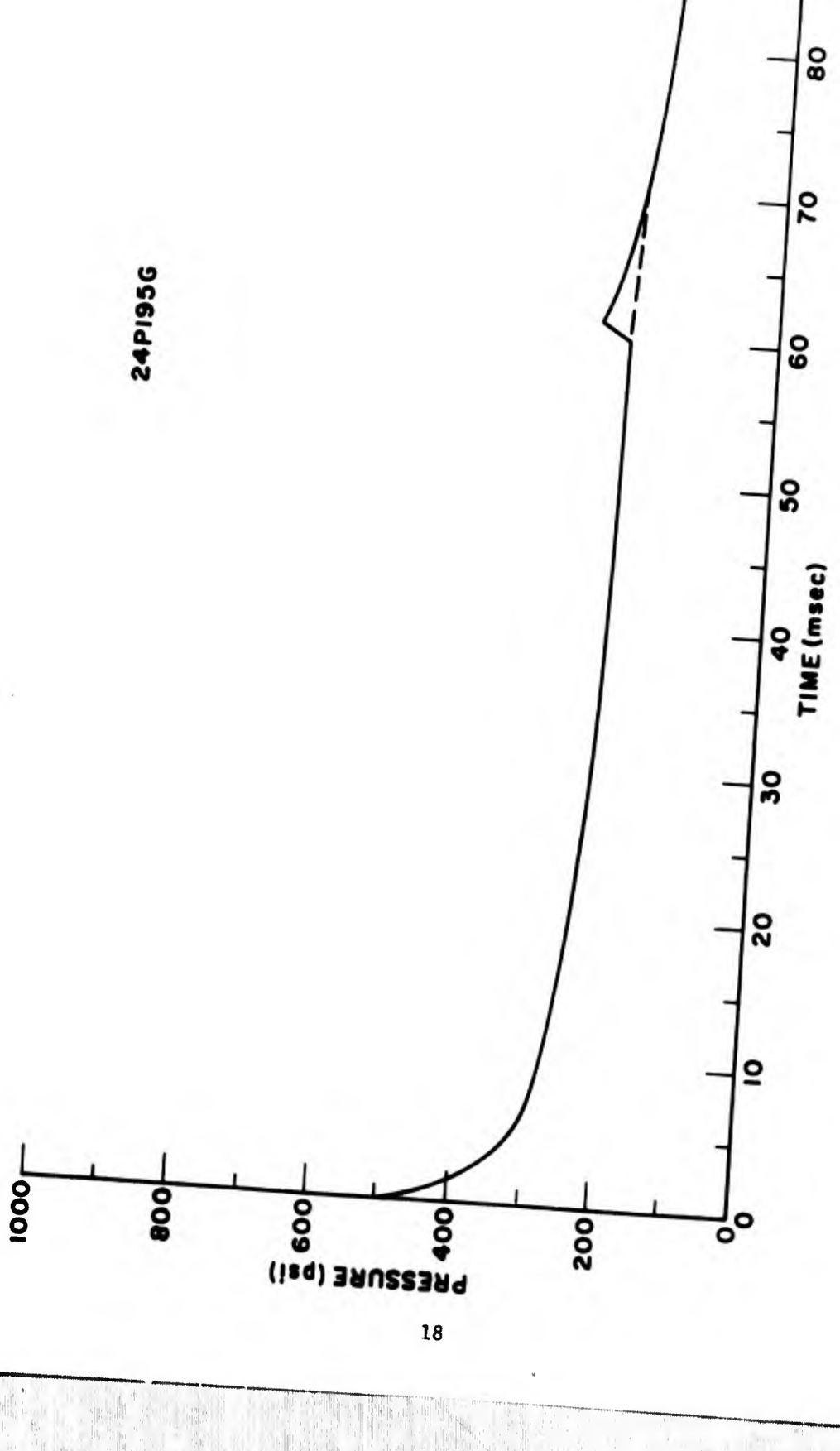

Figure 11. Overpressure-Time History 24P195G

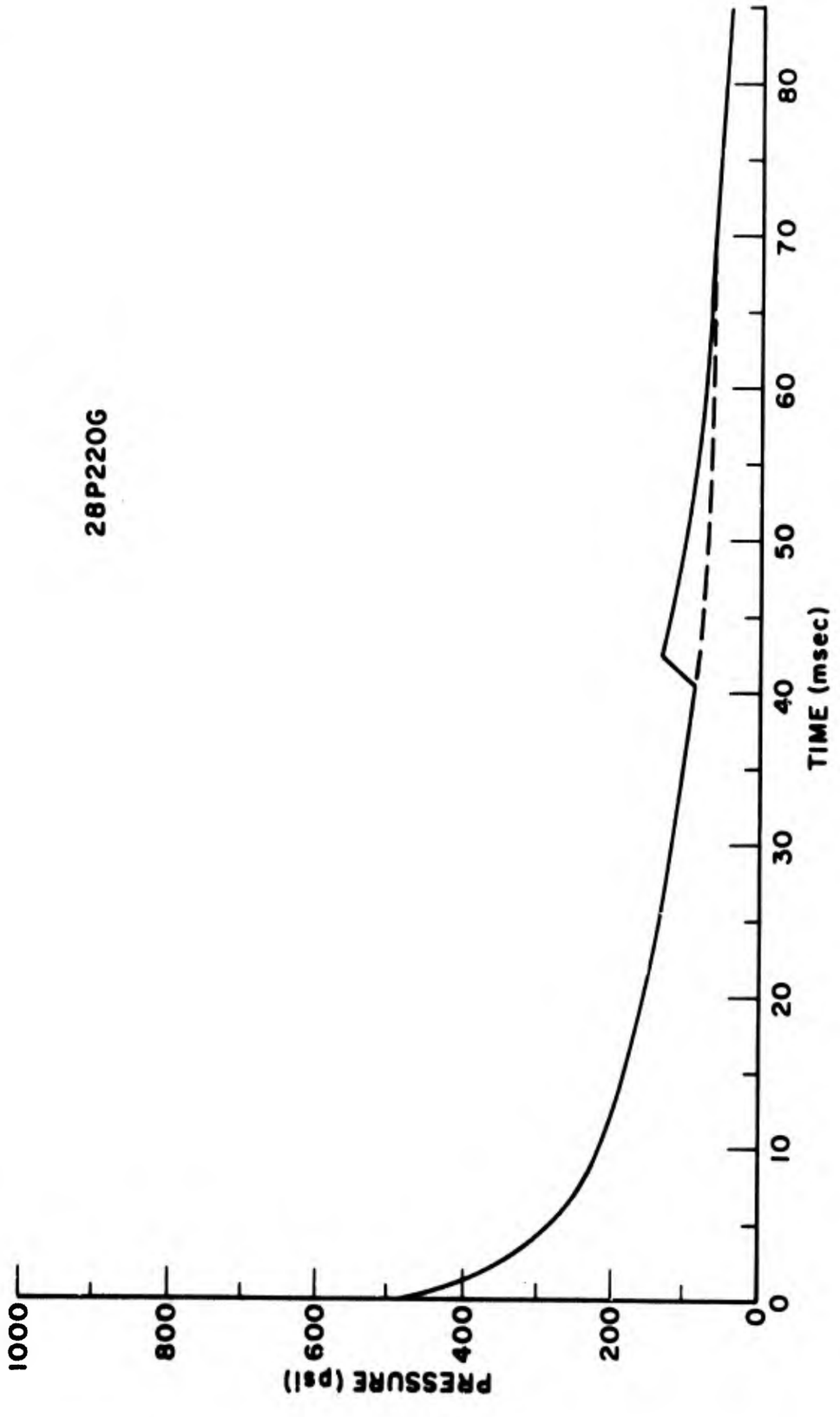

Figure 12. Overpressure-Time History 28P220G

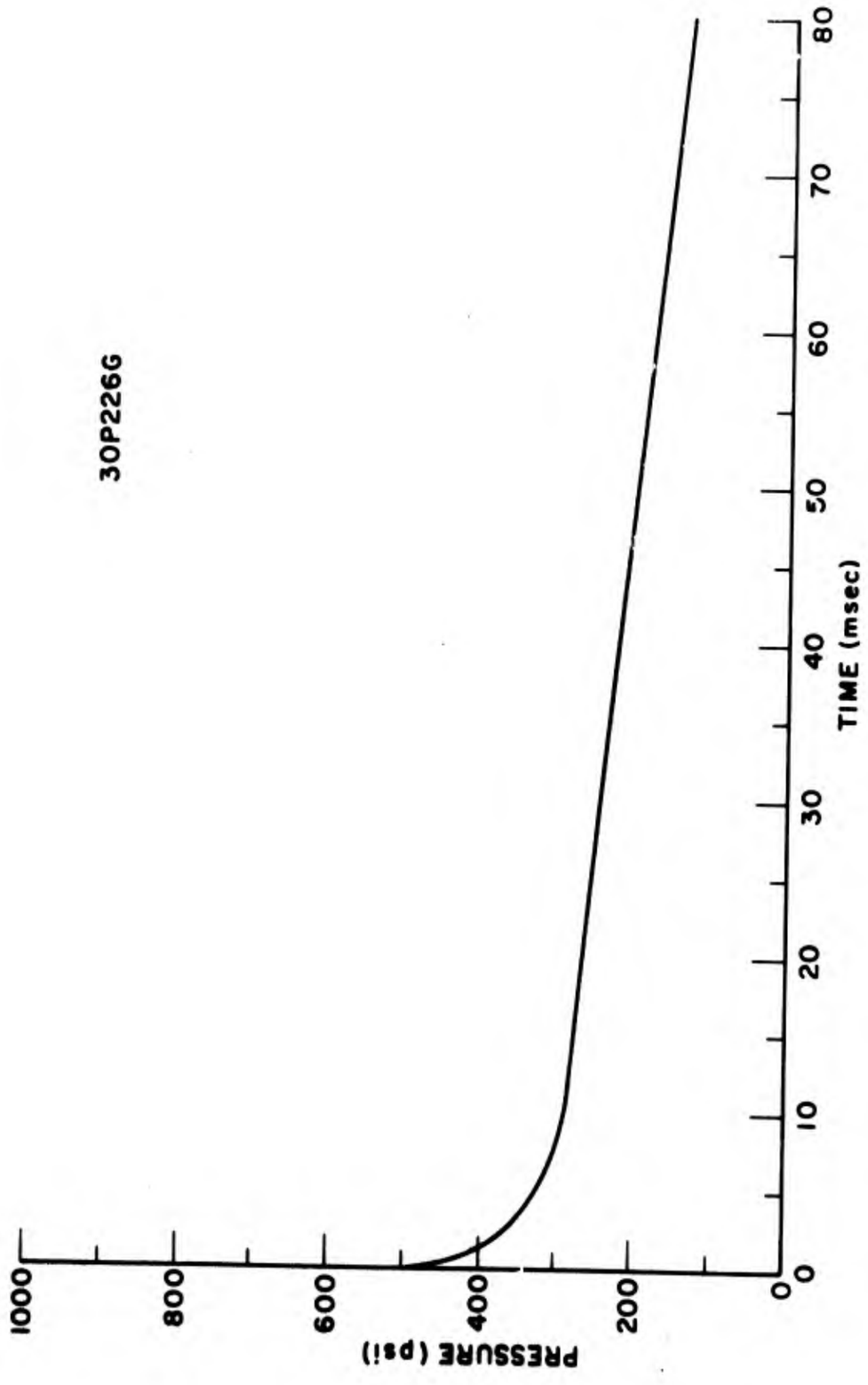

Figure 13. Overpressure-Time History 30P226G

The reflected peaks were ignored in computing the impulse. The reflected peaks are a result of the shock wave hitting the end of the test pit. The magnitude of the shock wave attenuated rapidly as it propagated against the air particle flow within the test pit.

Table III summarizes the pertinent data from the reduced pressure-time histories. With the exception of gage 10P121G, all gage readings were considered equally in the determination of the peak overpressures and impulses. All computed impulses and total times are corrected for baseline shifts except 28P220G. The baseline shift was considered to occur linearly with time, i.e., a straight line was drawn from zero time to the point at which pressure became constant. The complete baseline shift for 18P157G was assumed to occur immediately at $t = 0$, otherwise the gage would have negative pressures with significant impulse early in time. The average from the eight Norwood gages was 619 psi and from the two Bytrex gages was 513 psi. The spread of the data was 235 psi for the Norwood gages and 95 psi for the Bytrex gages.

Figure 14 represents the distance versus arrival time of the shock front. A least square fit in the form $y = a + bx$ was fit to the data points. This line represents a shock front velocity of 5640 feet per second. A 598-psi shock wave propagates at velocity of 6800 feet per second. Since the air-pressure gages were recorded on different magnetic tapes and the digitizing was not begun at the same real time for each tape, it was necessary to correct the shock front arrival time to account for this time difference. This correction is shown in table III. Shock-front arrival contours are shown in figure 15. This figure shows the position of the shock front within the test bed at various times after detonation. The apparent detonation time was 31.22 msec. This represents the delay between the time the fire signal was initiated and detonation began inside the pit.

Table III

SUMMARY OF AIR PRESSURE DATA

Gage	Peak overpressure (psi)	$T_{1/2}$ (msec)	Total duration (msec)	Impulse total (psi-sec)	Uncorrected t_a (msec)	Corrected t_a (msec)	Baseline shift (psi)
1P1G	595	6.0	179.0	24.10	11.0	47.0	+44.1
4P12G	670	18.0	148.5	16.37	26.7	---	+47.0
5P102G	735	6.5	180.0	10.40	13.0	47.0	+16.2
7P109G	630	6.0	170.0	16.74	27.5	42.3	+18.6
10P121G	---	---	---	---	---	---	---
14P141G	625	20.0	193.5	29.59	23.0	37.7	+59.5
18P157G	695	16.5	177.0	22.03	23.0	39.0	-95.9
22P183G	560	6.0	163.0	16.57	22.0	38.0	+88.0
24P195G	500	22.5	191.0	22.87	19.0	33.5	+47.0
28P220G	465	8.5	105.0	10.68	38.0	33.7	0
30P226G	503	29.0	196.0	23.12	19.0	33.5	+37.6
Average	597.8	---	172.2	19.25	---	---	---

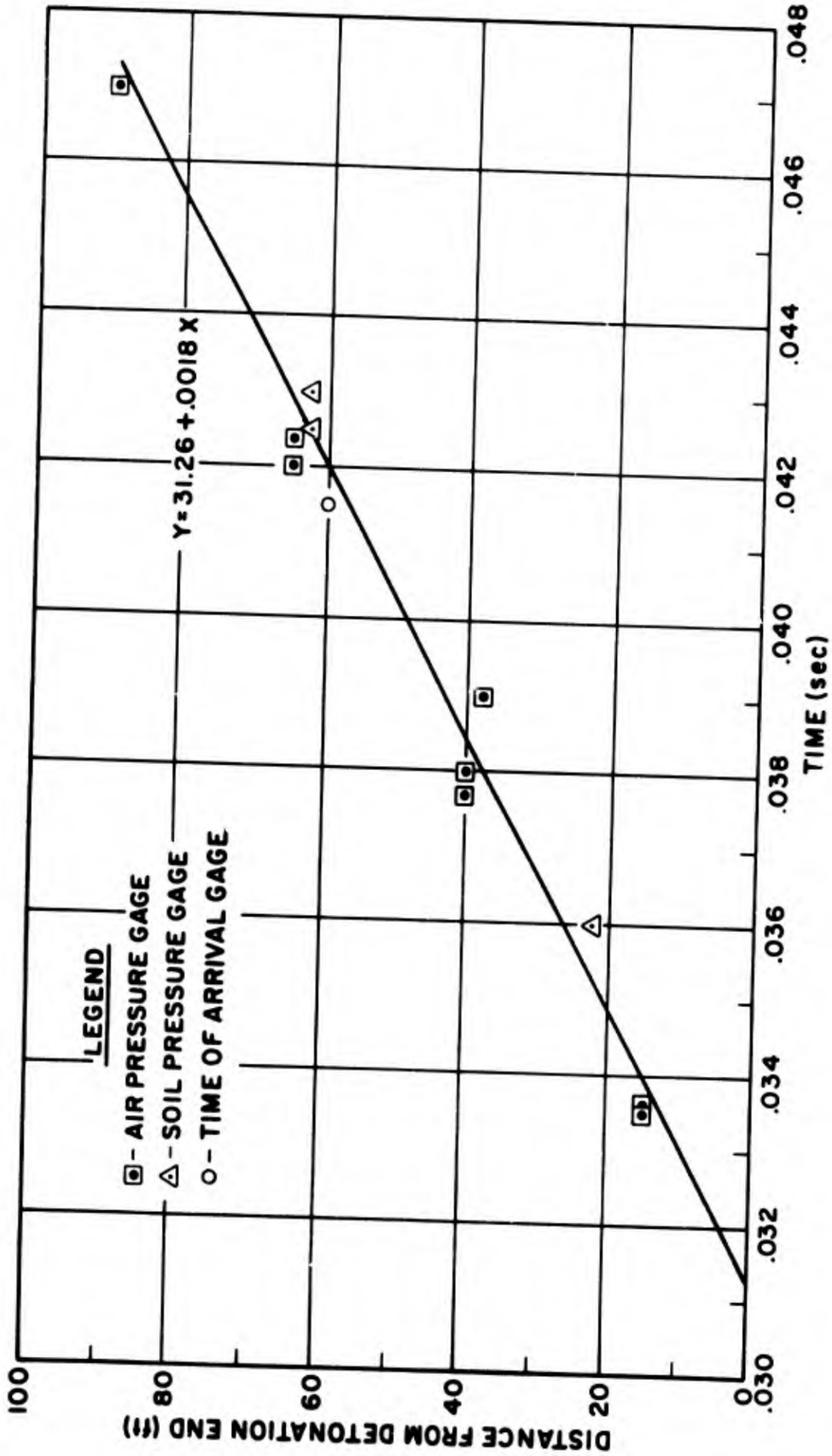

Figure 14. Airblast Time of Arrival

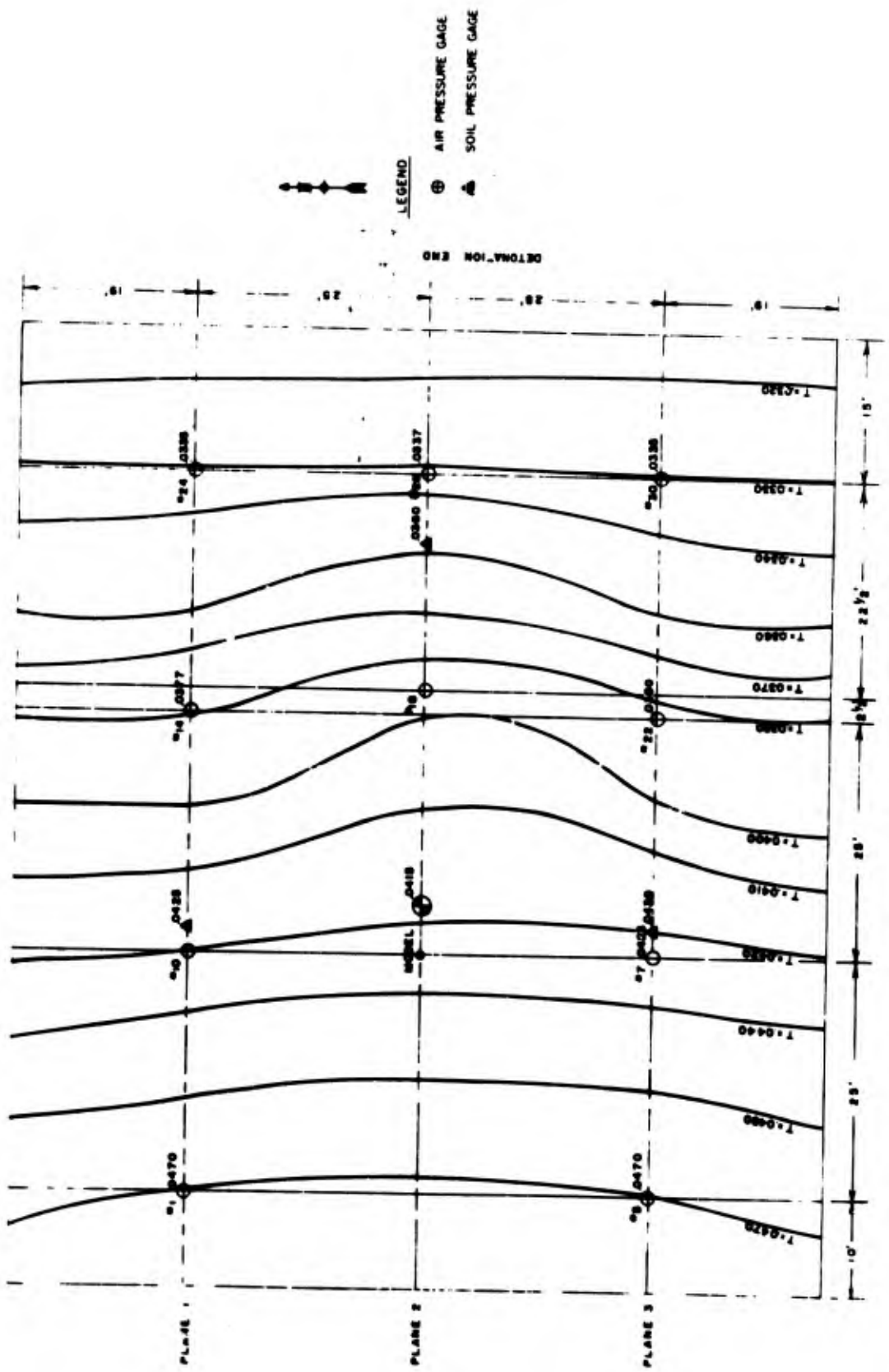

Figure 15. Surface Shock Front Arrival Contours

SECTION IV

EARTH FREE FIELD ENVIRONMENT

1. Subsurface Soil Properties

To evaluate the subsurface soil conditions, three exploratory drill holes were sampled. These samples were subjected to standard classification tests and dynamic one-dimensional multiple reflection compression tests. The soil profile, deduced from the exploration and testing, is shown in figure 16. The layering is essentially horizontal and well defined. The profile consists of alternating layers of sand and gravel with some silt and clay. The static water table was below 90 feet.

The constrained modulus tests were performed with a modified consolidometer,* using a rise time to peak stress of approximately 200 msec. The data shown in figure 17 are qualitative only and represent composite values. The curves are of the locking type indicating that an input shock condition should be maintained as the stress wave propagates. These curves show a large percentage of nonrecoverable strain. This is thought to be partially due to the testing arrangement as well as to the hysteritic properties of the soil. The soil properties are summarized in table IV.

The seismic velocity varied with depth as follows:

SEISMIC VELOCITY
HEST PHASE IIA

Depth (ft)	Seismic velocity (fps)
0-58	1700
58-268	2550
268-2000	6740

*Karol-Warner model 354 Consolidometer, Karol-Warner Co., Highland Park, NJ.

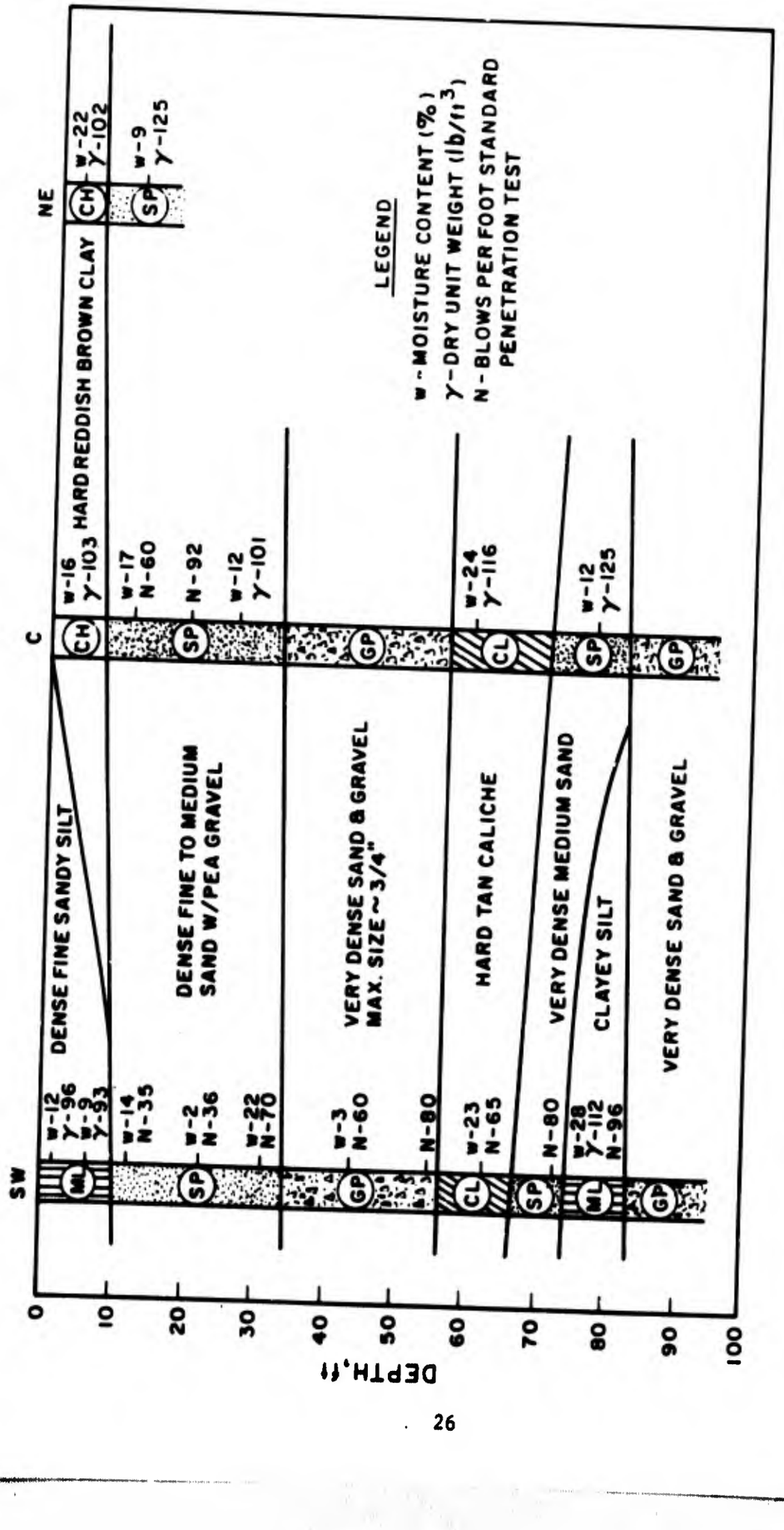

Figure 16. Subsurface Soil Profile

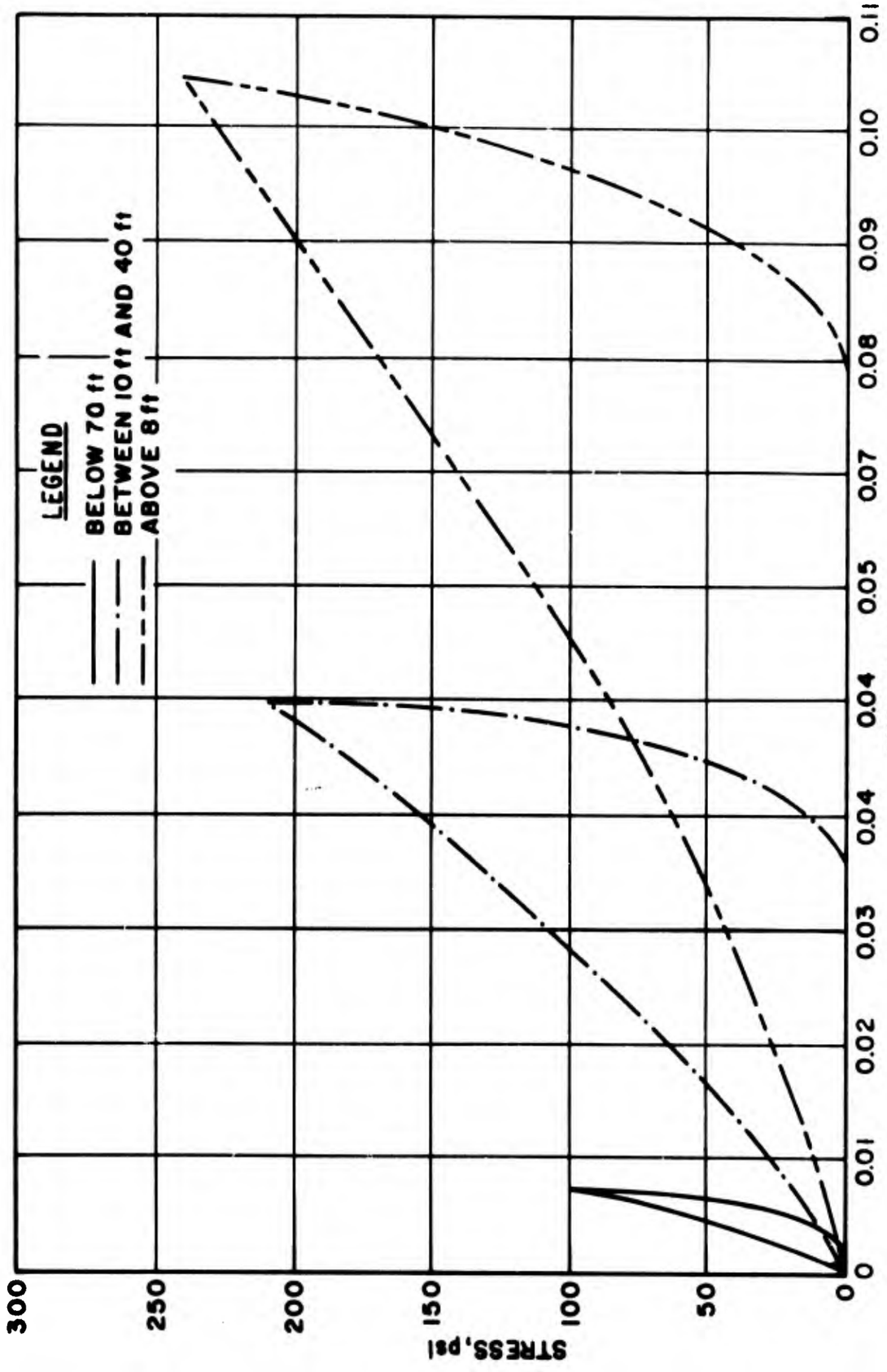

Figure 17. Constrained Modulus Tests

Table IV

SOIL PROPERTIES LDHEST PHASE IIA

Hole No.	Sample No.	Sample depth (ft)	Soil type	Soil condition properties		
				Moisture content (%)	Dry density (lb/ft^3)	Penetration resistance (blows/ft)
SW	1	1	ML	12	96	---
	2	7	ML	9	---	---
	3	15	SP	14	---	35
	4	20	SP	2	---	36
	5	30	SP	22	---	70
	6	45	GP	3	---	60
	7	55	GP	---	---	80
	8	60	CL	23	---	65
	9	70	SP	---	---	80
	10	80	ML	28	112	96
	11	90	GP	---	---	---
C	1	1	CH	10	103	---
	2	12	SP	17	---	60
	3	20	SP	---	---	92
	4	30	SP	12	101	---
	5	60	CL	24	116	---
	6	75	SP	12	125	---
NE	1	1	CH	22	102	---
	2	15	SP	19	125	---

2. Soil Stress

Ten soil-stress* gages were used in this test. Three were buried at a depth of 6 inches in holes 8, 11, and 16. The traces from the gages are shown in figures 39, 40, and 41. The data from these gages, summarized in table V, indicate soil stresses of 900, 870, and 740 psi, respectively. These data are not considered reliable because of the high peak pressures. The average overregistration factor based on the average air pressure was 1.40. The overregistration factor for the Phase II experiment (Ref. 1) and for the HIP-1A experiment were 1.85 and 1.60, respectively. (The results of HIP-1A are to be published.) At the present time, this factor cannot be determined from laboratory calibration tests. The high pressure results in a high impulse; therefore, the gages were disregarded in the overpressure analysis.

The data from the seven gages buried in hole 21 are shown in figures 42 through 48. These data cannot be considered reliable because (1) the frequency registered by the gages is too great to represent soil stress, (2) the data show large negative stresses the gage is not physically capable of measuring, and (3) the soil stress shows no increase in rise time or attenuation with depths as the other ground-motion data indicate.

3. Soil Strain

Sets of 4-inch-diameter soil-strain gages** were placed at depths of 1, 5, 10, 20, 40, 60, 80, and 100 feet in hole number 42 (figure 1) located 20 feet from the detonation end of the test pit. The details of the gage design, gage placement, and recording are found in reference 5, pages 71 through 74. The gages were oriented to measure strain in a vertical direction over a gage length of 6 inches. Plots of strain versus time for the eight gages are shown in figure 49. From these curves, the peak strains were determined and are plotted in figure 18. Assuming that the smooth curve shown in the figure represents the data, a total displacement of 11 inches at the surface and 3.3 inches at 20 feet is indicated. This is in good agreement with the displacements shown in figure 24. The data show a rapid attenuation of strain in the upper 20 feet, becoming much more gradual below that depth. This is in agreement with the other displacement data.

---

*University of New Mexico soil stress gage
**IITRI coil strain gage

Table V

SUMMARY OF NEAR-SURFACE SOIL STRESS DATA

Gage No.	Peak stress (psi)	Impulse (psi-sec)	Duration (msec)	$t_{1/2}$ (msec)
8L110G	900	17.1	132.0	6.2
11L112G	870	31.7	186.0	23.0
16L151G	740	22.6	191.0	21.0
Average	837	23.8	170.0	16.7

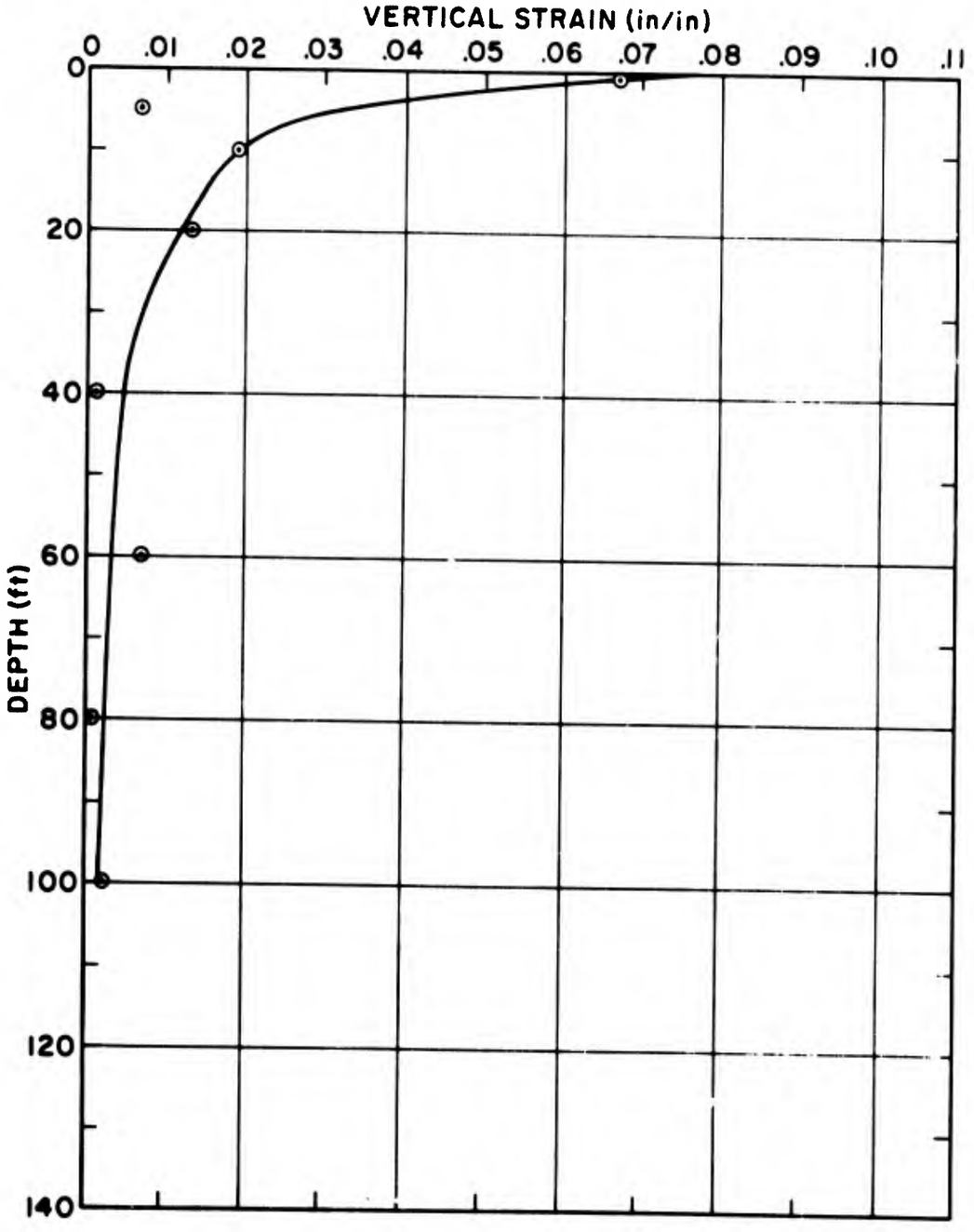

Figure 18. Peak Vertical Strain-Depth

In the data, there are certain anomalies (tension, second peaks) that cannot be explained, but are probably a result of cable squeeze, reflections, or related phenomena.

4. Velocity

The particle velocity data represents the best quality ground-motion data which was obtained in this test. Of the 15 gages installed, 12 were successfully recorded. The signal to noise ratio was very low and only two gages, 12V-125-60 and 25V-204-1, exhibited baseline shifts. In integration of these gages, the baseline shift was assumed to occur linearly with time. The peak vertical particle velocities are plotted in figure 19. The acceleration records were of poor quality and no attempt was made to integrate them for velocity. The scatter in the velocity data is limited and seems to be random, i.e., the data from one hole are not consistently high or low. The data show a rapid attenuation in the upper 20 feet, becoming much more gradual below that depth.

From the velocity-time histories, figures 50 through 61, the rise time to peak velocity was calculated. This is plotted in figure 20. Also shown as dashed lines is the rise time, calculated assuming that the peak of the stress wave propagated at a velocity equal to one-half the seismic propagation velocity. This predicted rise time agrees with the observed rise time quite well to a depth of about 50 feet. If the data point from hole 12 at a 60-foot depth, which is questionable due to the shape of velocity-time history (figure 25), were ignored, the agreement would be quite good below 50 feet also. However, at this depth, the stress wave has become quite soft-fronted and the hard caliche at about 60 feet exhibited a locking stress-strain behavior under dynamic loading. This would cause a shocking-up (decrease in rise time) of the stress front. Since both the stress-strain data and the rise time data are limited, it is not possible to determine whether the data point should be eliminated or the caliche actually caused the wave to shock-up.

To determine the velocity at which the stress wave propagated into the ground (wave propagation velocity), the travel time of the stress wave front and peak were determined from the velocity records. These data are plotted in figures 21 and 22. The three holes were normalized by shifting the arrival time of the airblast over the hole to zero time so that only propagation of the stress wave through the soil might be considered. Also shown for comparison

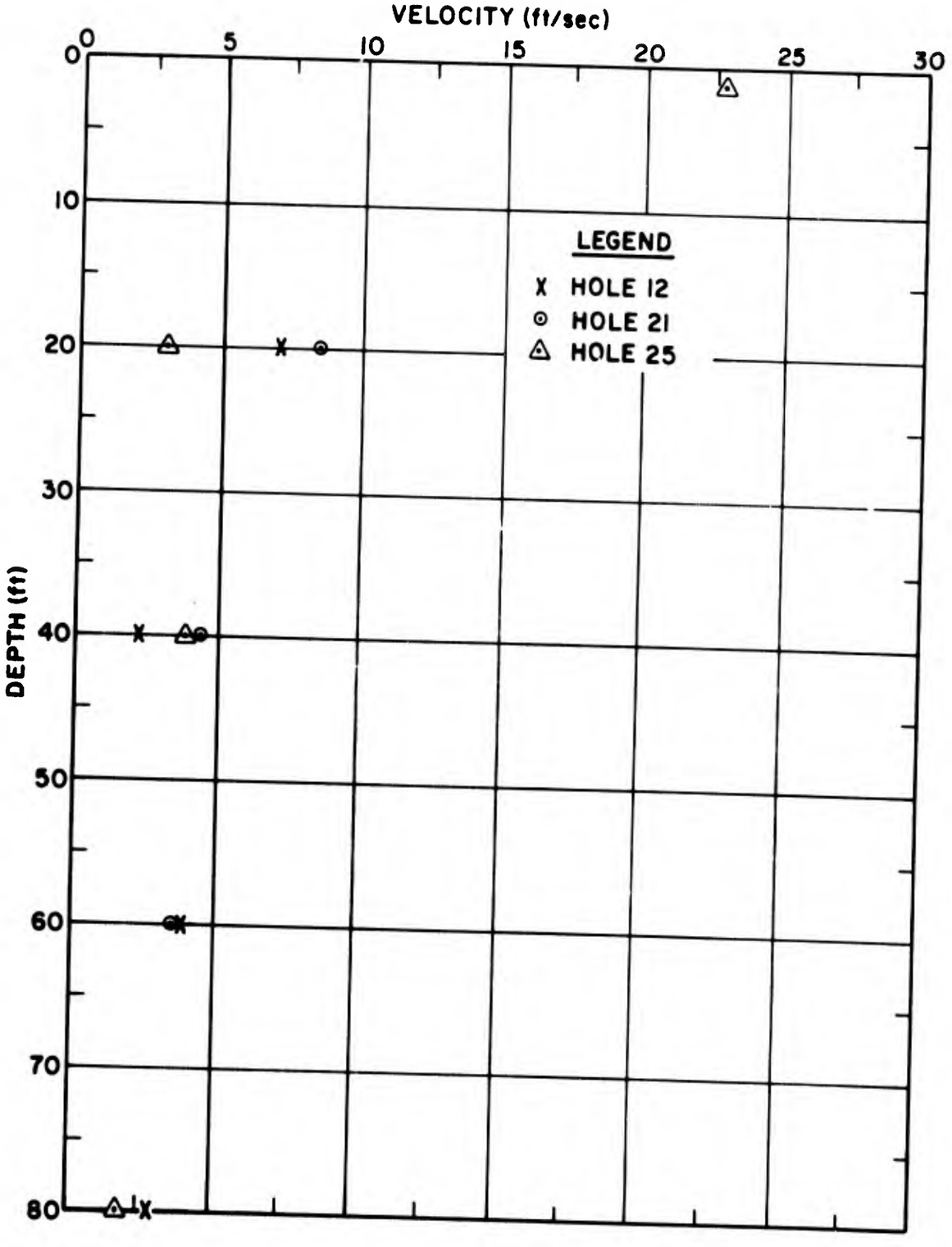

Figure 19. Peak Particle Velocities

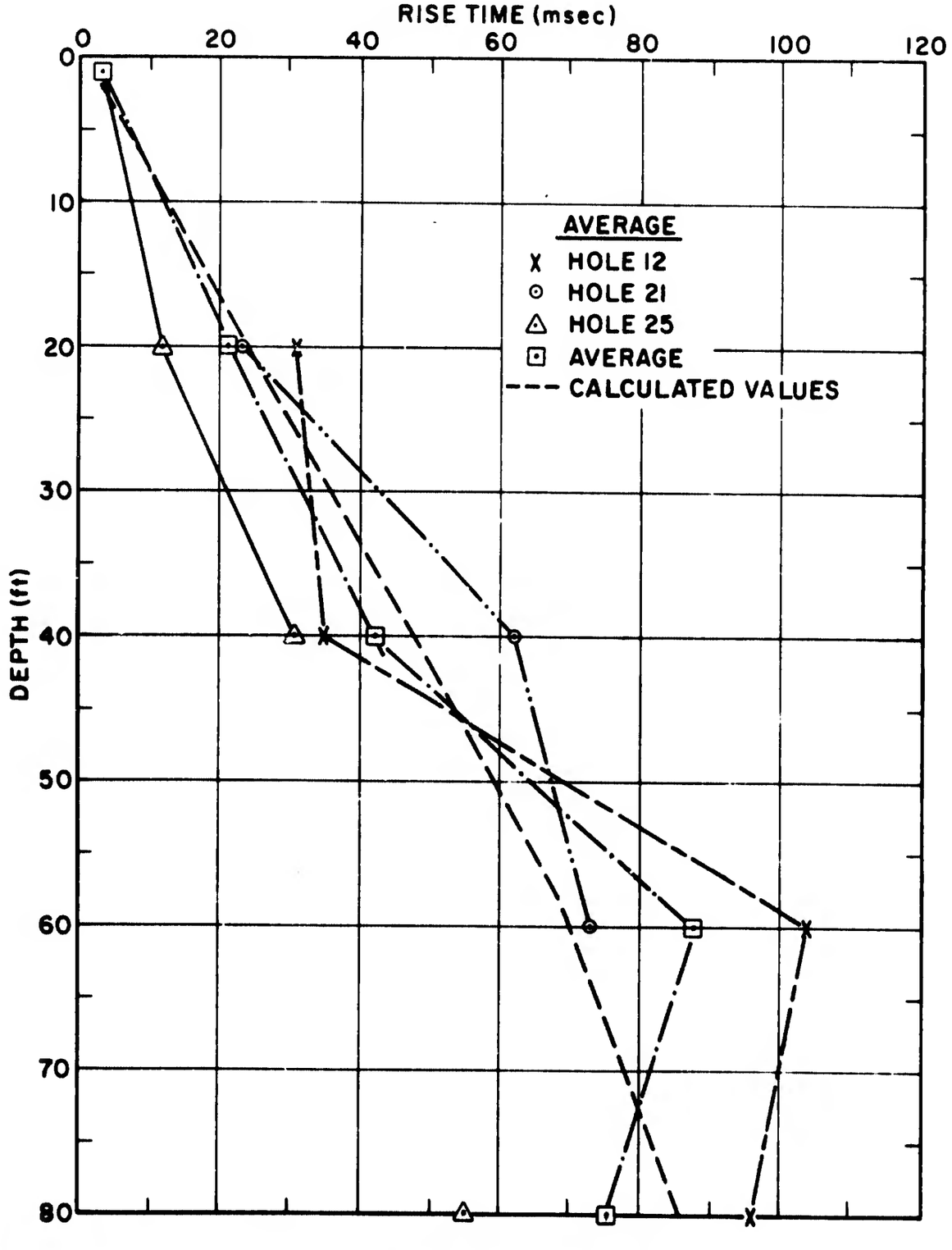

Figure 20. Rise Time to Peak Velocity

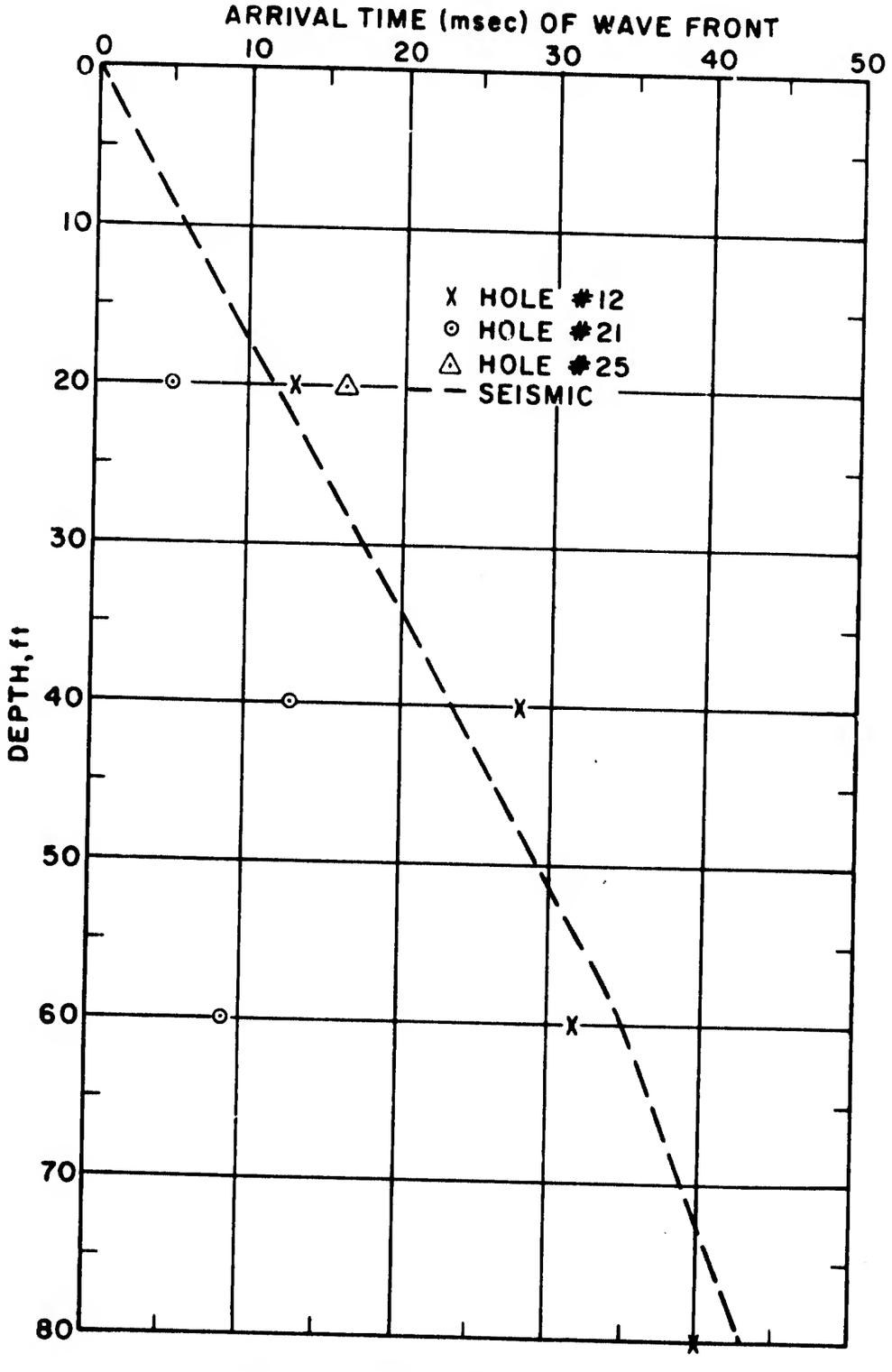

Figure 21. Arrival Time of Stress Front

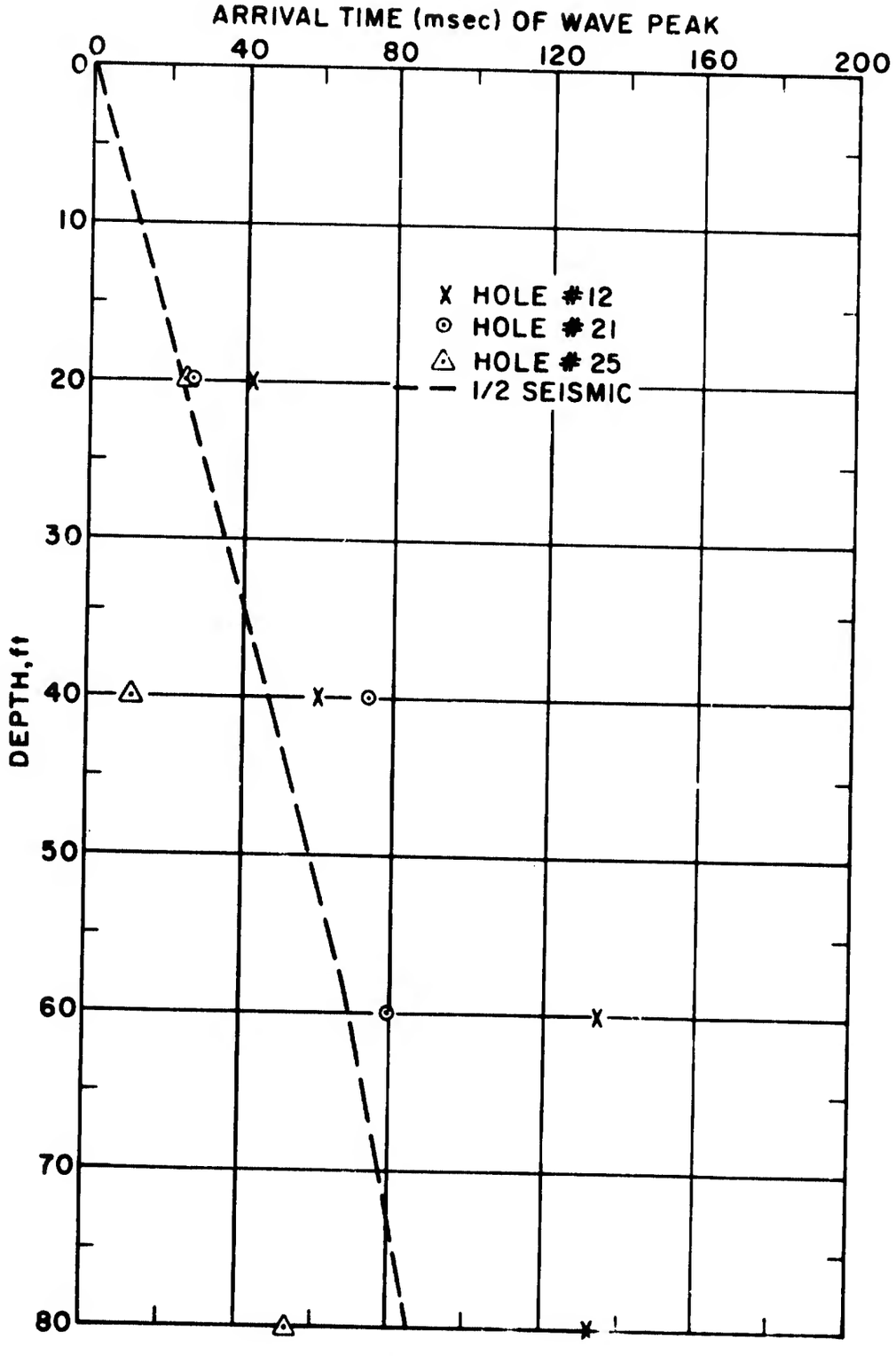

Figure 22. Arrival Time of Stress Peak

are the arrival times of the seismic wave and the arrival times of a wave traveling at one-half the seismic velocity. For this case, these values represent a good approximation of the data.

5. Acceleration

Twelve accelerometers were used to record particle acceleration at depths between 10 and 70 feet. The digitized traces are shown in figures 62 through 71. The peak downward accelerations are plotted in figure 23. The agreement among the data from the three holes is very good with the exception of the gages at 10 feet. As a comparison, the maximum slopes of the velocity-time histories were determined and are also plotted in figure 23. The agreement between the two methods of determining particle acceleration is very good. These data are tabulated in table VI. The acceleration from the slope of velocity gage at 1-foot depth of burial was 1,120 g. Many of the spikes on the air-pressure traces are above 1000 psi and these probably are not filtered by the soil at a depth of 1 foot. Since the particle acceleration is primarily peak pressure sensitive for very short rise times, one would expect a very high acceleration. This value is in good agreement with more recent measurements of acceleration very near the surface.

Generally, the data are of poor quality due to the high signal-to-noise ratio.

6. Displacement

Three long-span displacement gages were used to measure the relative displacement between the surface and deadmen at 40 feet, 70 feet, and 100 feet. The gage with a 40-foot span was overdriven before reaching a maximum value. This is probably a result of the spring (which takes up the slack in the wire) not being extended sufficiently on installation. The velocity gages were integrated for displacement and are plotted along with the long-span displacement gages in figure 24. The digitized displacement data are shown in figures 72 through 74. The long-span data are plotted assuming the deadman at 100 feet did not move; therefore absolute displacement is recorded. Any displacement at 100 feet would be directly additive to the values shown. The soil-strain data reaches zero at 161 feet, and assuming a linear decay below 80 feet, a peak transient displacement of 0.6 inch at 100 feet is obtained. It is significant to note that the long-span displacement gages show more displacement than both the intergrated velocity records and the soil-strain gages.

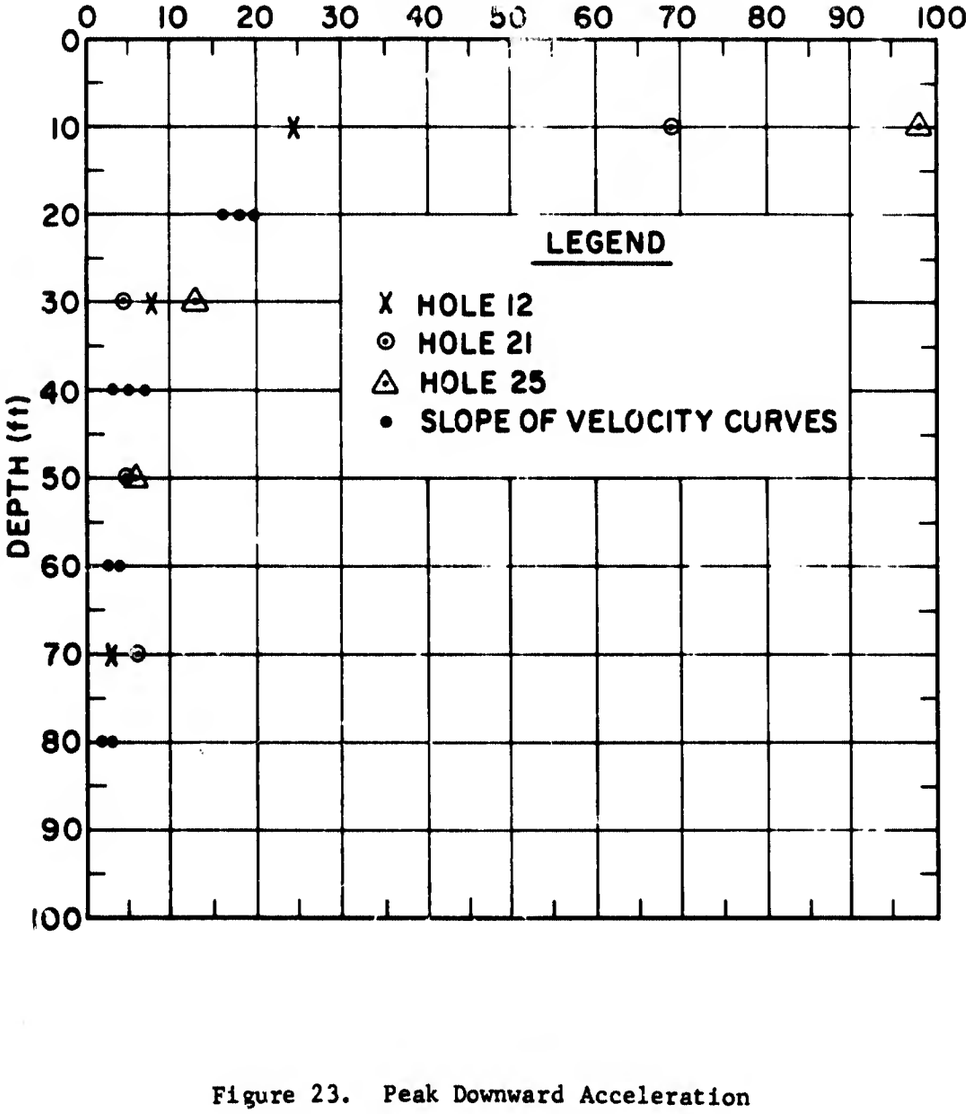

Figure 23. Peak Downward Acceleration

Table VI

PEAK PARTICLE ACCELERATION

Hole No.	Depth (ft)	Acceleration (g)	
		Directly measured	Slope of velocity-time history
12A-10	10	24.5	---
12V-20	20	---	16.3
12A-30	30	8.0	---
12V-40	40	---	3.11
12A-50	50	---	---
12V-60	60	---	2.48
12A-70	70	3.5	---
12V-80	80	---	2.17
21A-10	10	69.0	---
21V-20	20	---	19.4
21A-30	30	5.0	---
21V-40	40	---	4.45
21A-50	50	4.8	---
21V-60	60	---	3.54
21A-70	70	6.2	---
25V-1	1	---	1120.0
25A-10	10	97.0	---
25V-20	20	---	17.7
25A-30	30	12.0	---
25V-40	40	---	7.04
25V-80	80	---	1.81

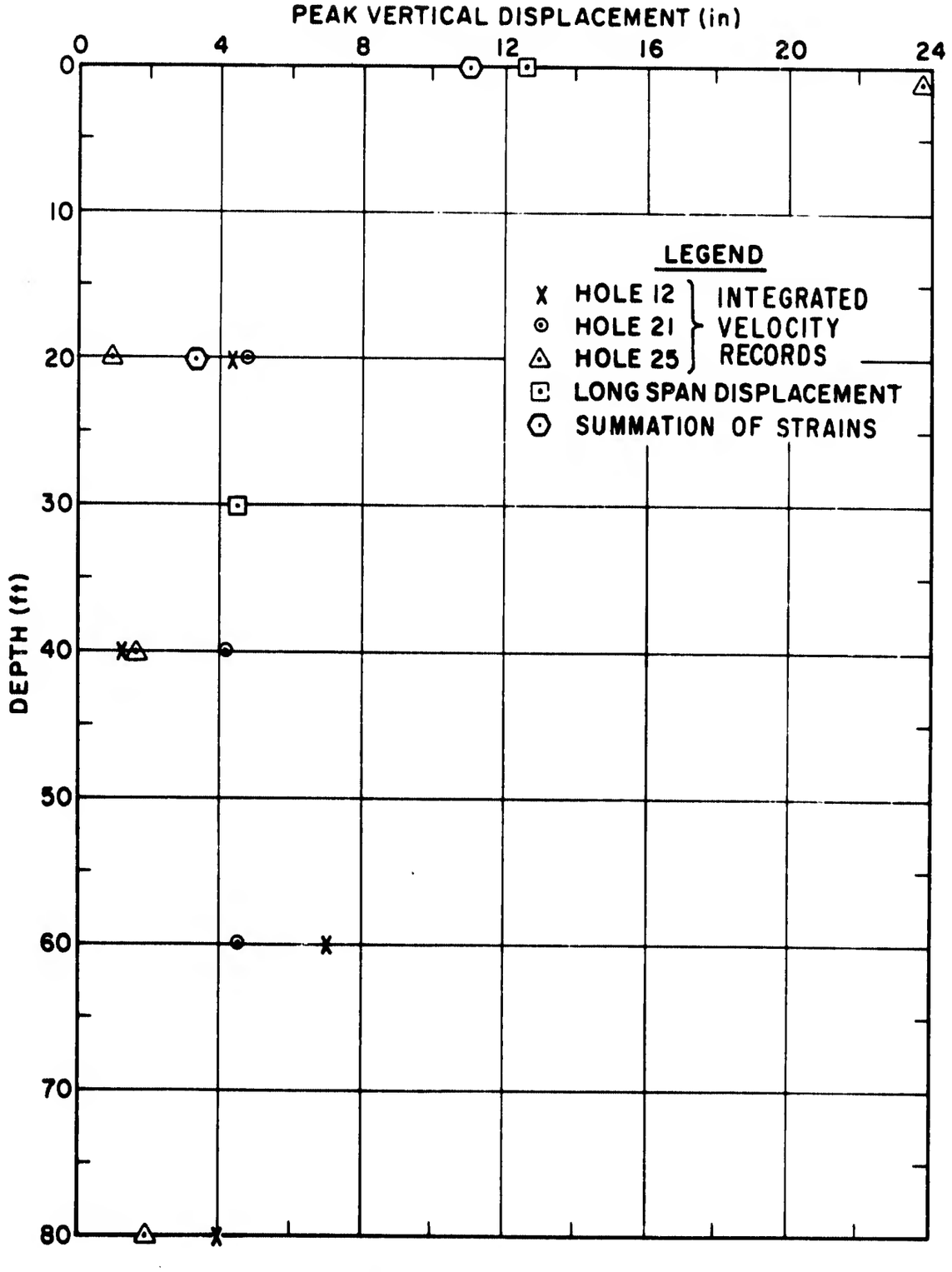

Figure 24. Peak Vertical Displacement-Depth

7. Time of Arrival

The time of arrival of the shock front at the surface is shown in figure 15. Figures 25 through 27 are cross sections of the test pit illustrating the variation of the arrival of the shock front as a function of depth. The time interval of the contour is 0.002 sec. The angle of incidence of the shock front ranges from 10° to 27°, the smaller angles of incidence being found near the surface at the detonation end of the test pit, and generally greater at increased distance and depth from the detonation. The average angle of incidence is approximately 18°. All gage types were used in the determination of the arrival of the shock front. These data agree very well with the angle of incidence one would calculate (17° 40') by using a wave front velocity of 5640 feet per second and a seismic velocity of 1700 feet per second.

In determining the propagation velocity of the stress wave, the values given in figures 25 through 27 should be used rather than the values from the digitized records. The records do not have the same zero times because digitization of the various tapes was not begun at the same time. The values in figures 25 through 27 have all been normalized to a common zero time.

8. Summary

It should be reemphasized, in conclusion, that in this report no attempt has been made to rigorously analyze these data, but they seem internally consistent. Given the uncertainties of measurements of this type, the data seem reliable and are of the order one predicts using a one-dimensional calculation procedure and a reasonable soil model which accounts for the energy absorption on cyclic loading.

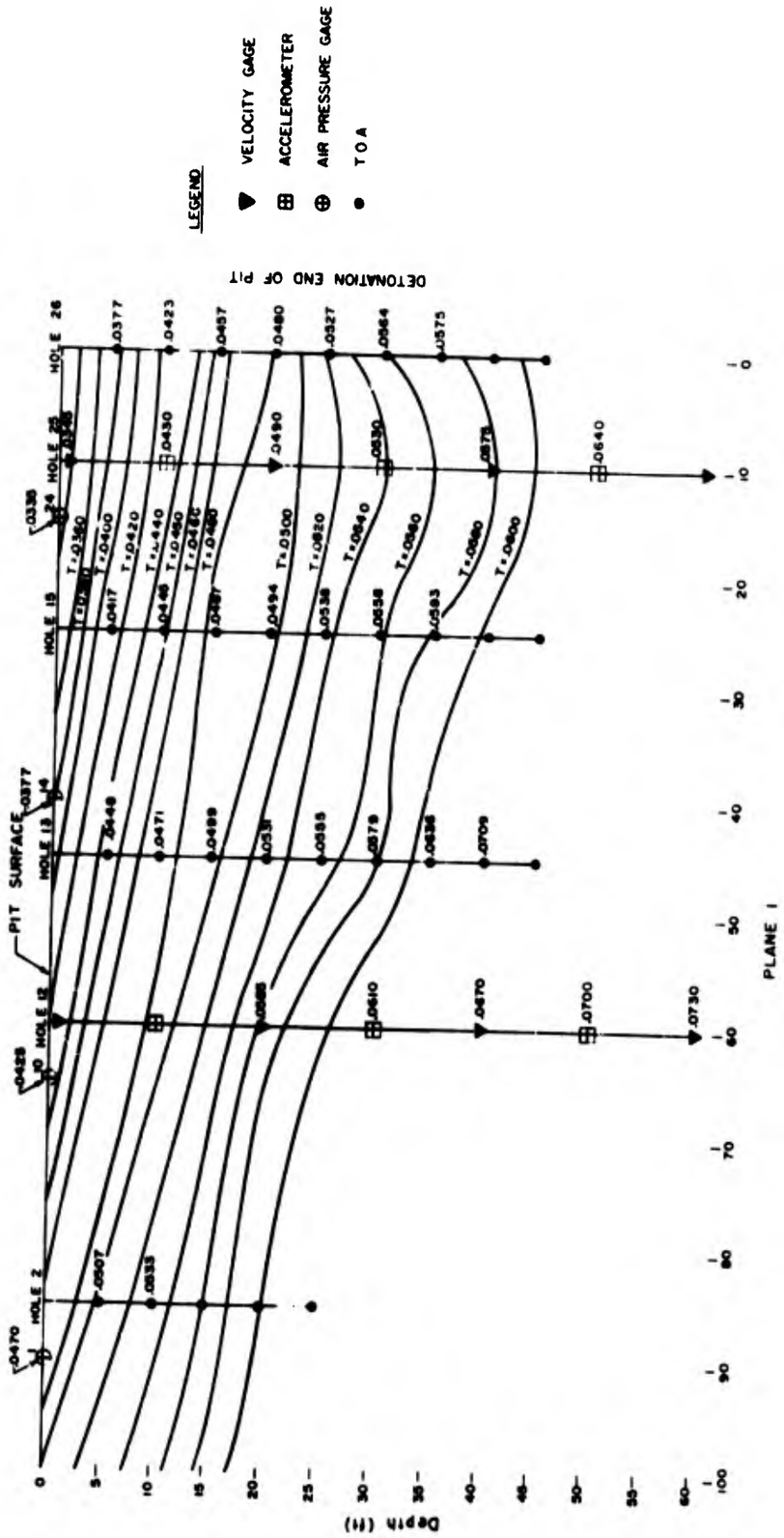

Figure 25. Cross Section of Test Pit Showing Time of Arrival Contours (Plane 1)

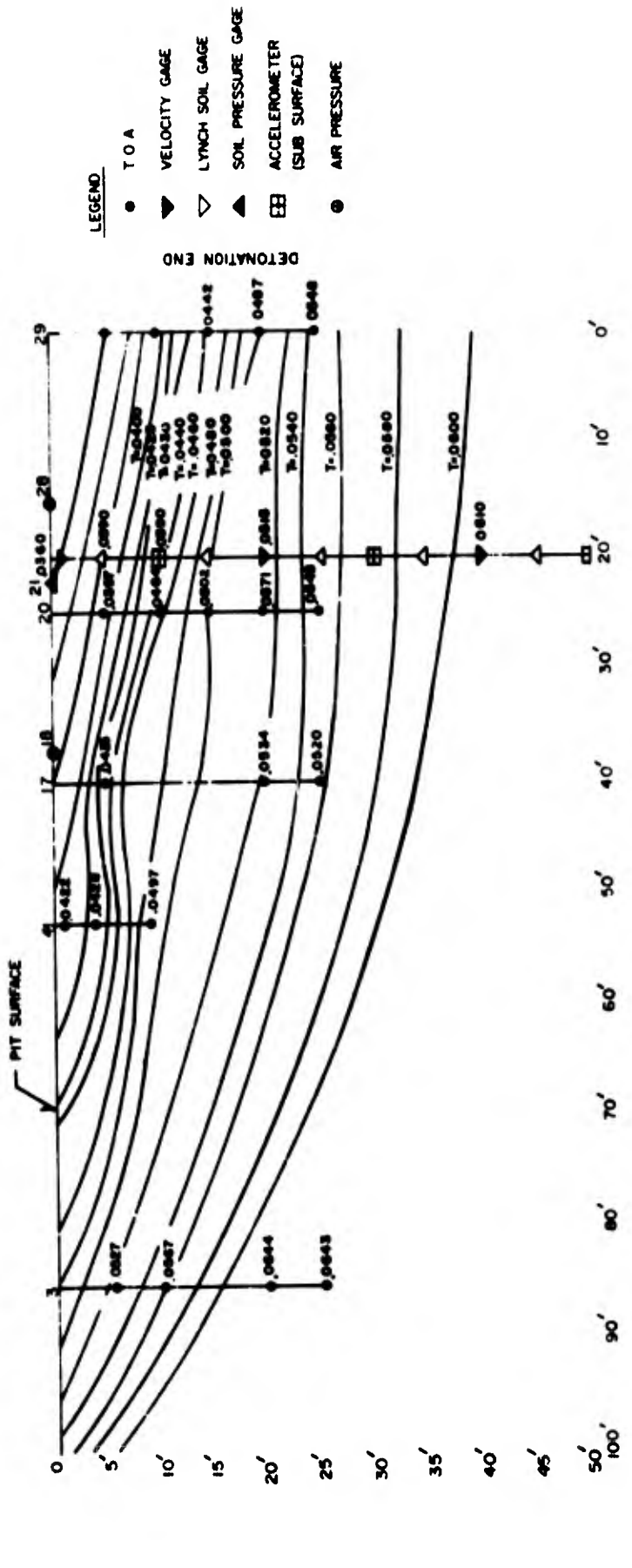

Figure 26. Cross Section of Test Pit Showing Time of Arrival Contours (Plane 2)

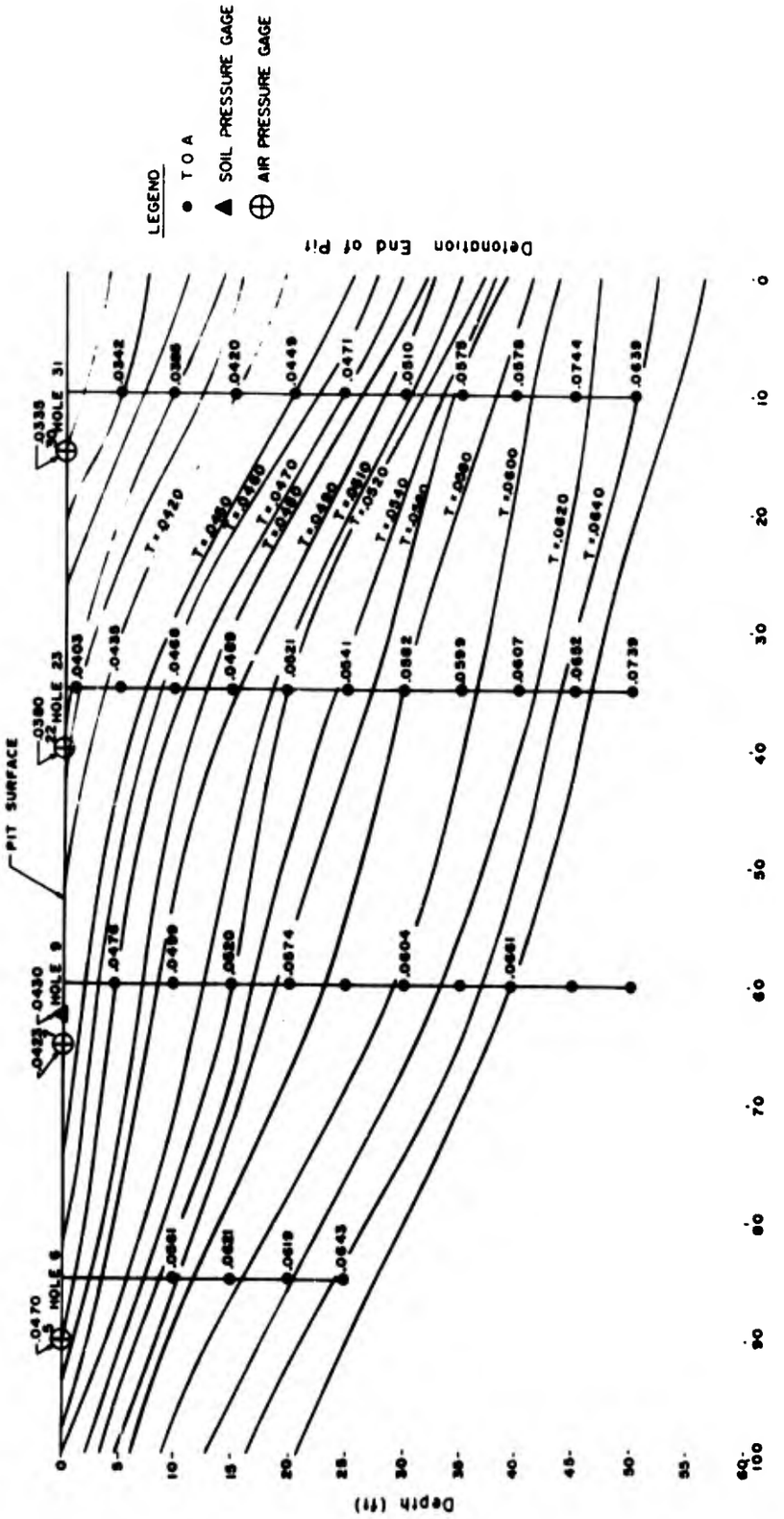

Figure 27. Cross Section of Test Pit Showing Time of Arrival Contours (Plane 3)

APPENDIX

DIGITIZED RECORDS

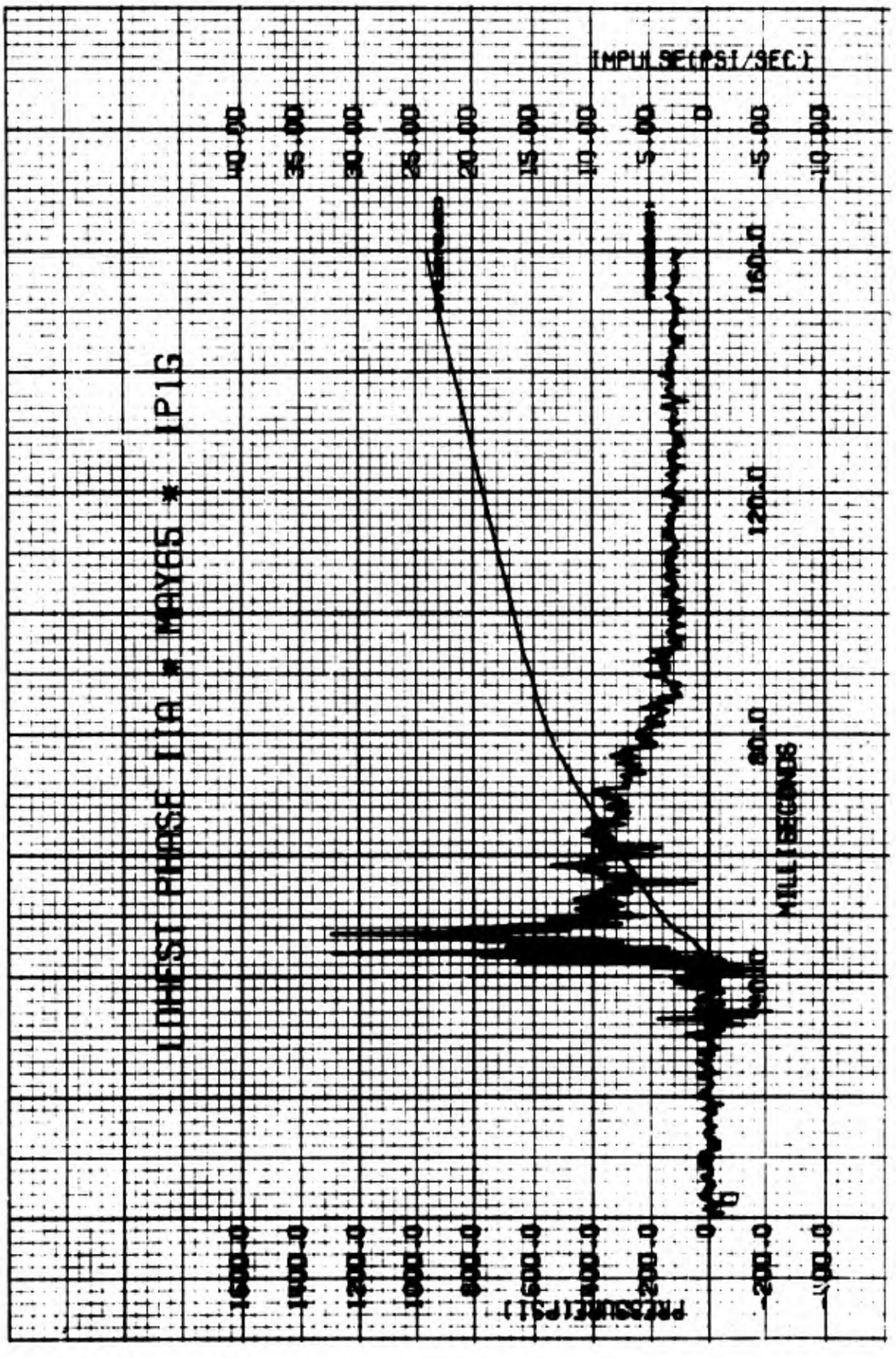

Figure 28. Overpressure-Time Histories

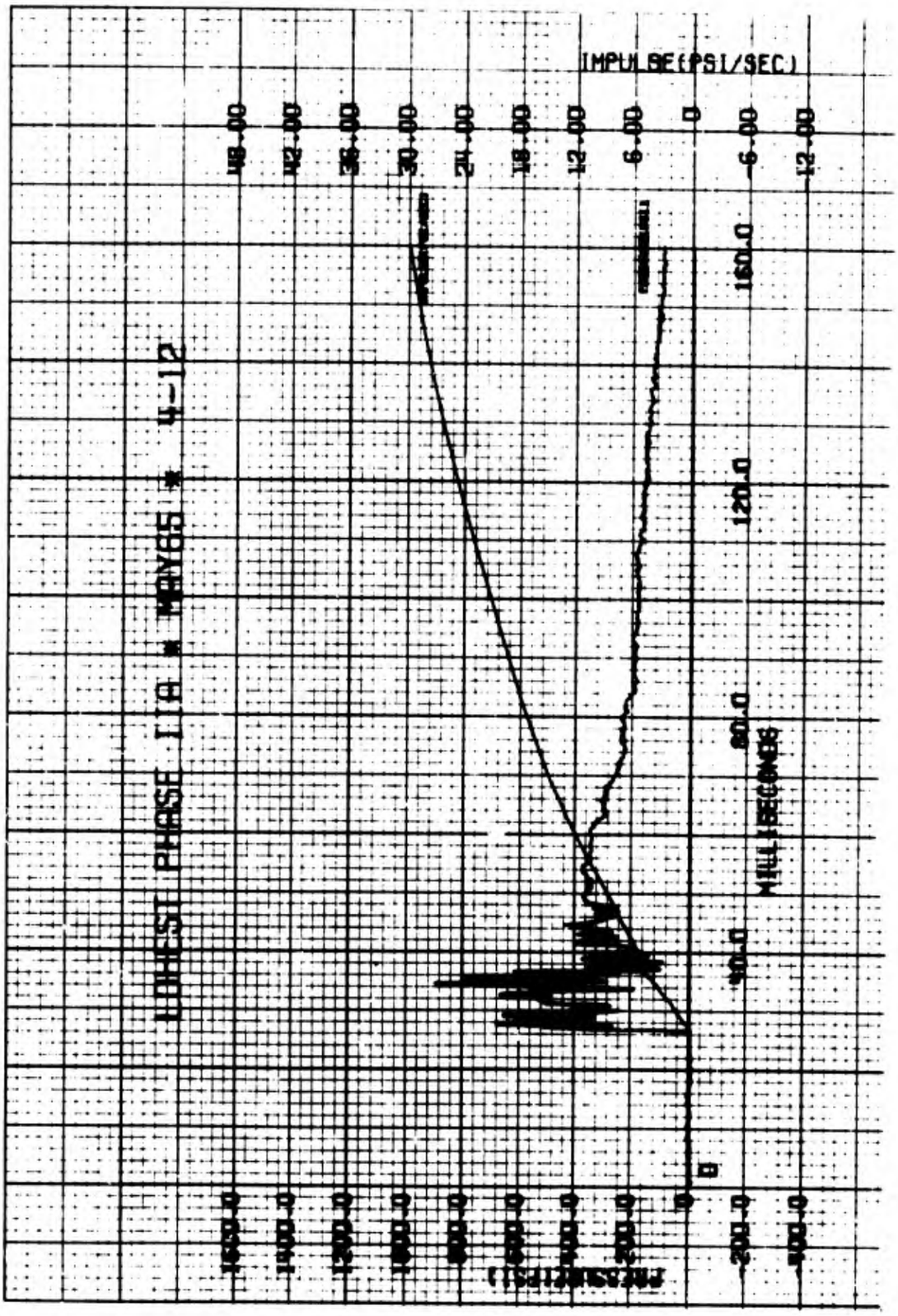

Figure 29. Overpressure-Time Histories

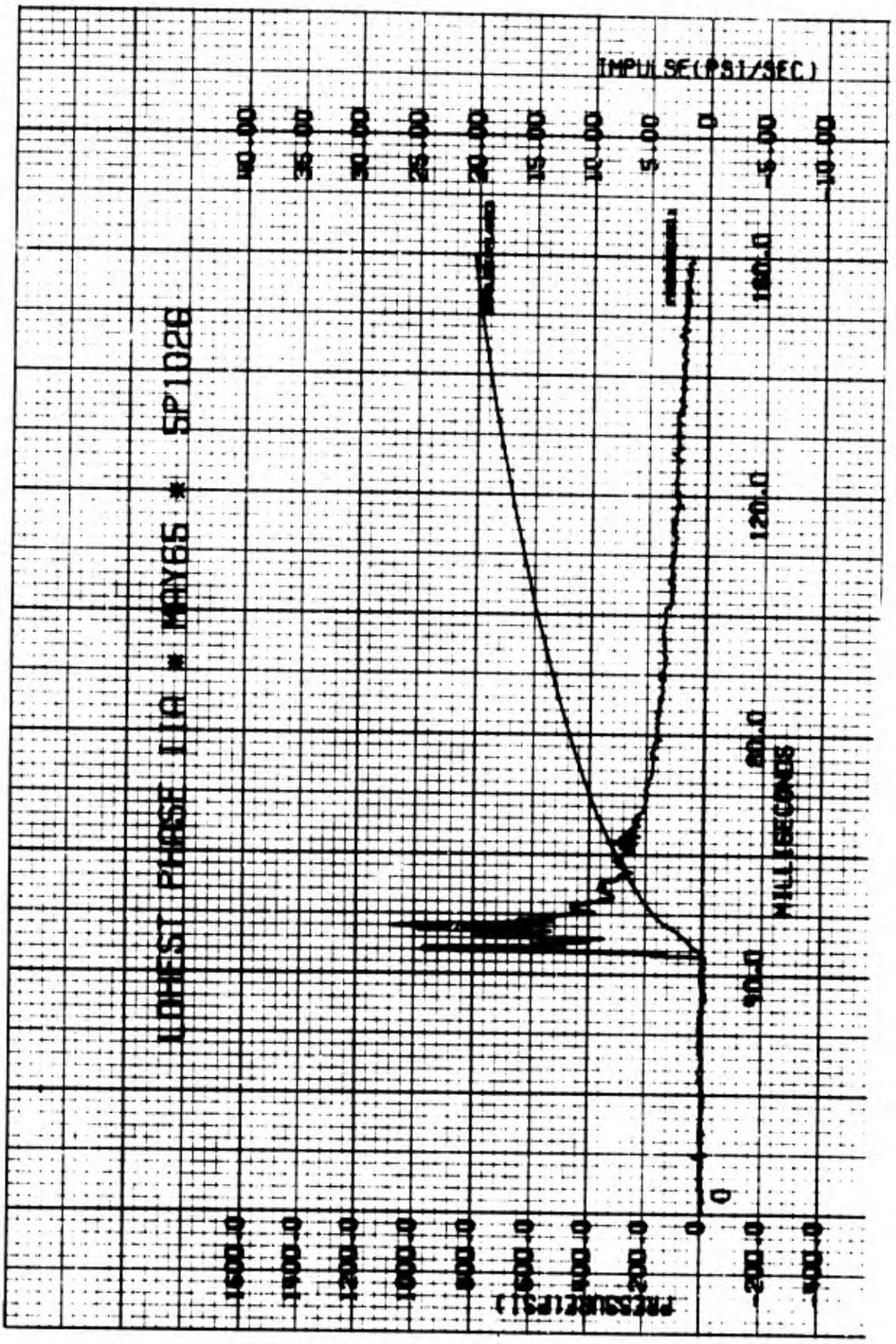

Figure 30. Overpressure-Time Histories

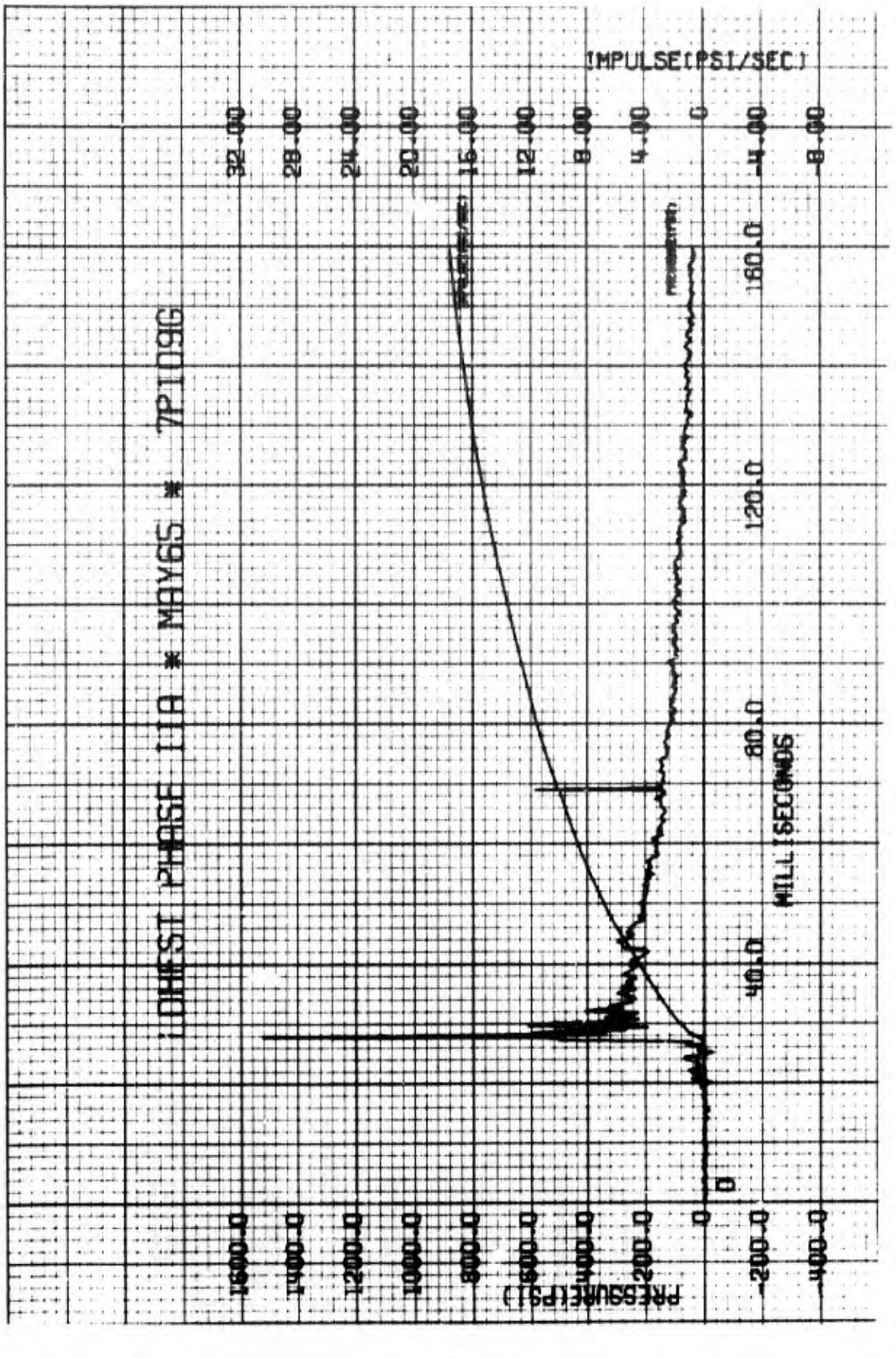

Figure 31. Overpressure-Time Histories

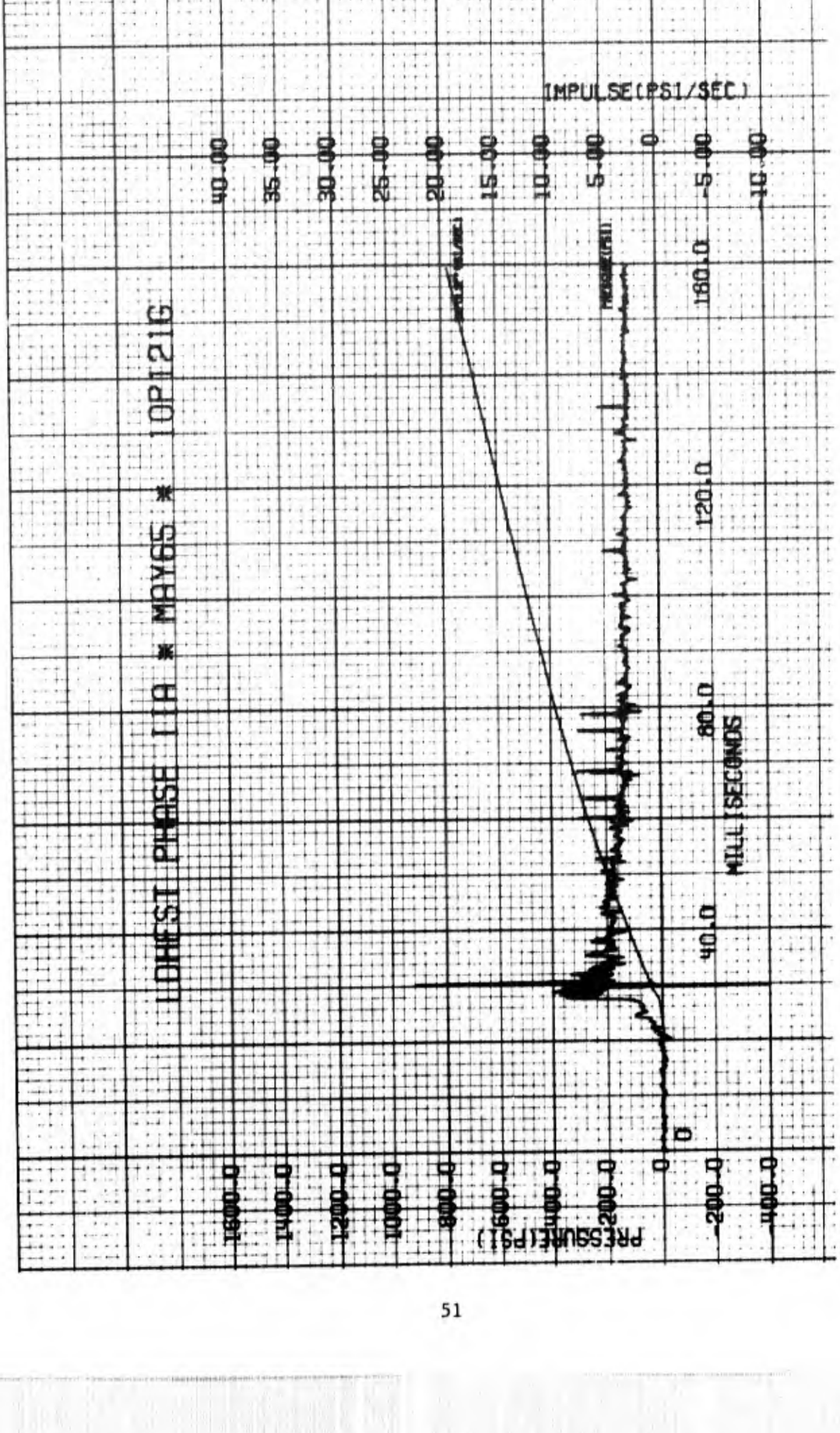

Figure 32. Overpressure-Time Histories

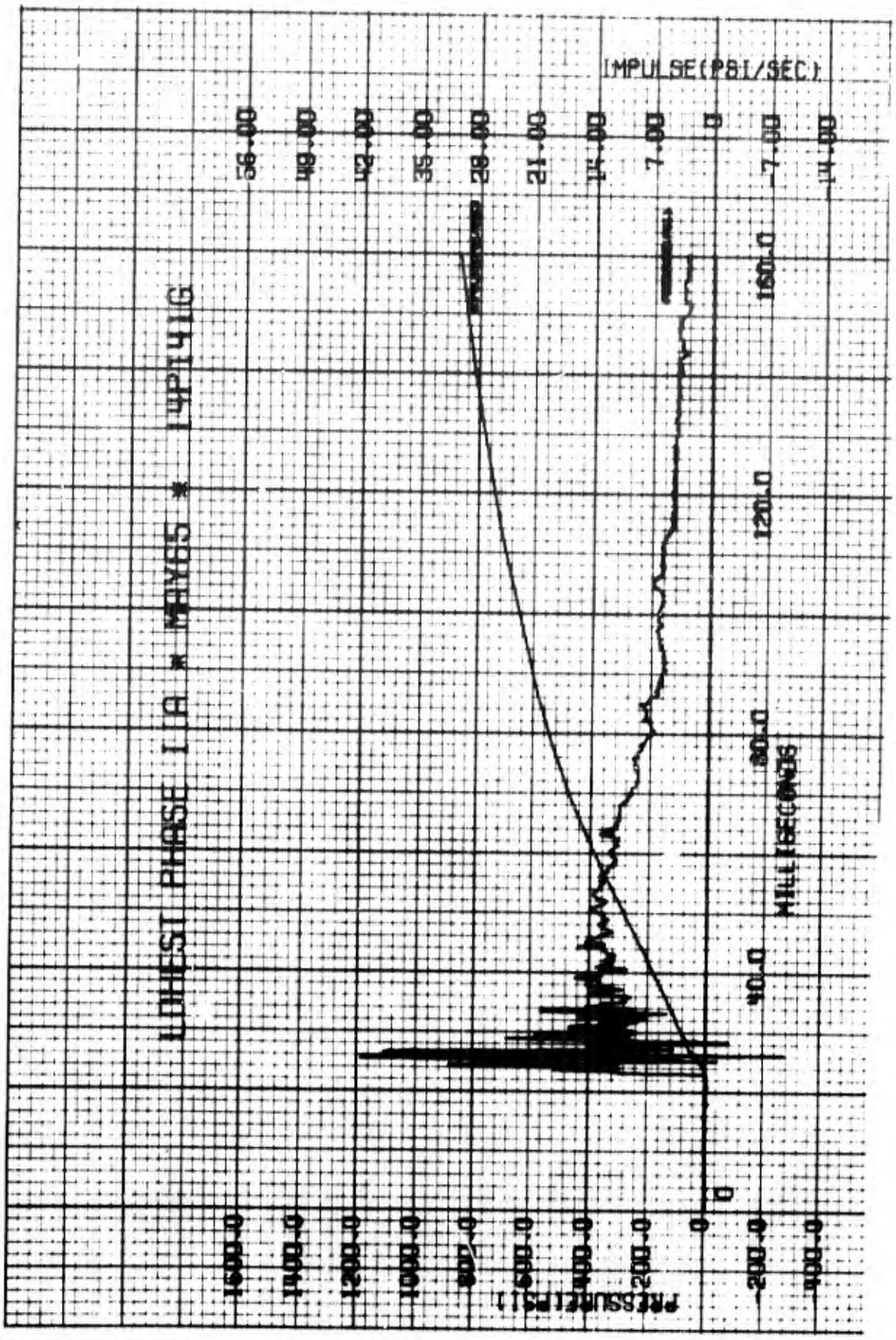

Figure 33. Overpressure-Time Histories

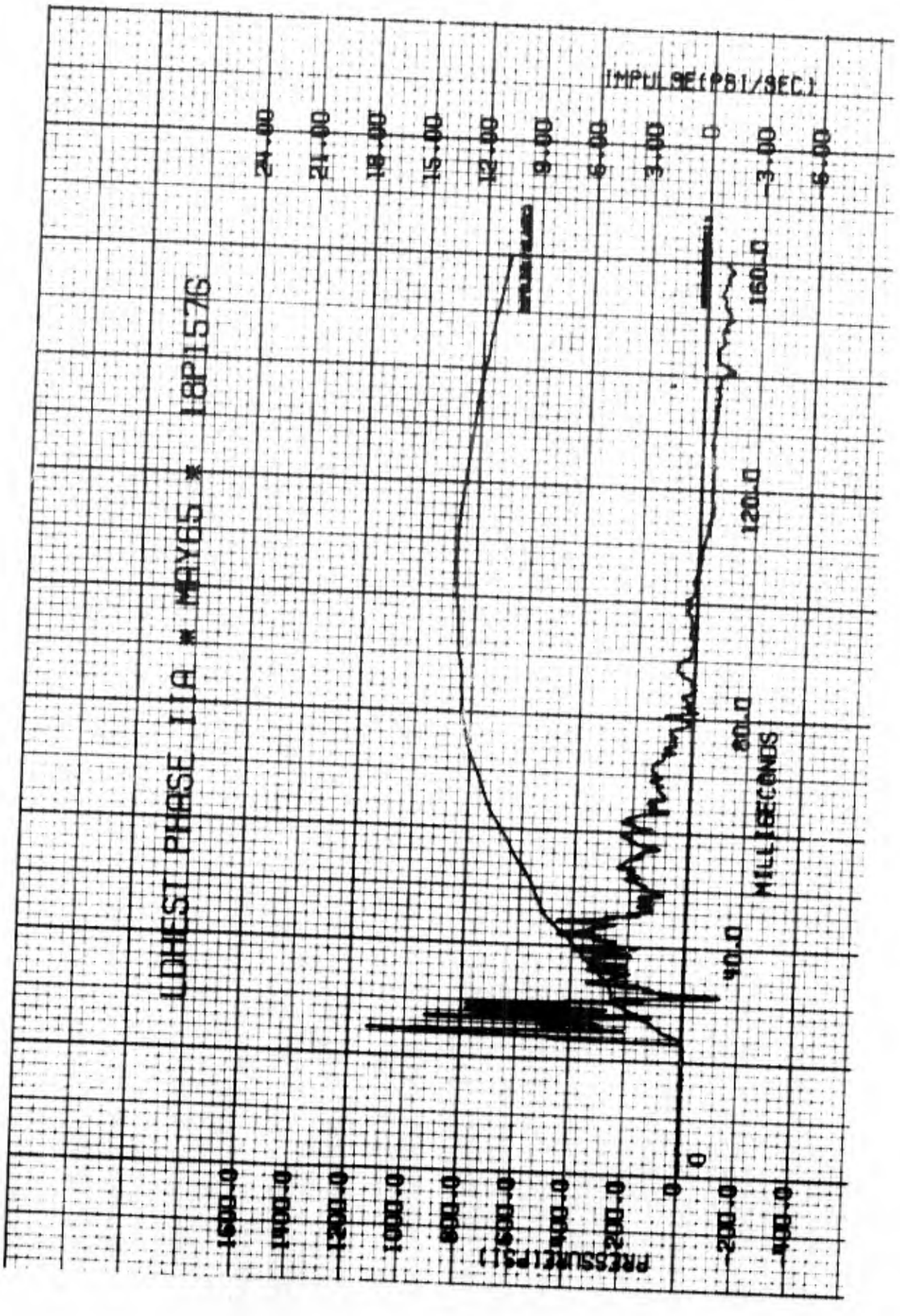

Figure 34. Overpressure-Time Histories

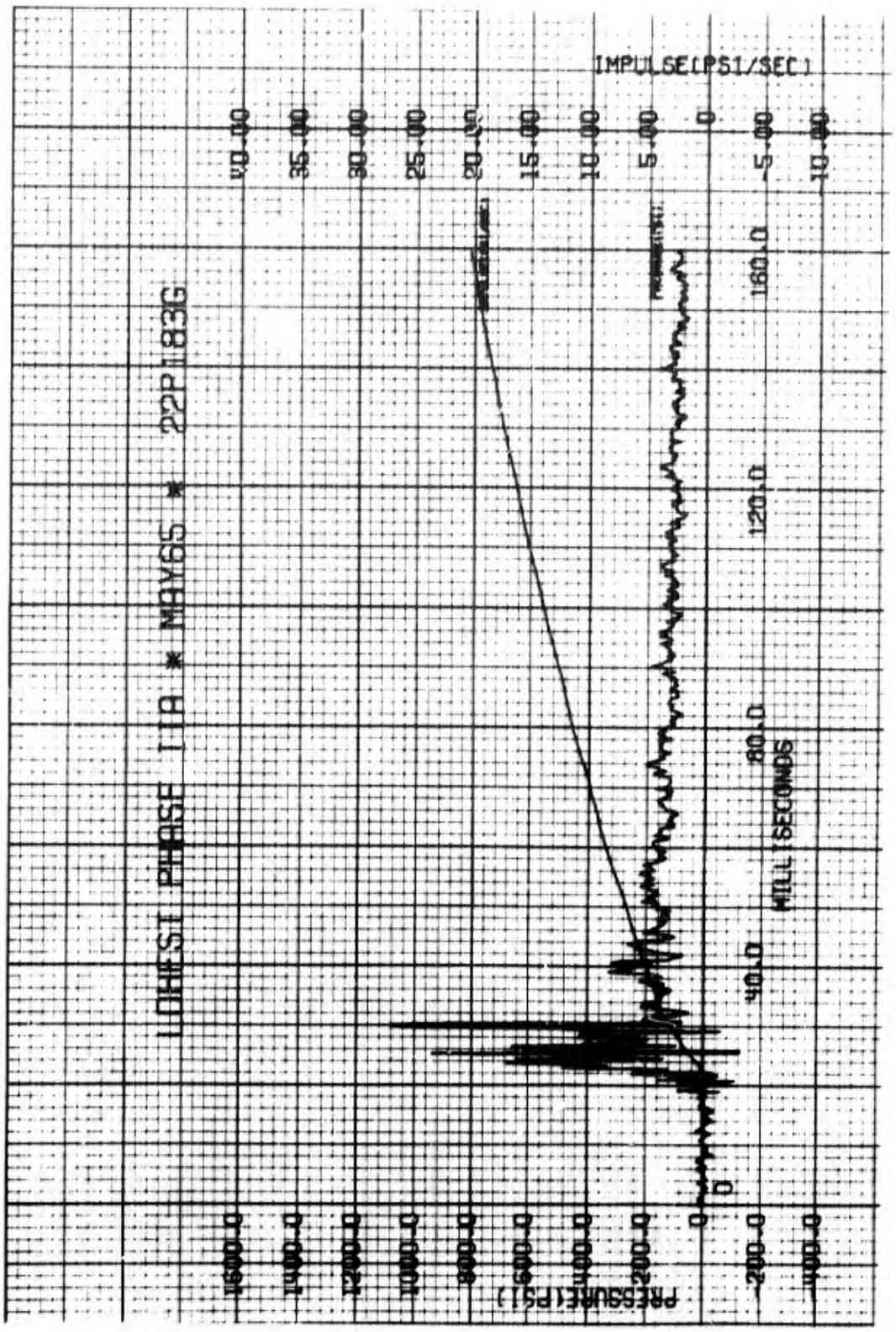

Figure 35. Overpressure-Time Histories

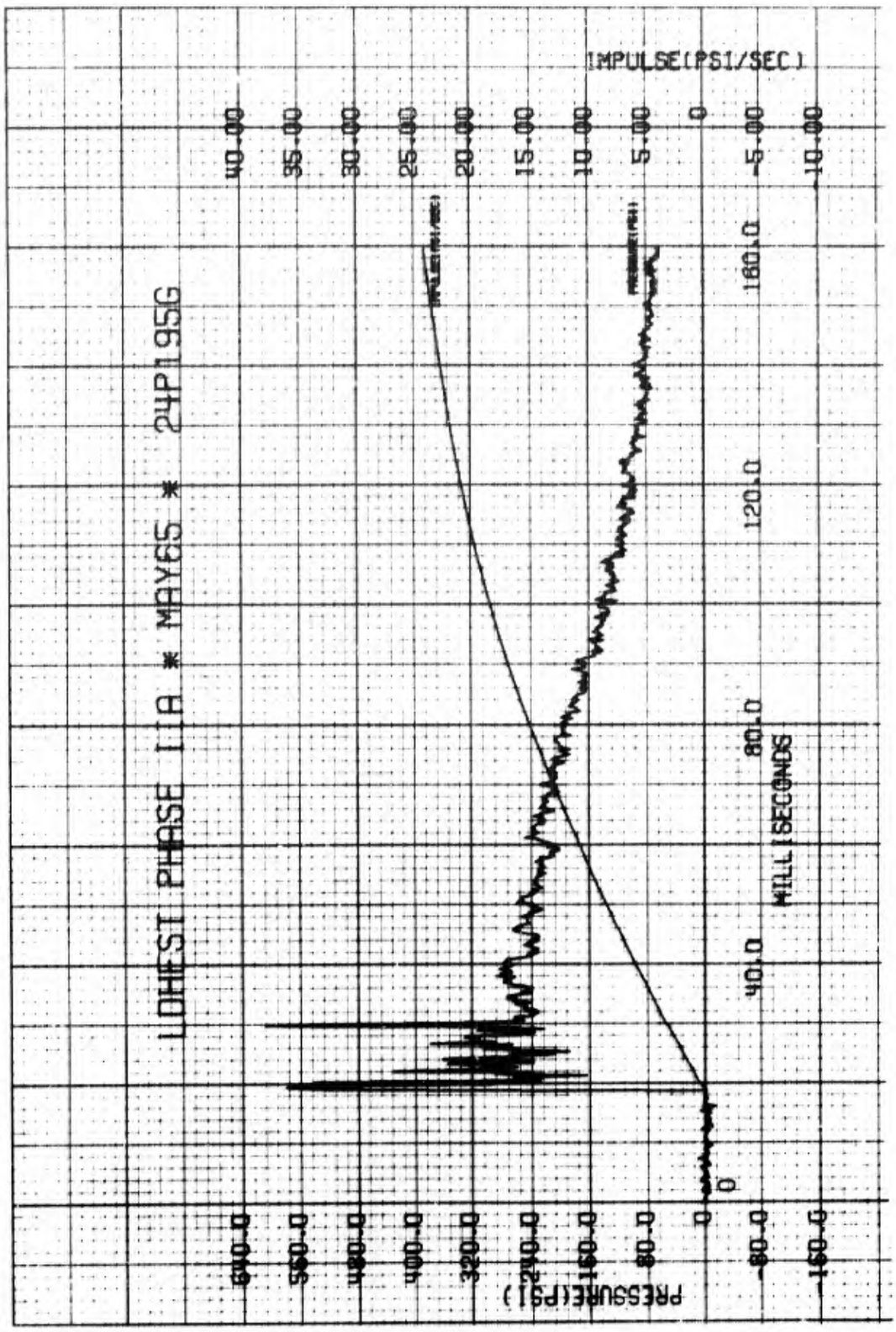

Figure 36. Overpressure-Time Histories

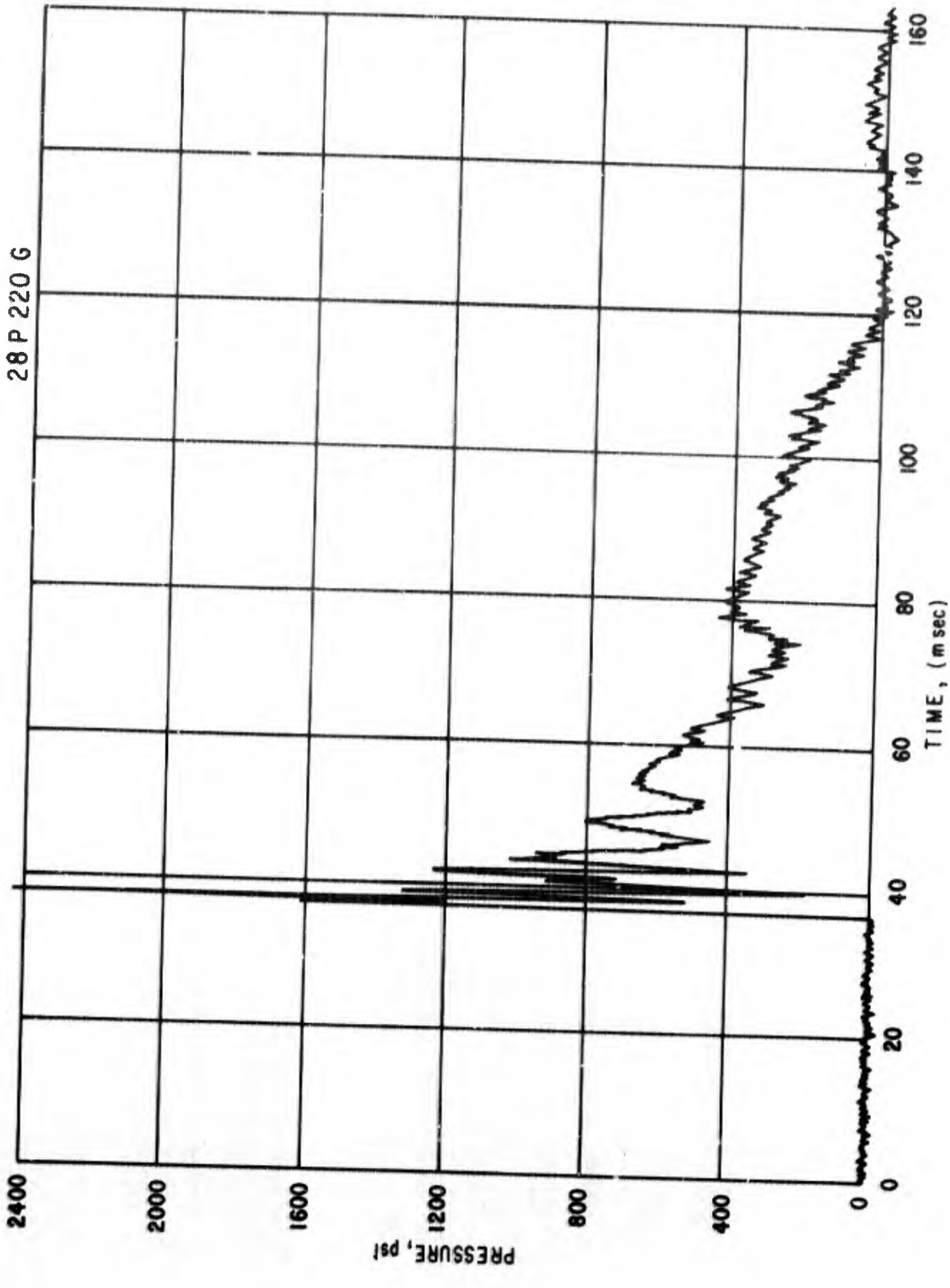

Figure 37. Overpressure-Time Histories

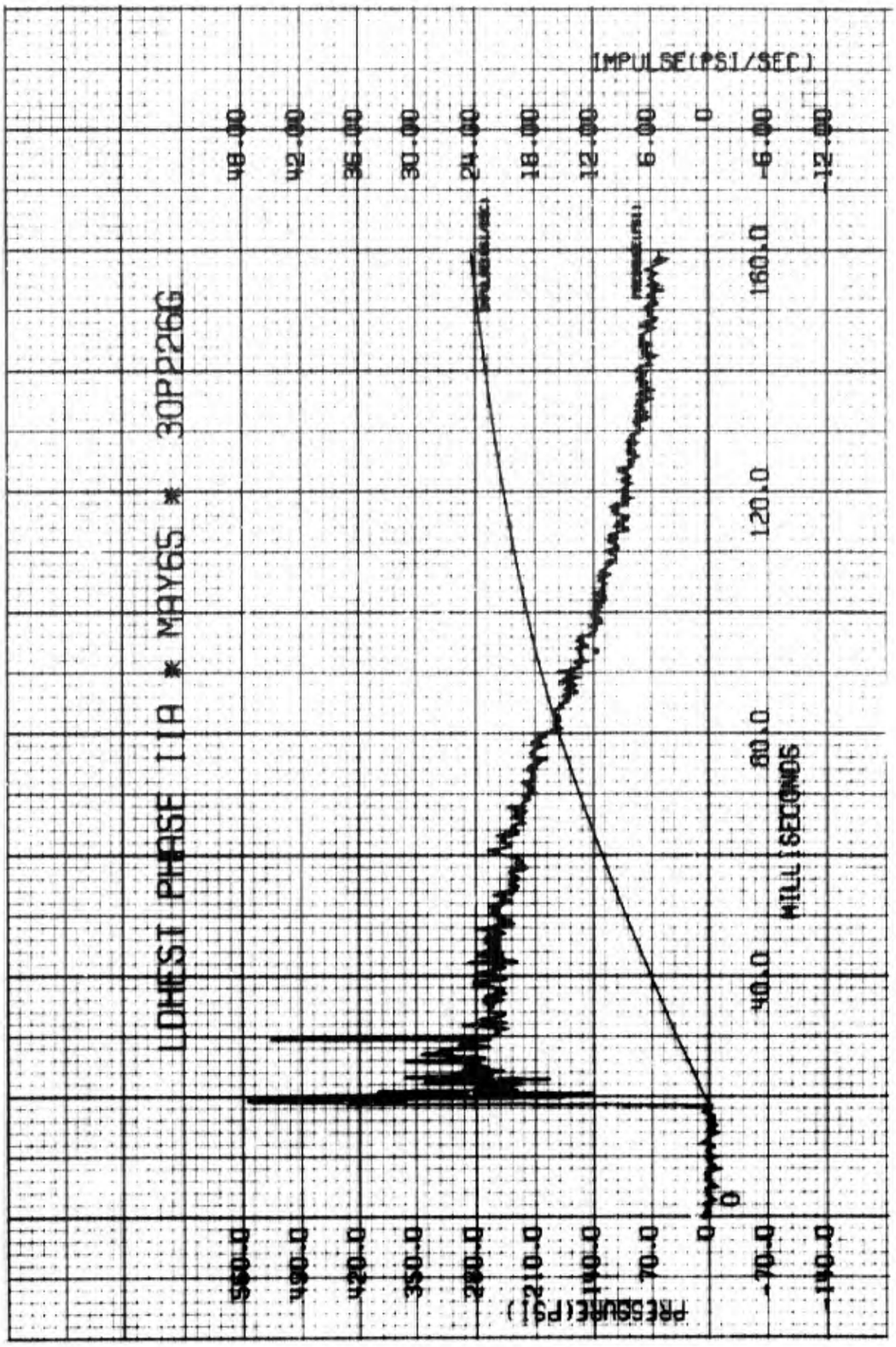

Figure 38. Overpressure-Time Histories

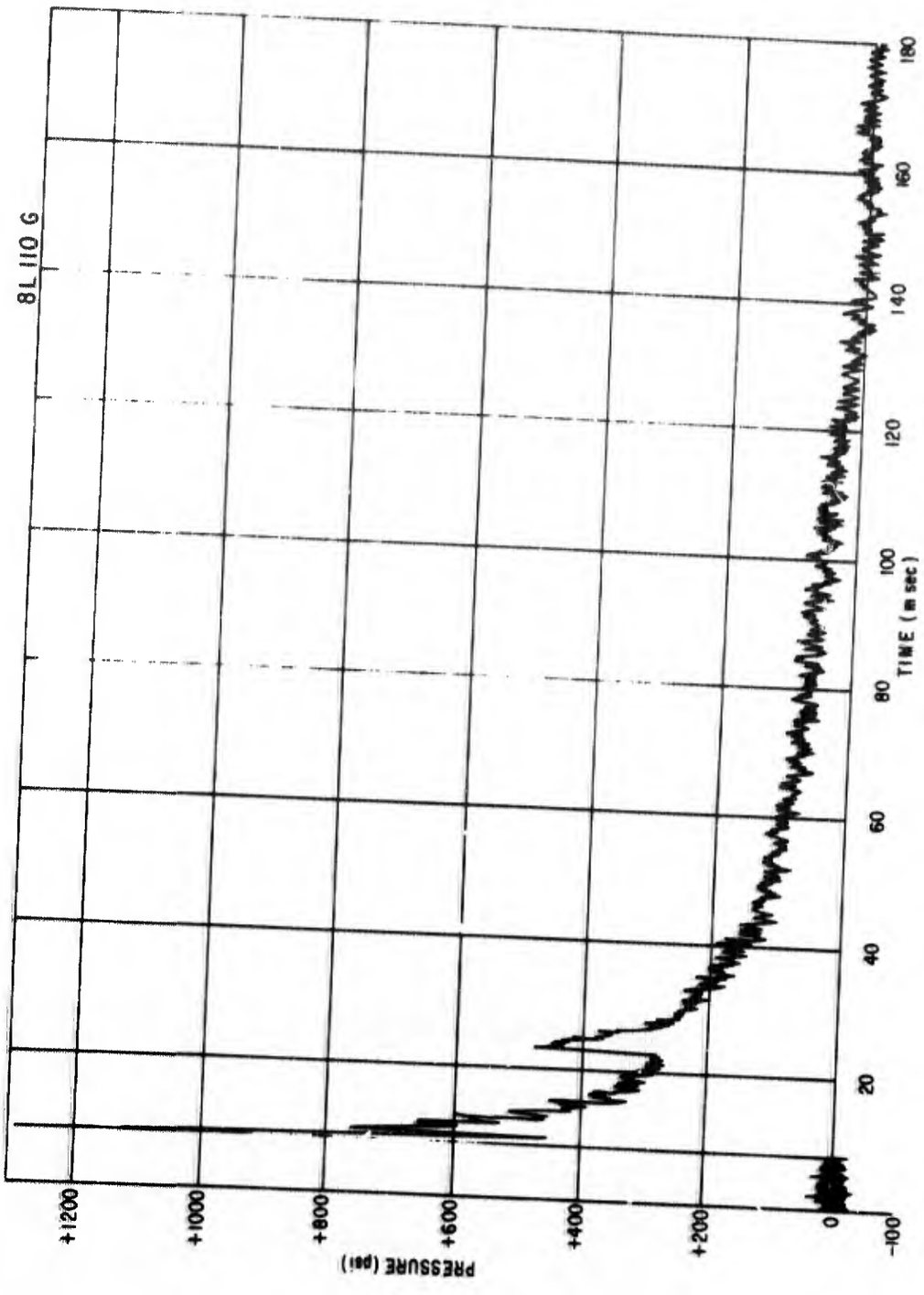

Figure 39. Near Surface Soil Stress

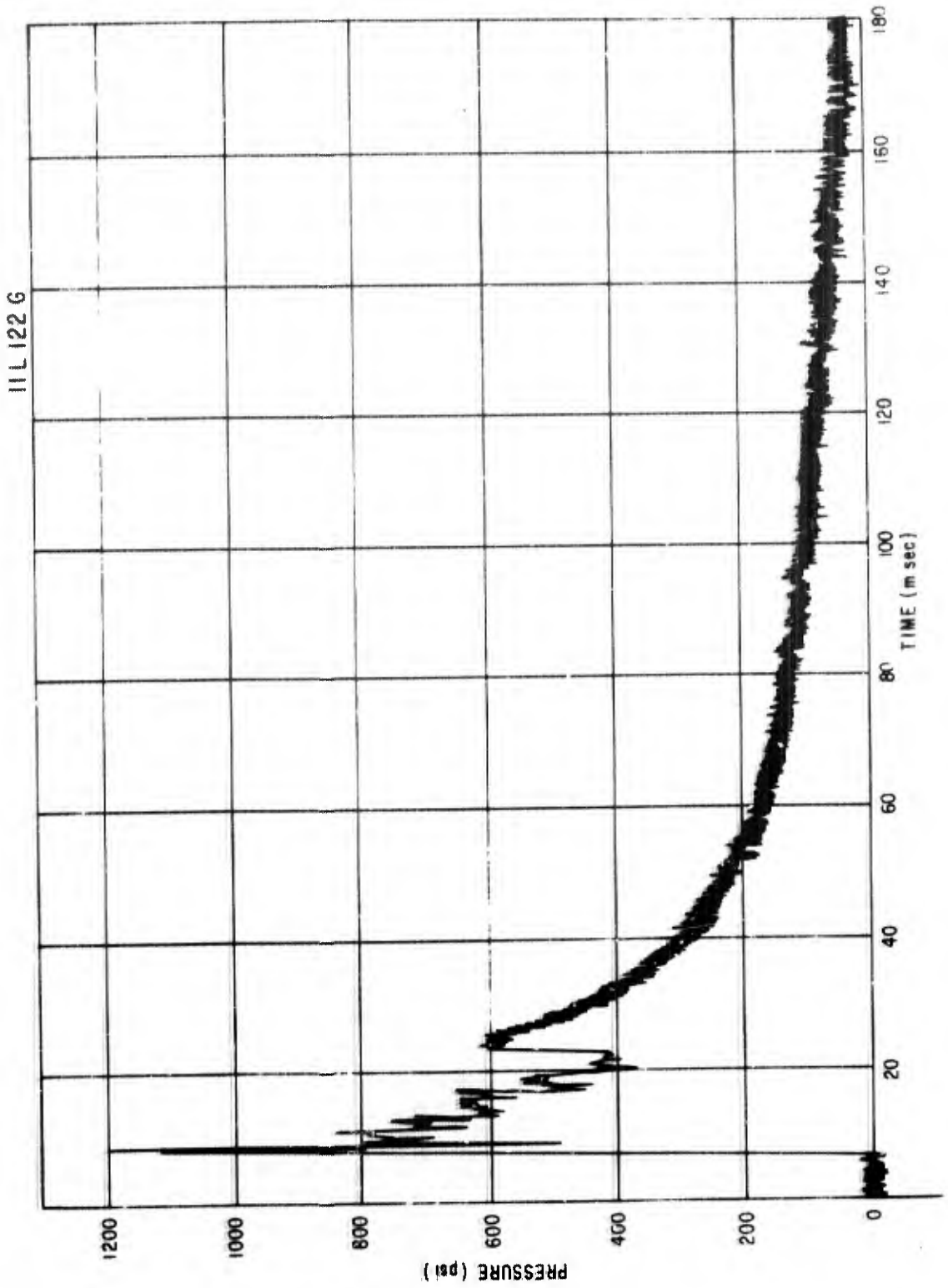

Figure 40. Near Surface Soil Stress

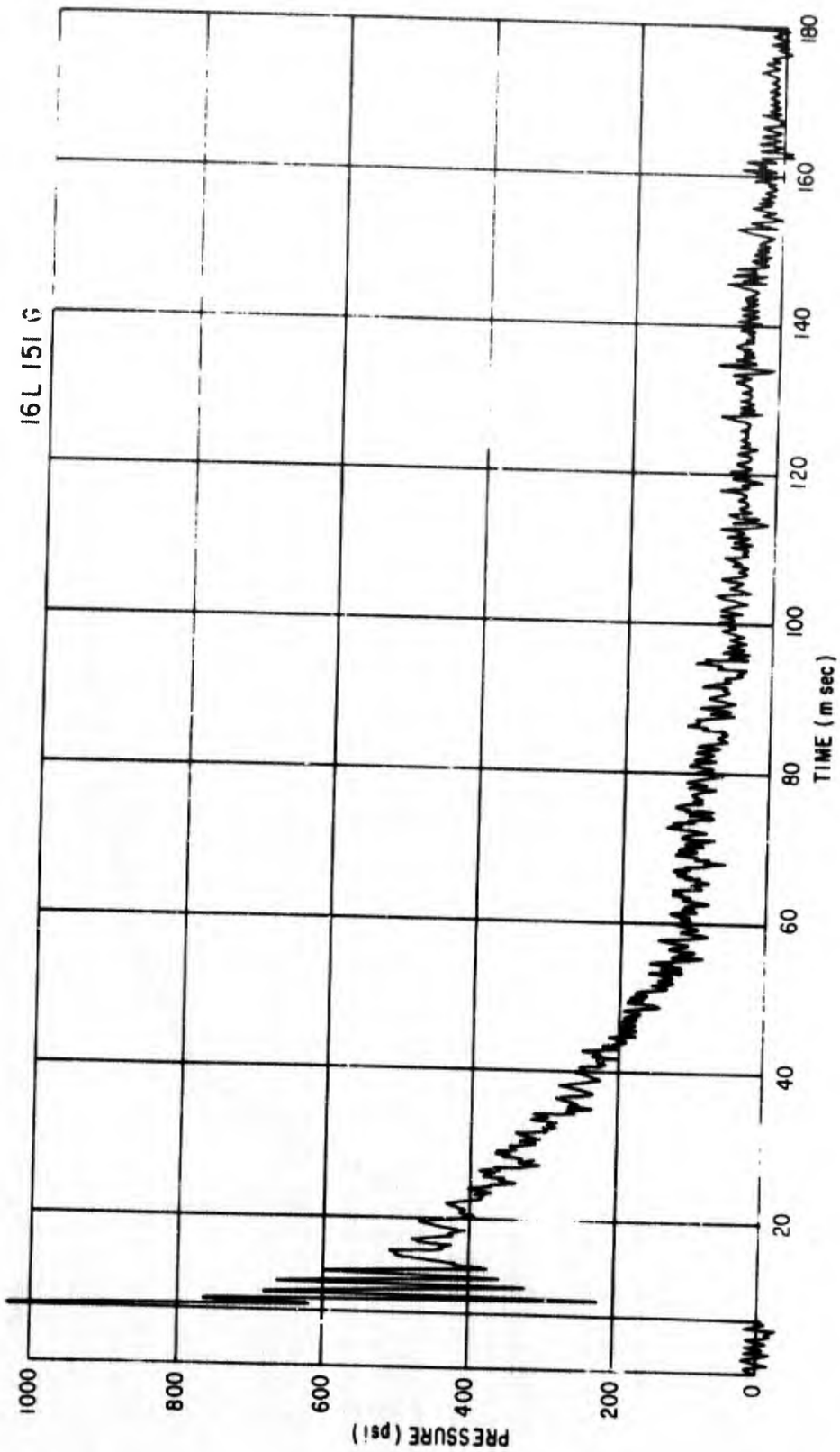

Figure 41. Near Surface Soil Stress

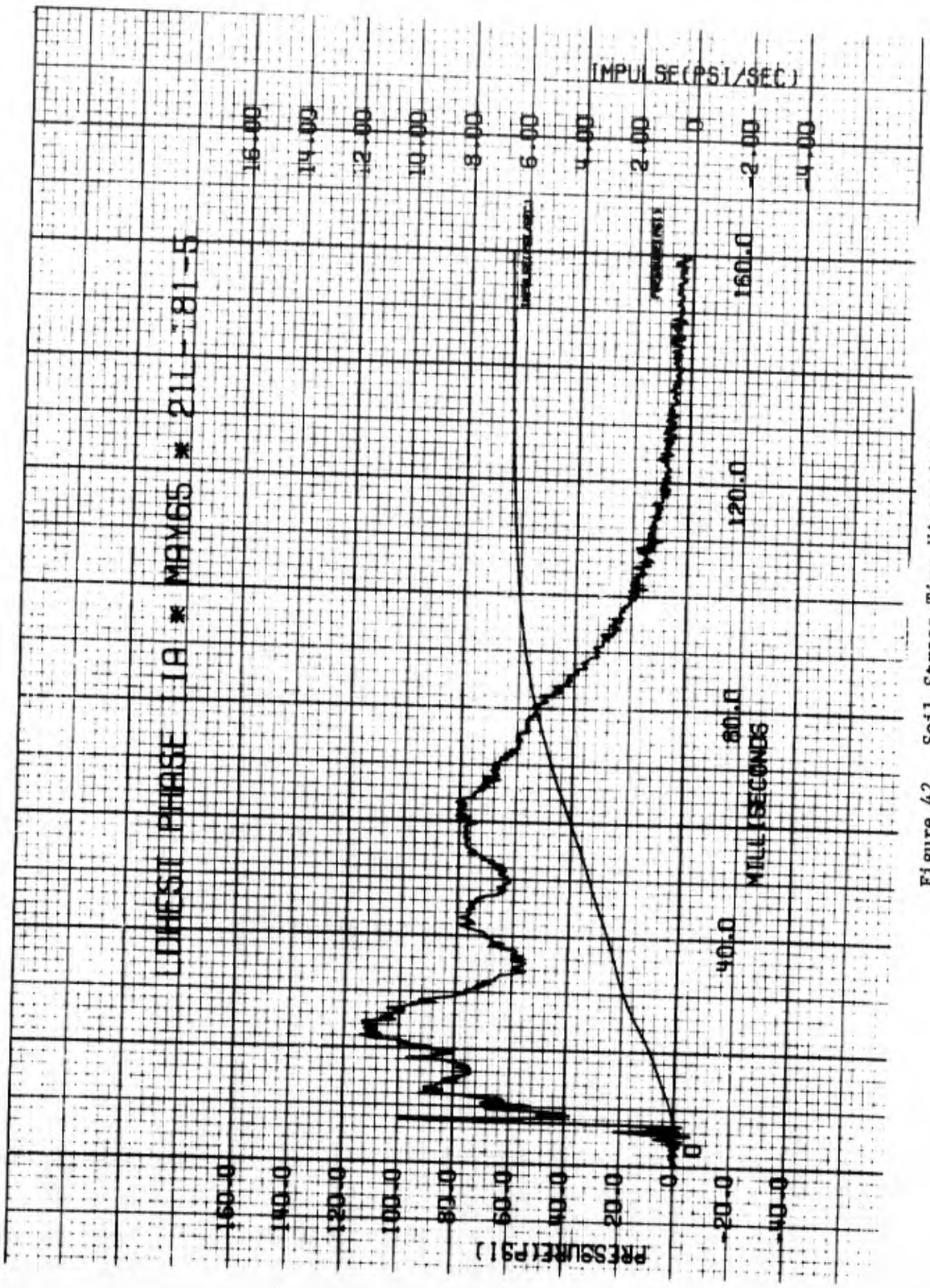

Figure 42. Soil Stress-Time Histories

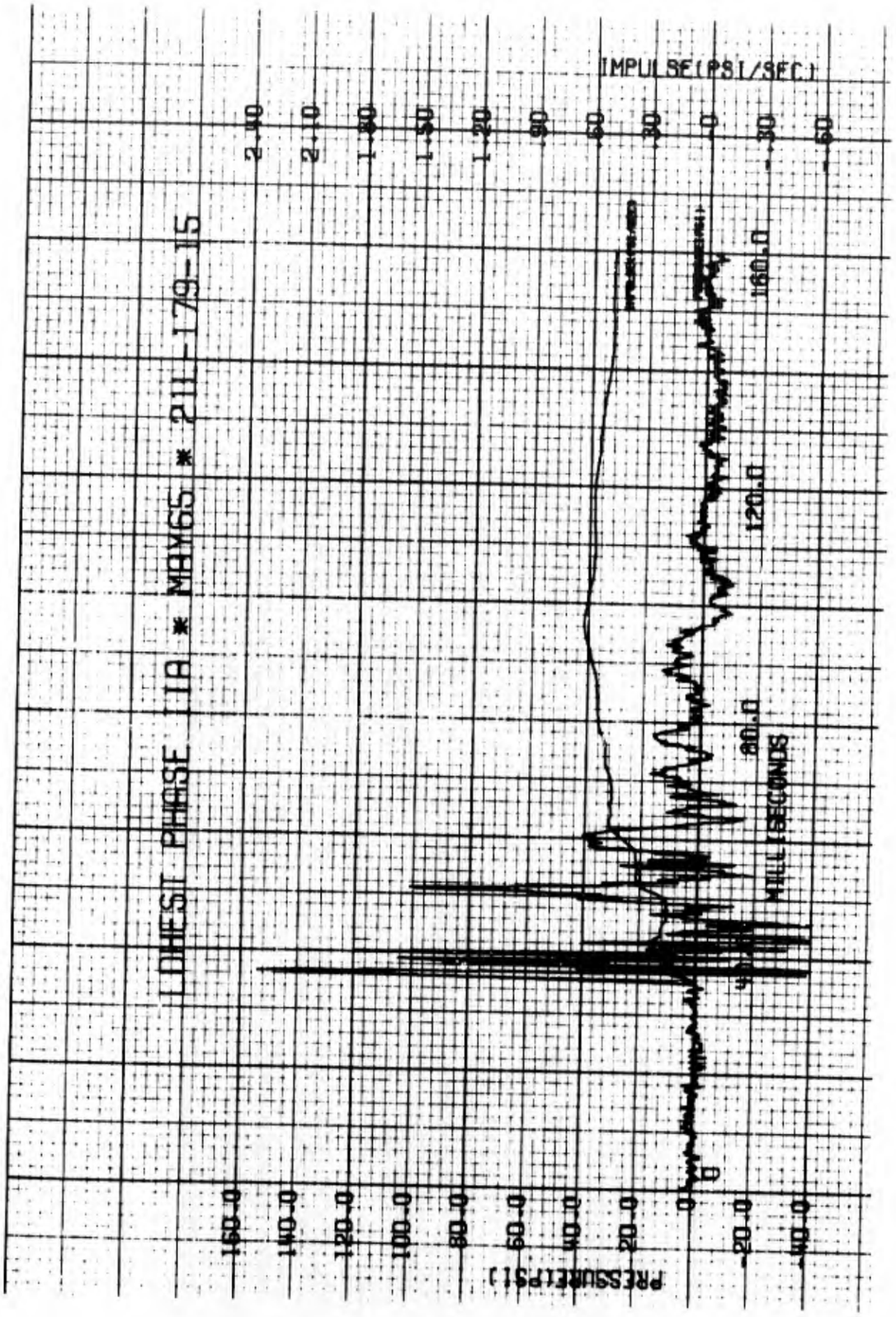

Figure 43. Soil Stress-Time Histories

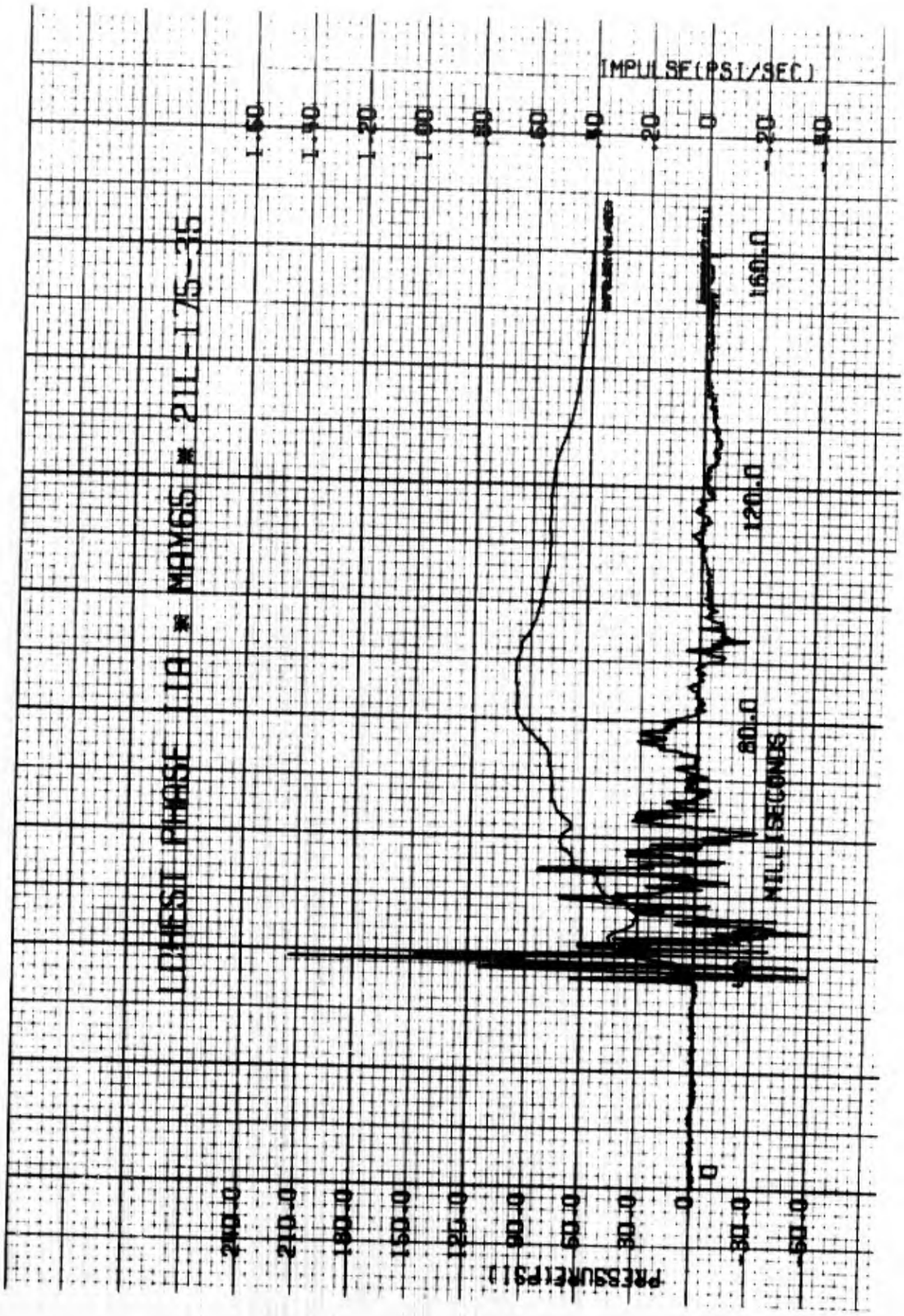

Figure 44. Soil Stress-Time Histories

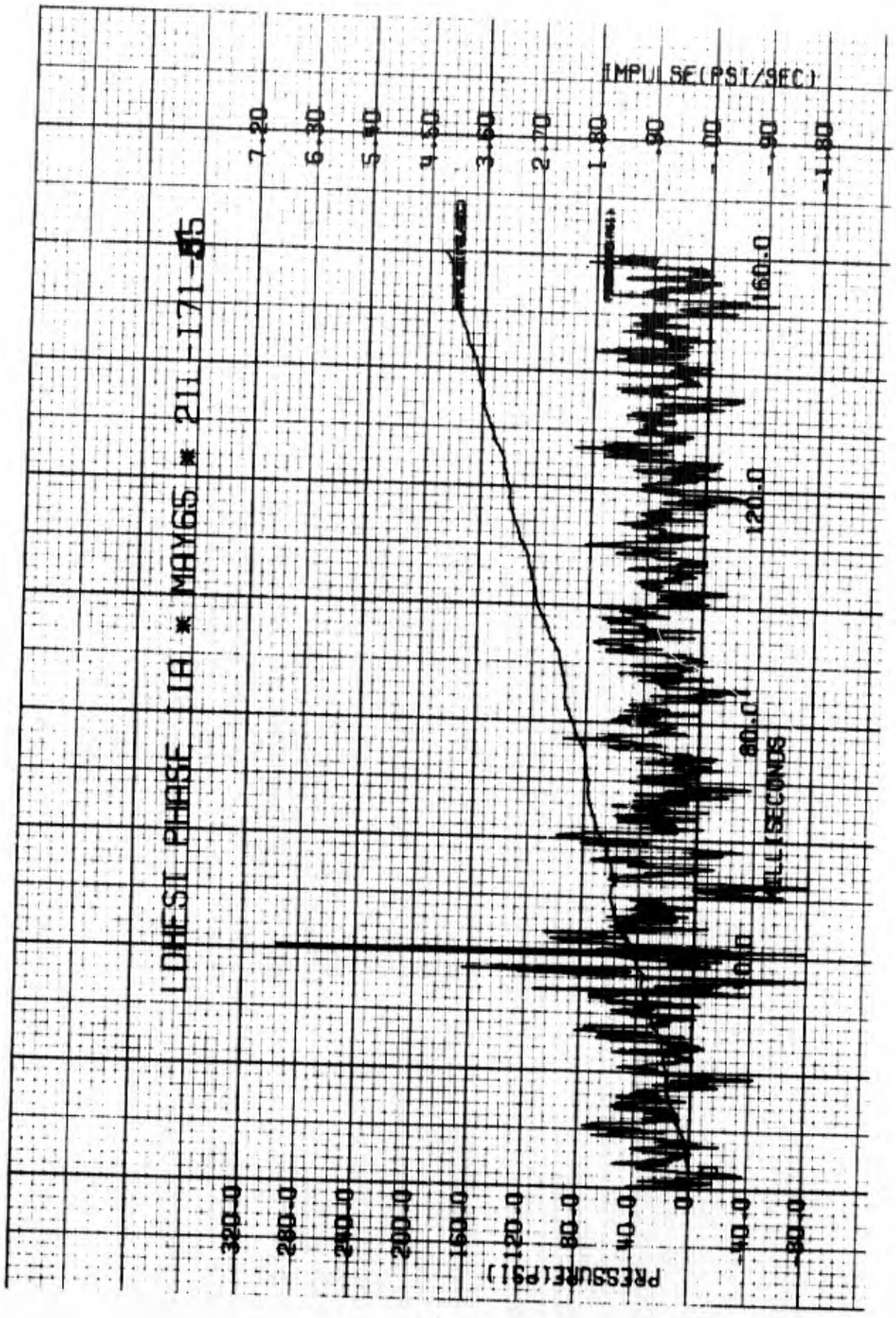

Figure 45. Soil Stress-Time Histories

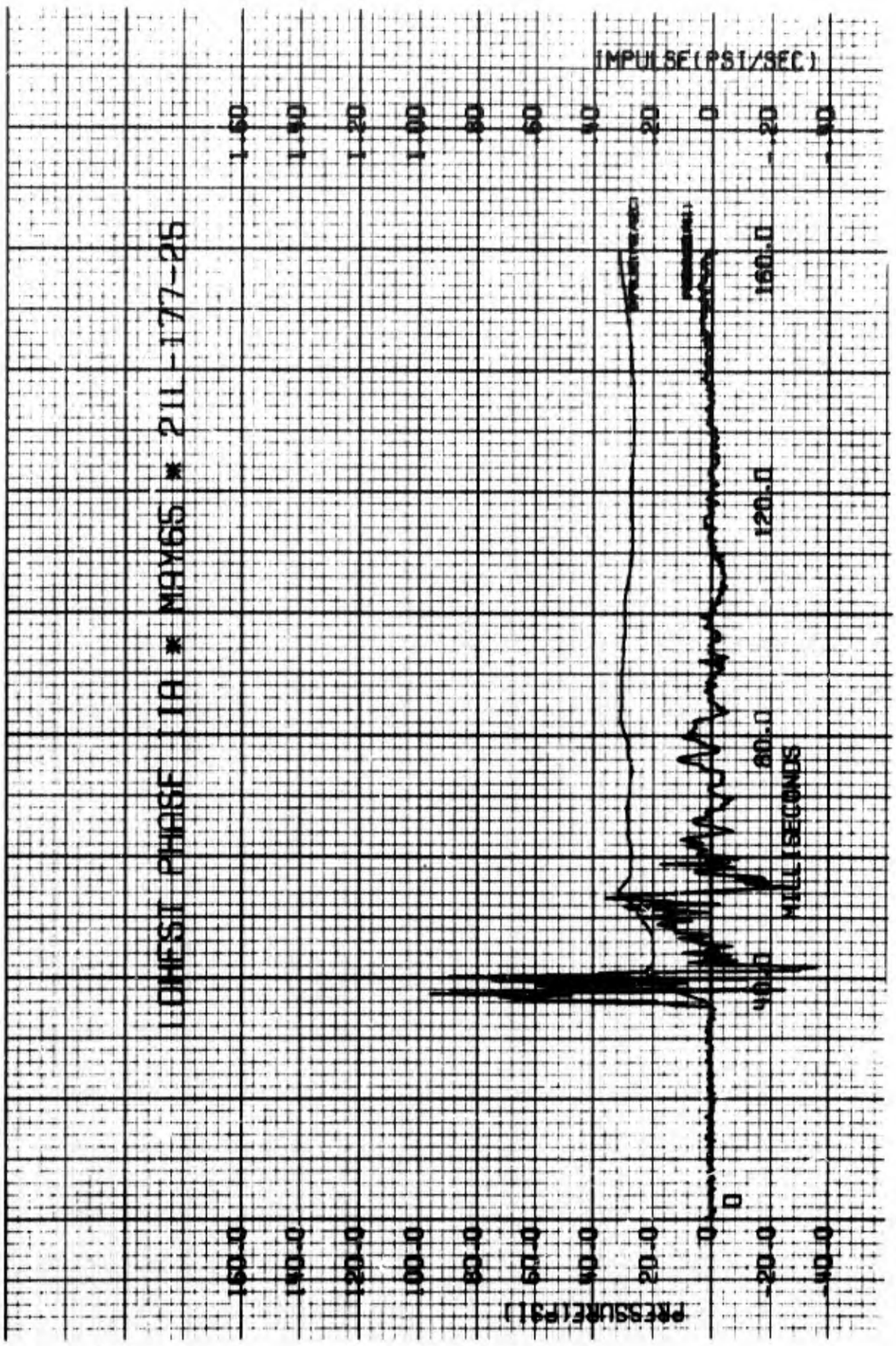

Figure 46. Soil Stress-Time Histories

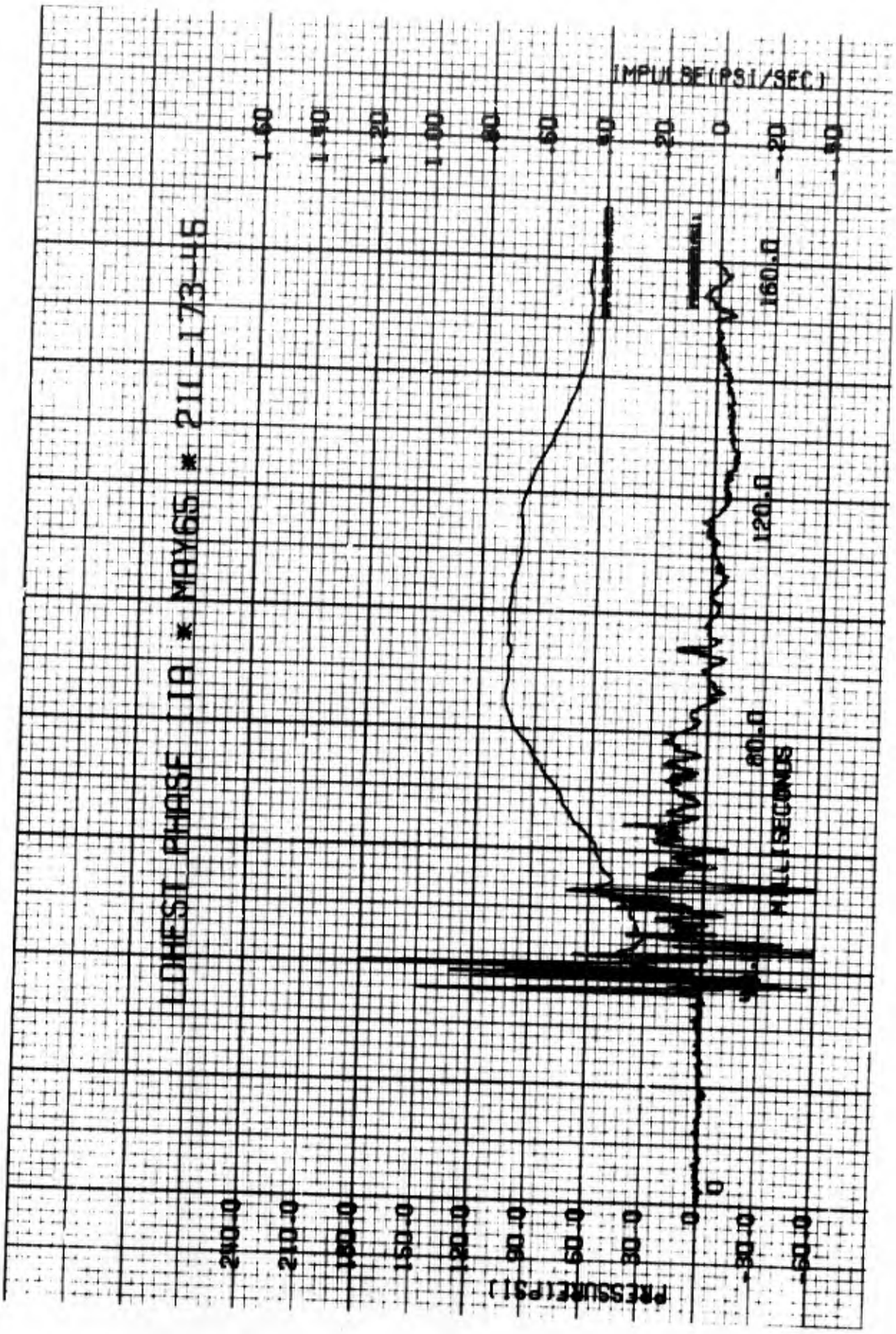

Figure 47. Soil Stress-Time Histories

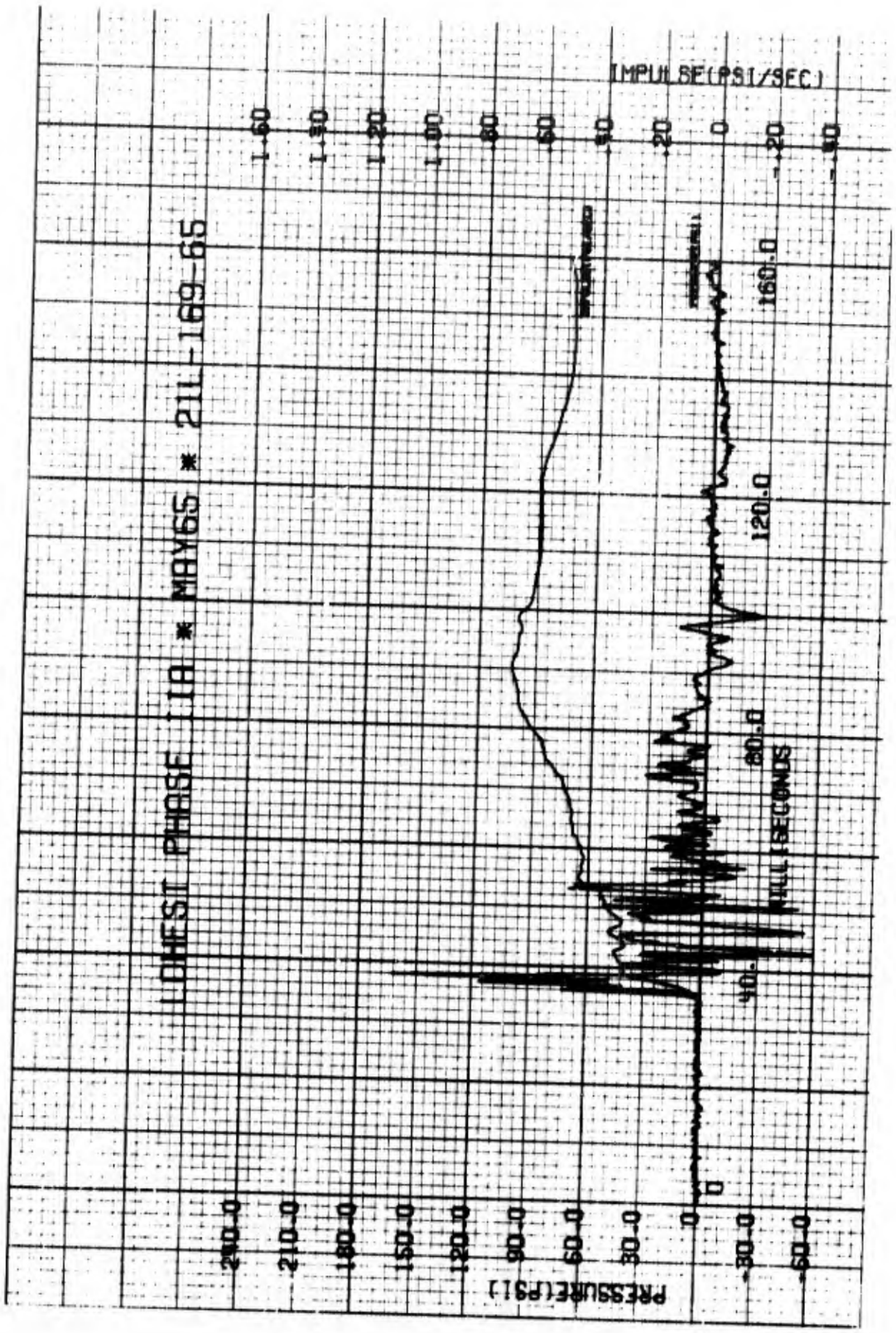

Figure 48. Soil Stress-Time Histories

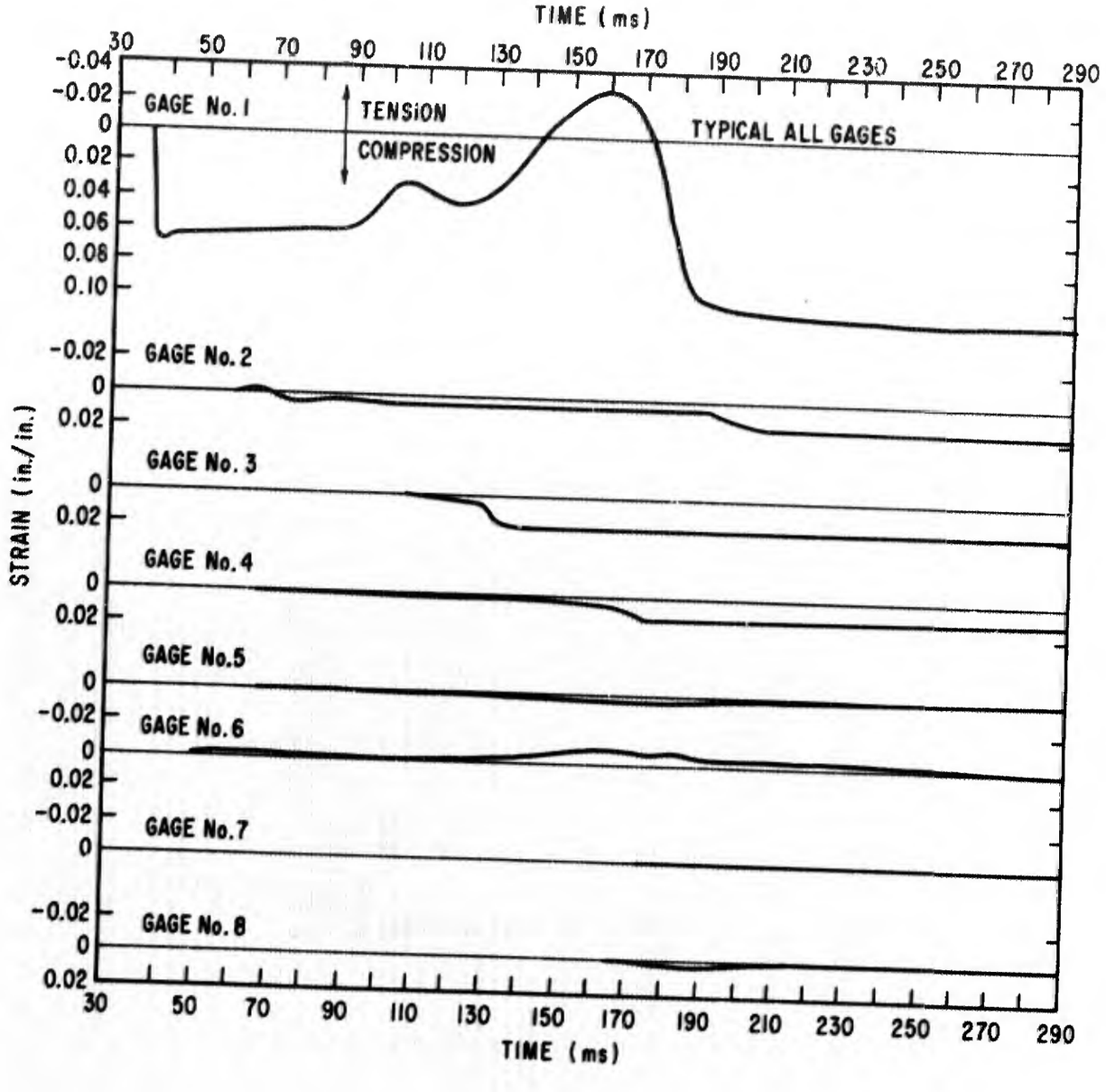

Figure 49. Strain versus Time

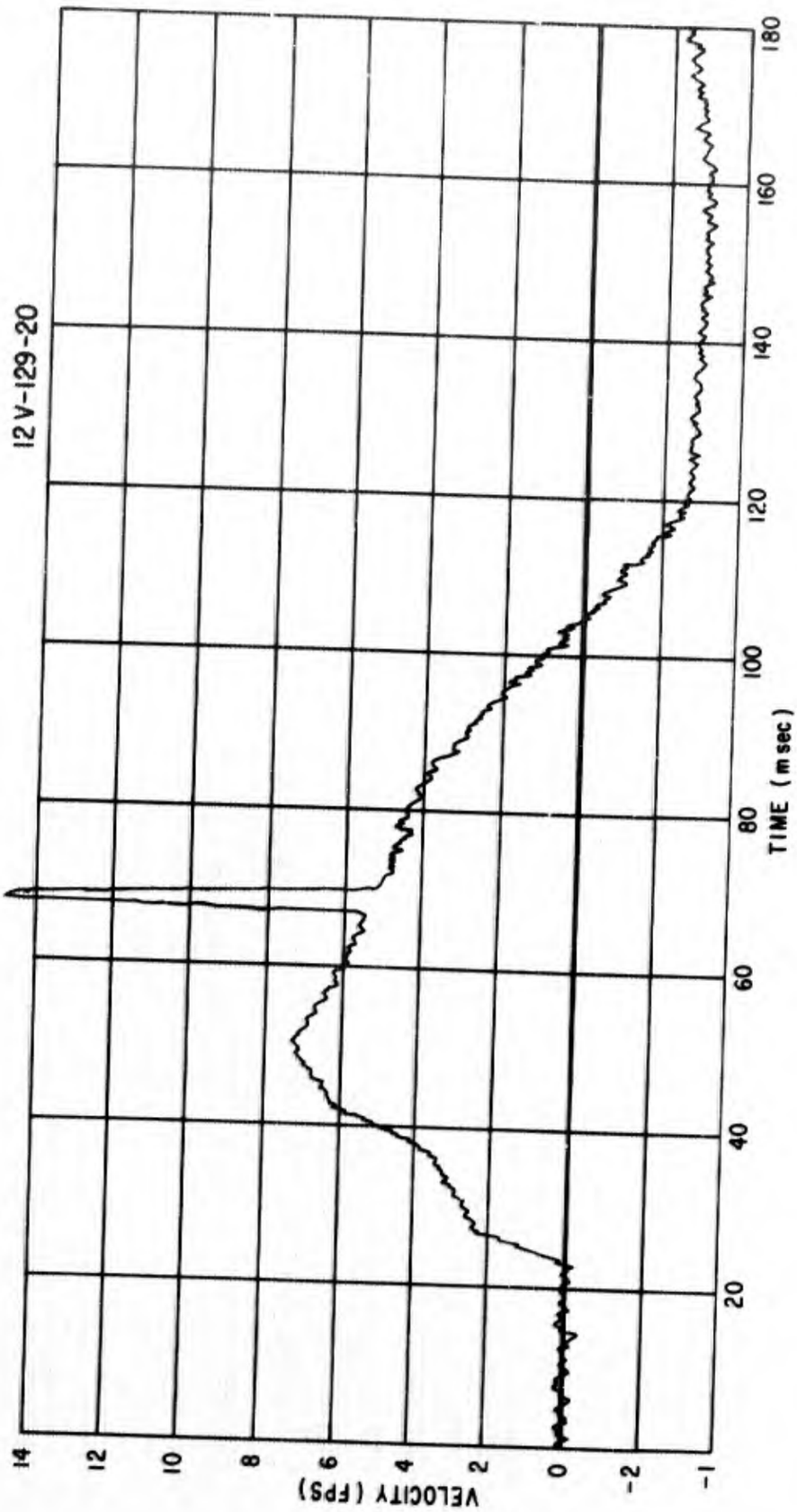

Figure 50. Particle Velocity-Time Histories

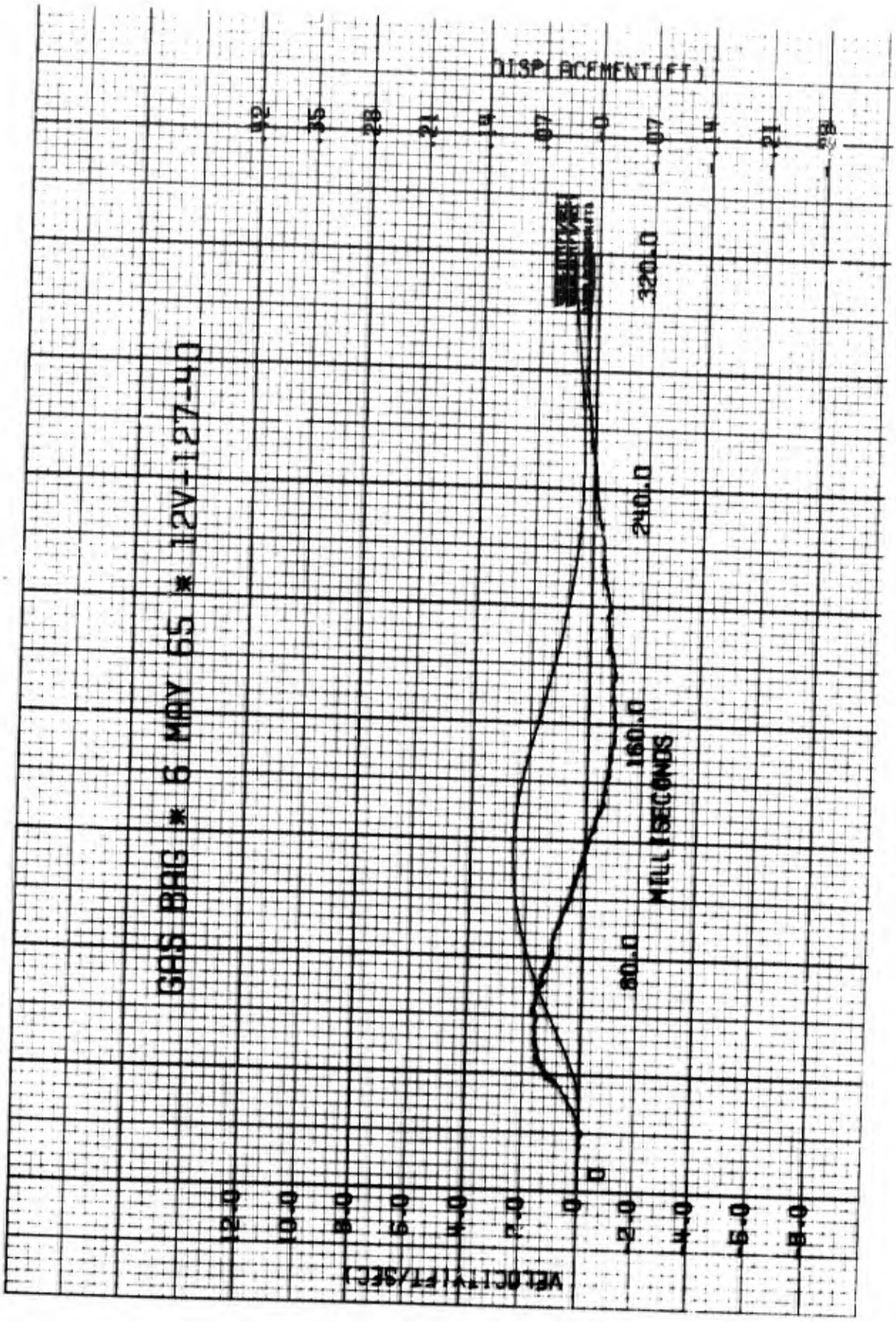

Figure 51. Particle Velocity-Time Histories

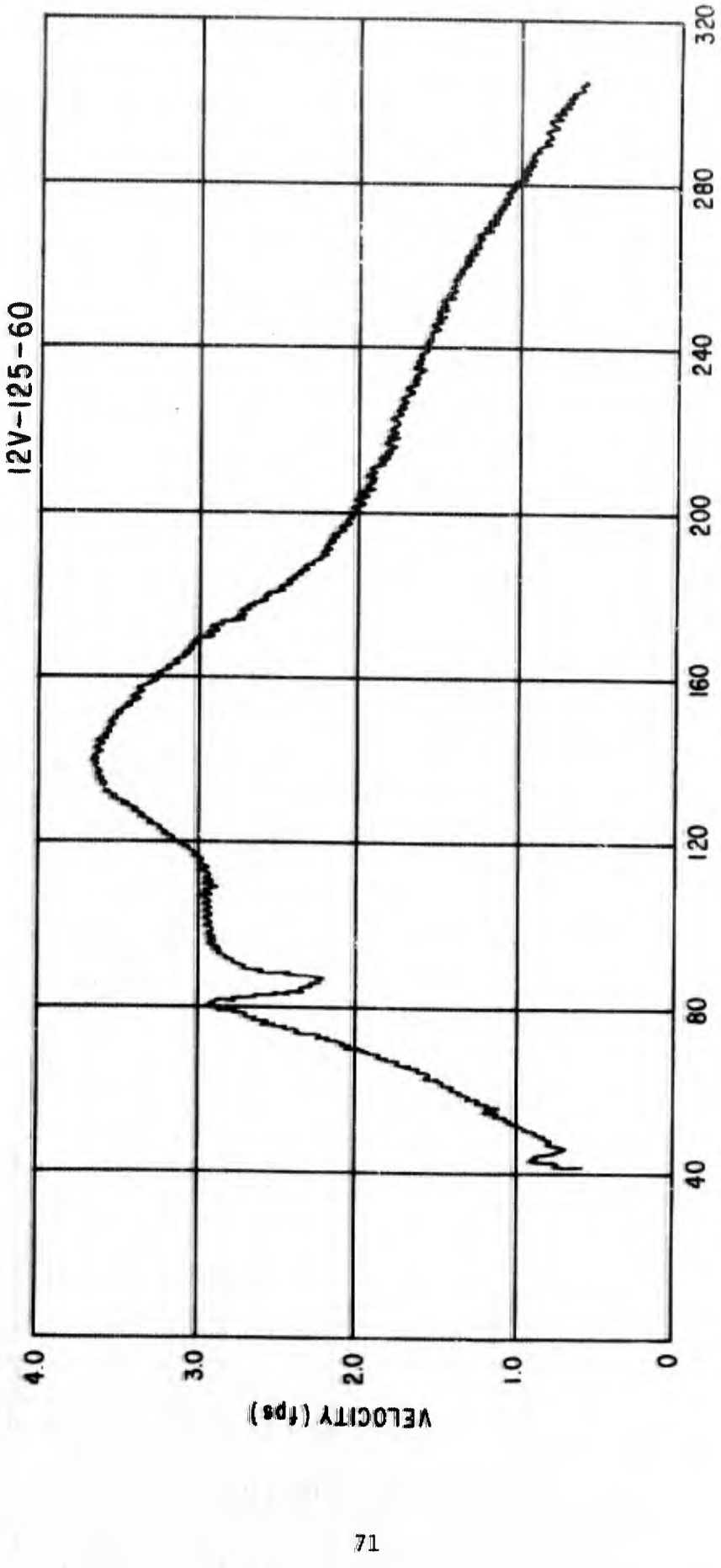

Figure 52. Particle Velocity-Time Histories

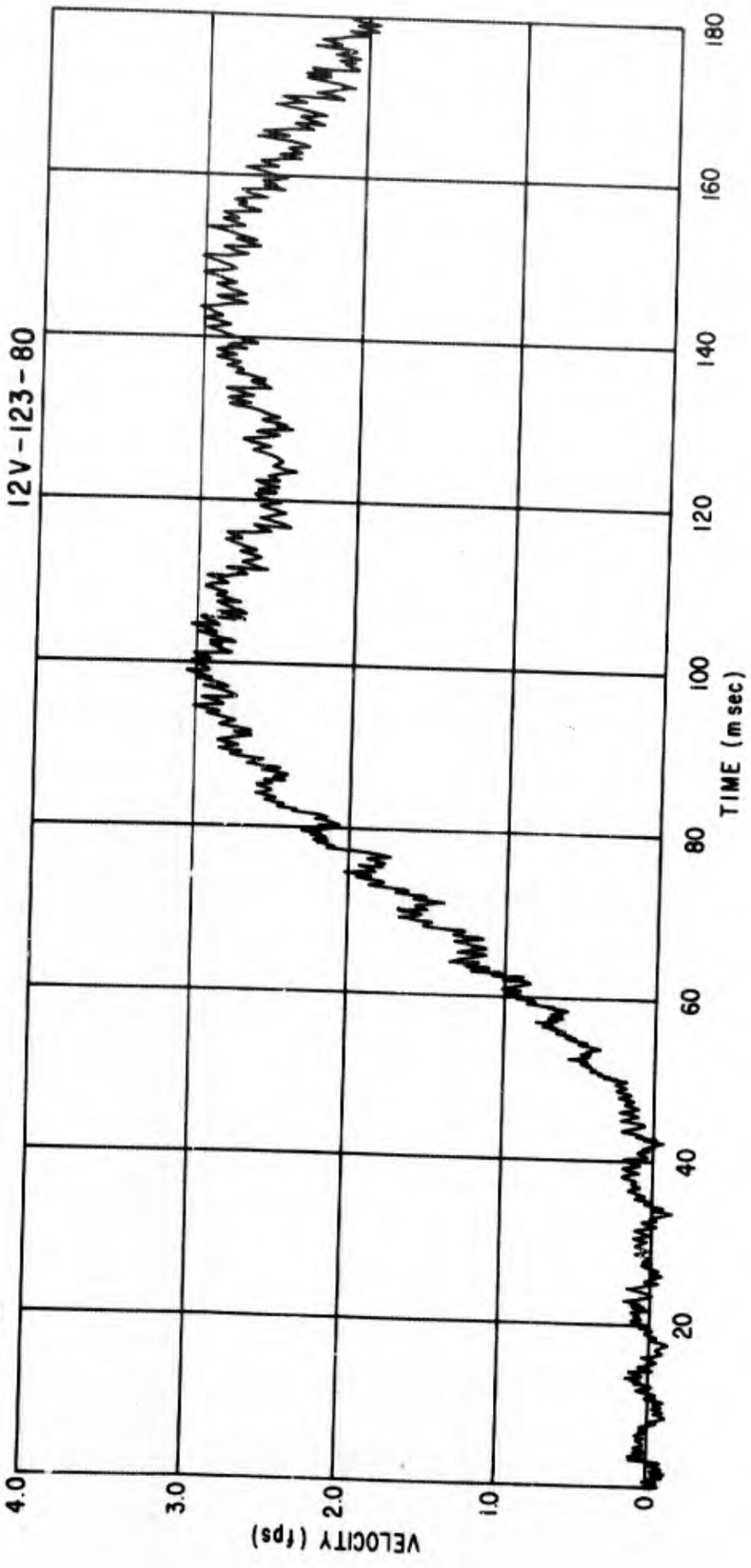

Figure 53. Particle Velocity-Time Histories

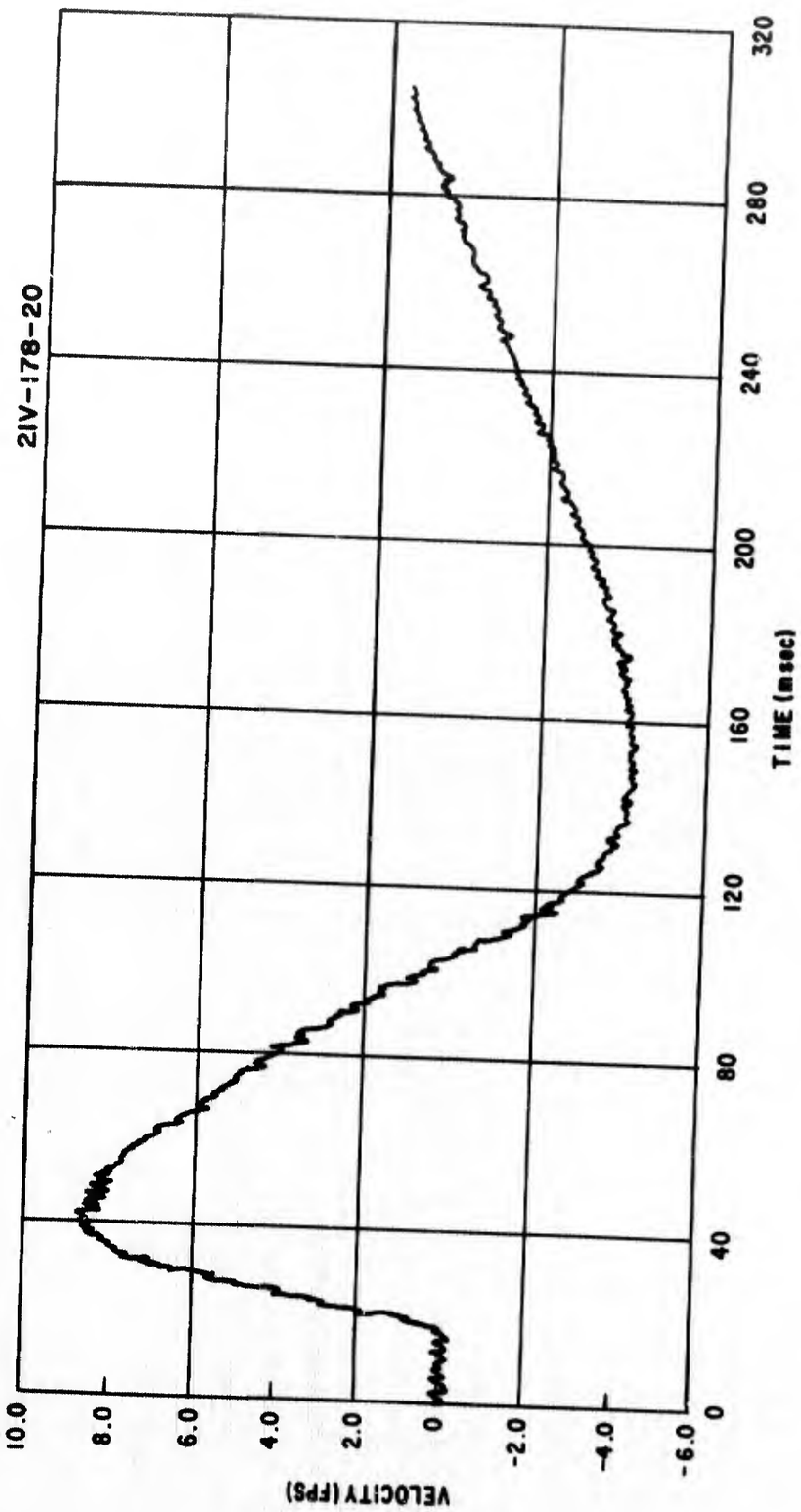

Figure 54. Particle Velocity-Time Histories

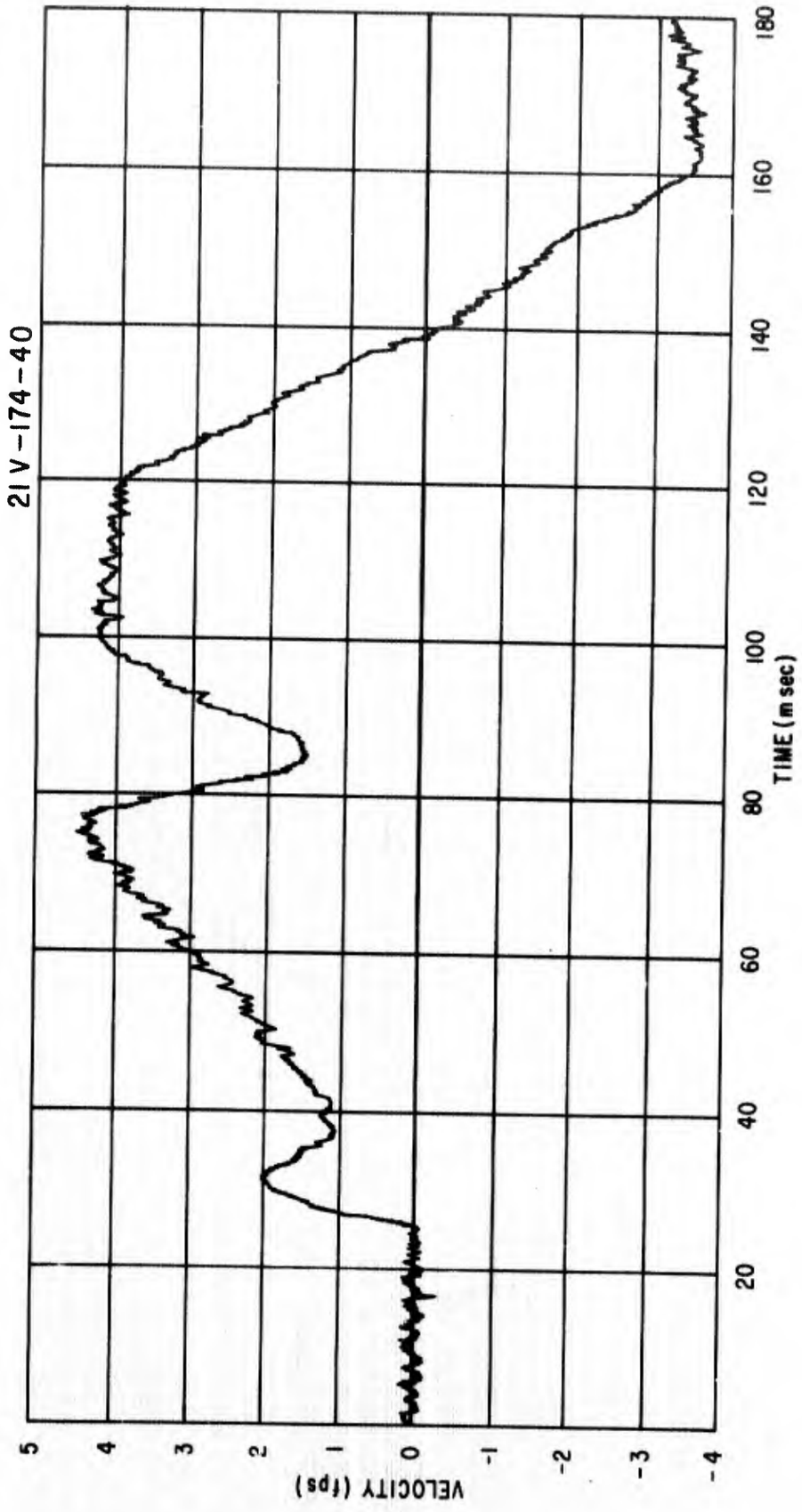

Figure 55. Particle Velocity-Time Histories

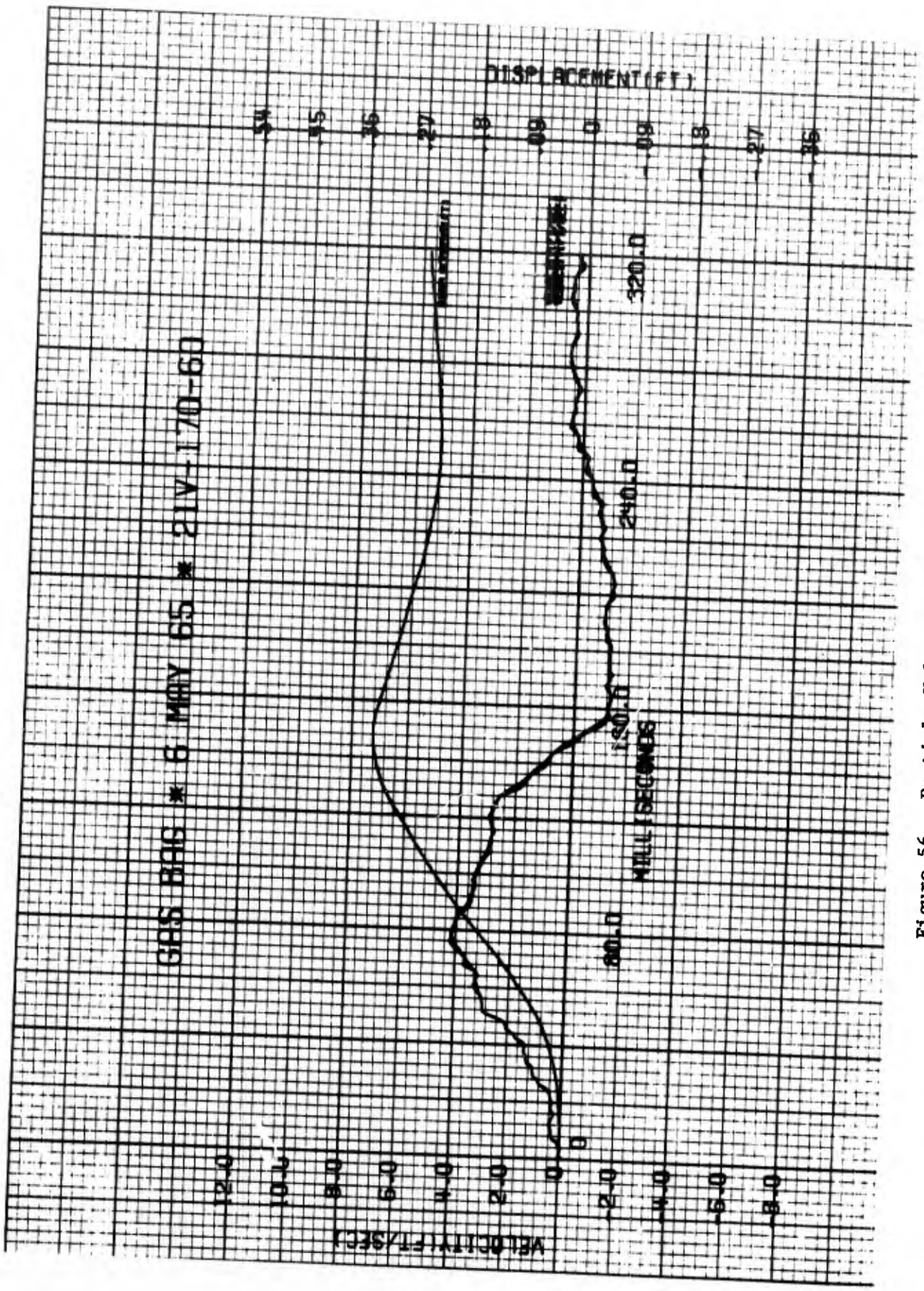

Figure 56. Particle Velocity-Time Histories

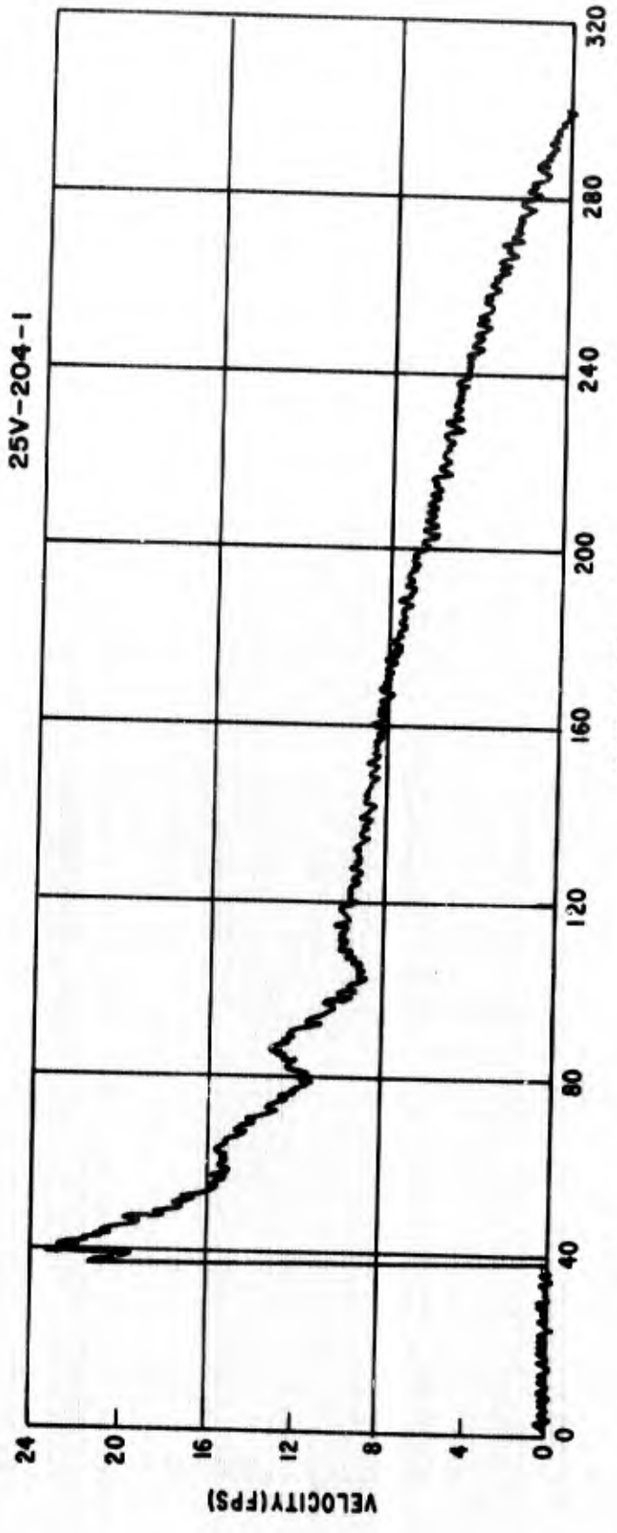

Figure 57. Particle Velocity-Time Histories

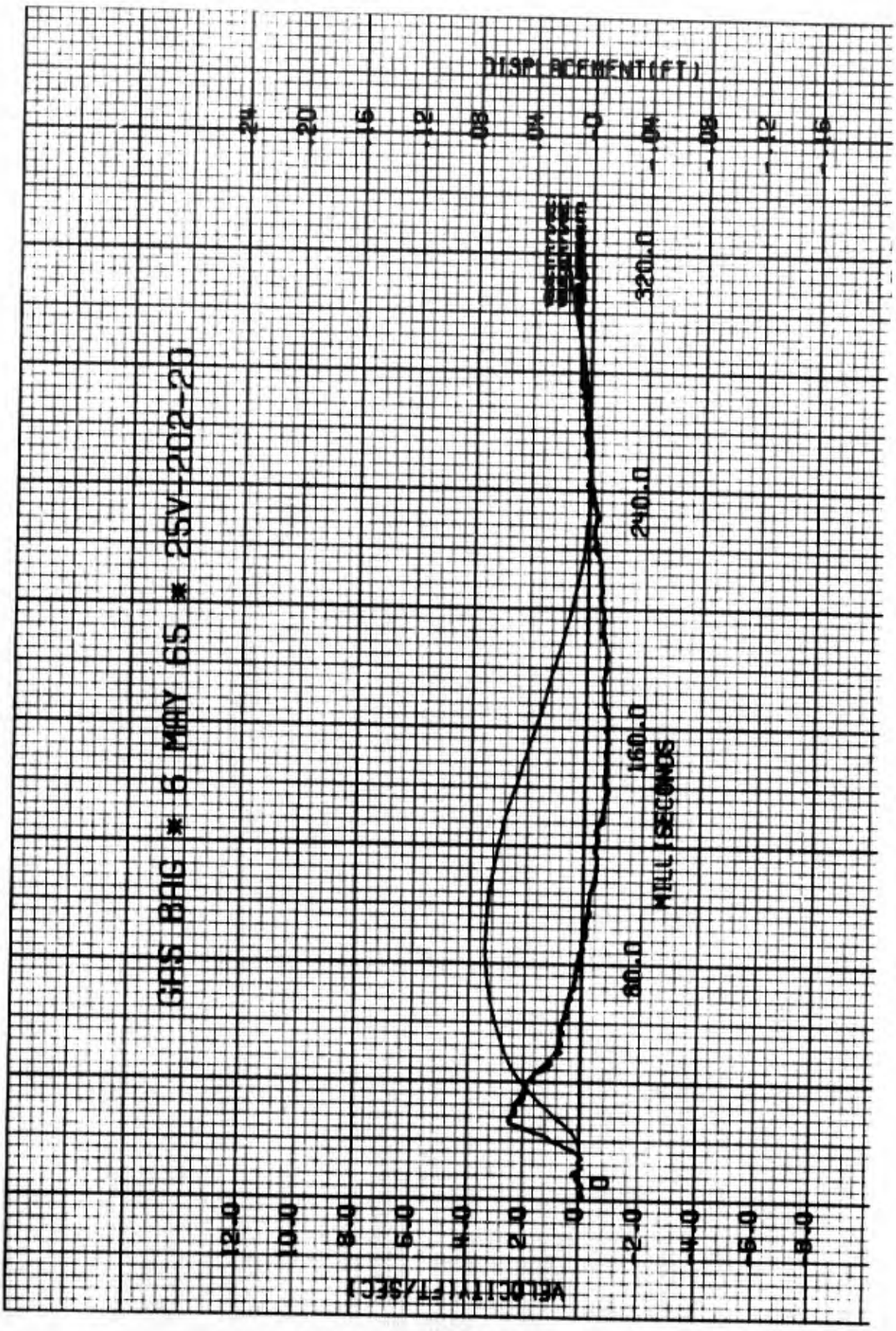

Figure 58. Particle Velocity-Time Histories

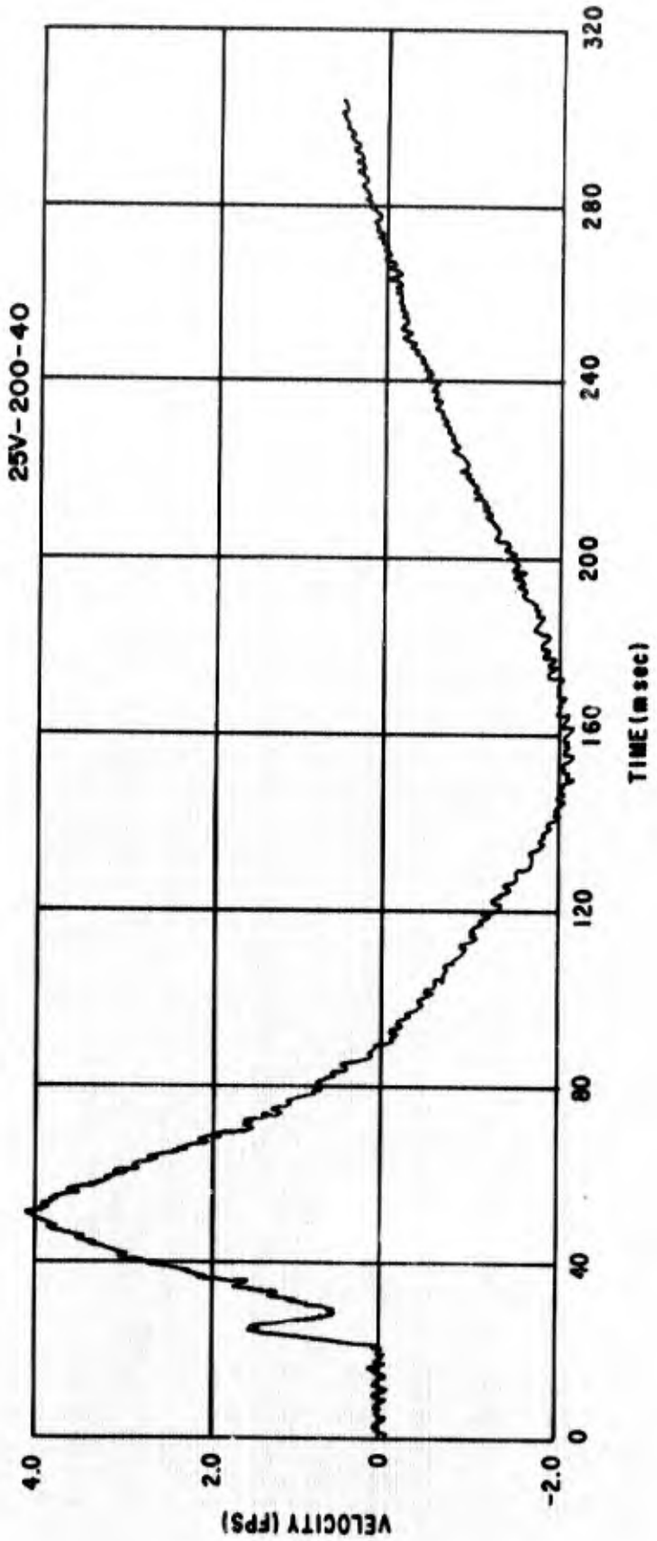

Figure 59. Particle Velocity-Time Histories

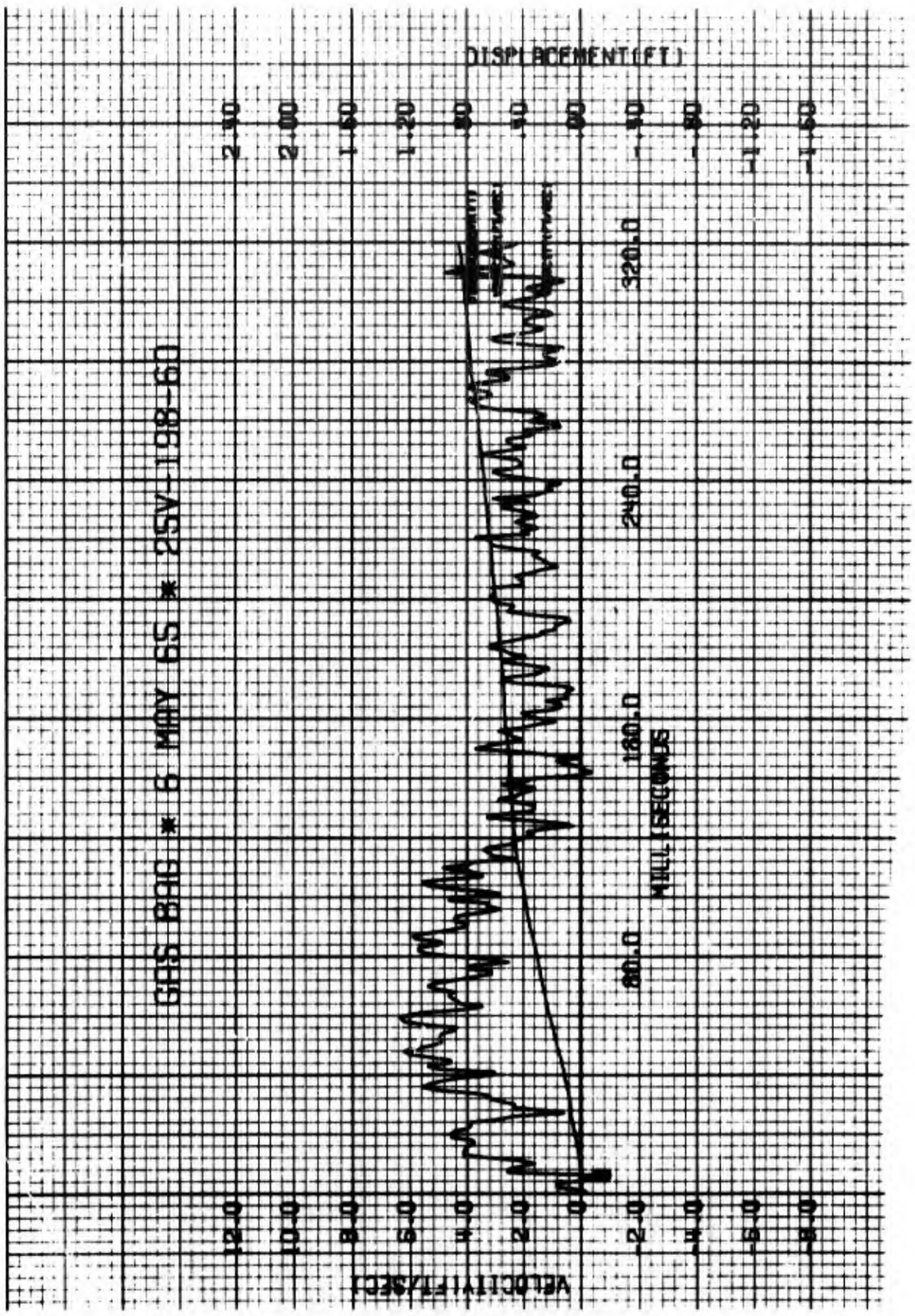

Figure 60. Particle Velocity-Time Histories

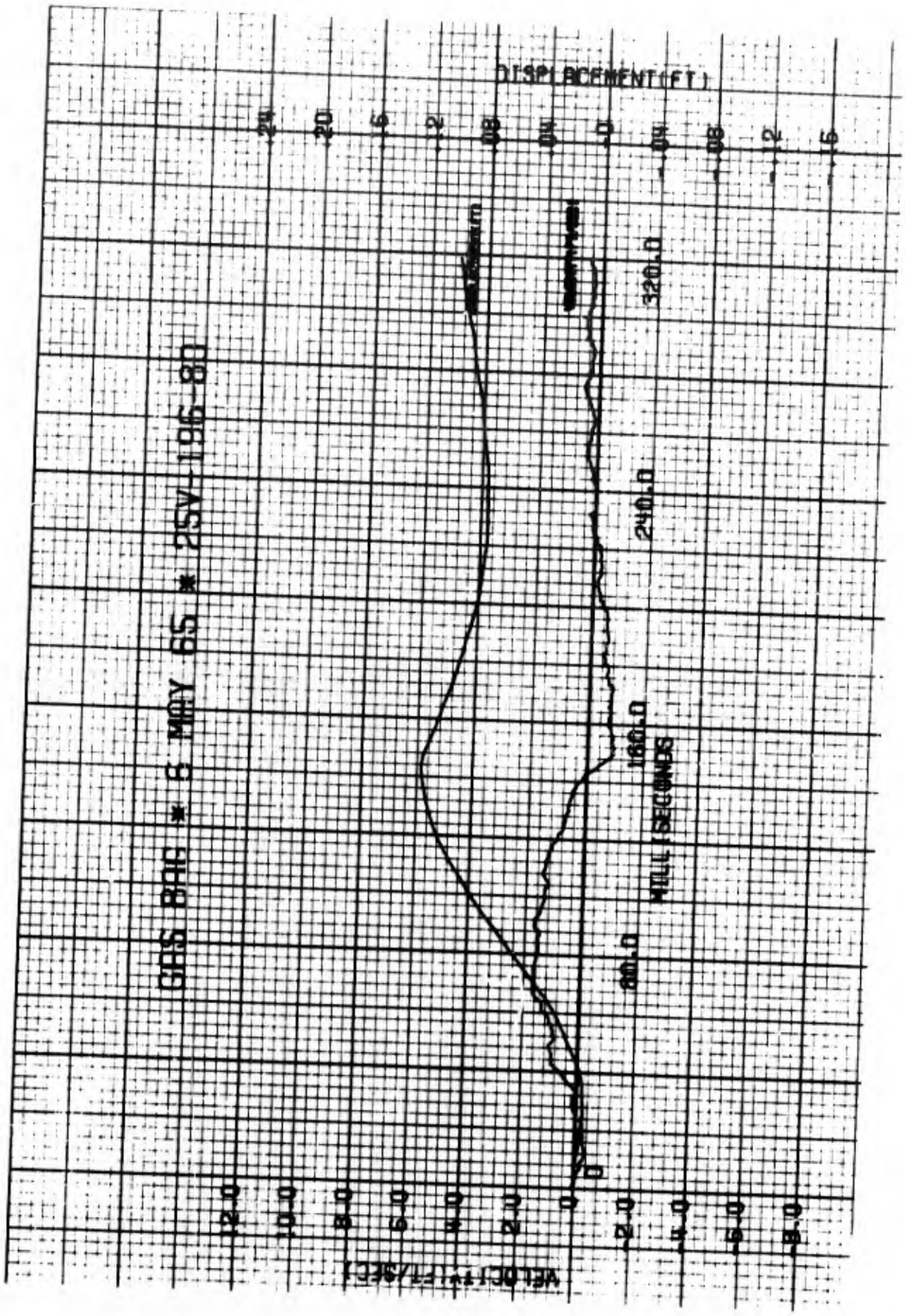

Figure 61. Particle Velocity-Time Histories

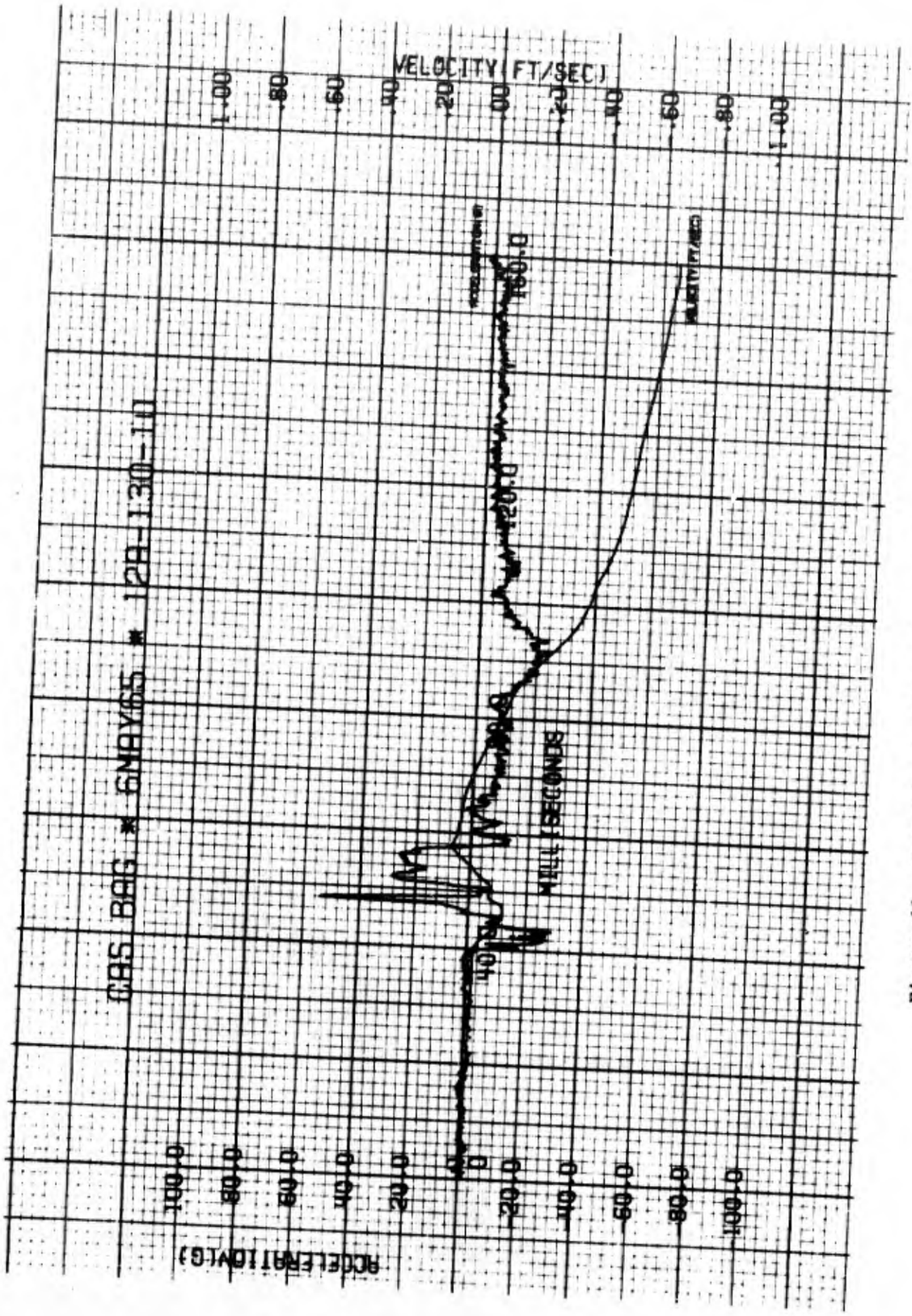

Figure 62. Particle Acceleration-Time Histories

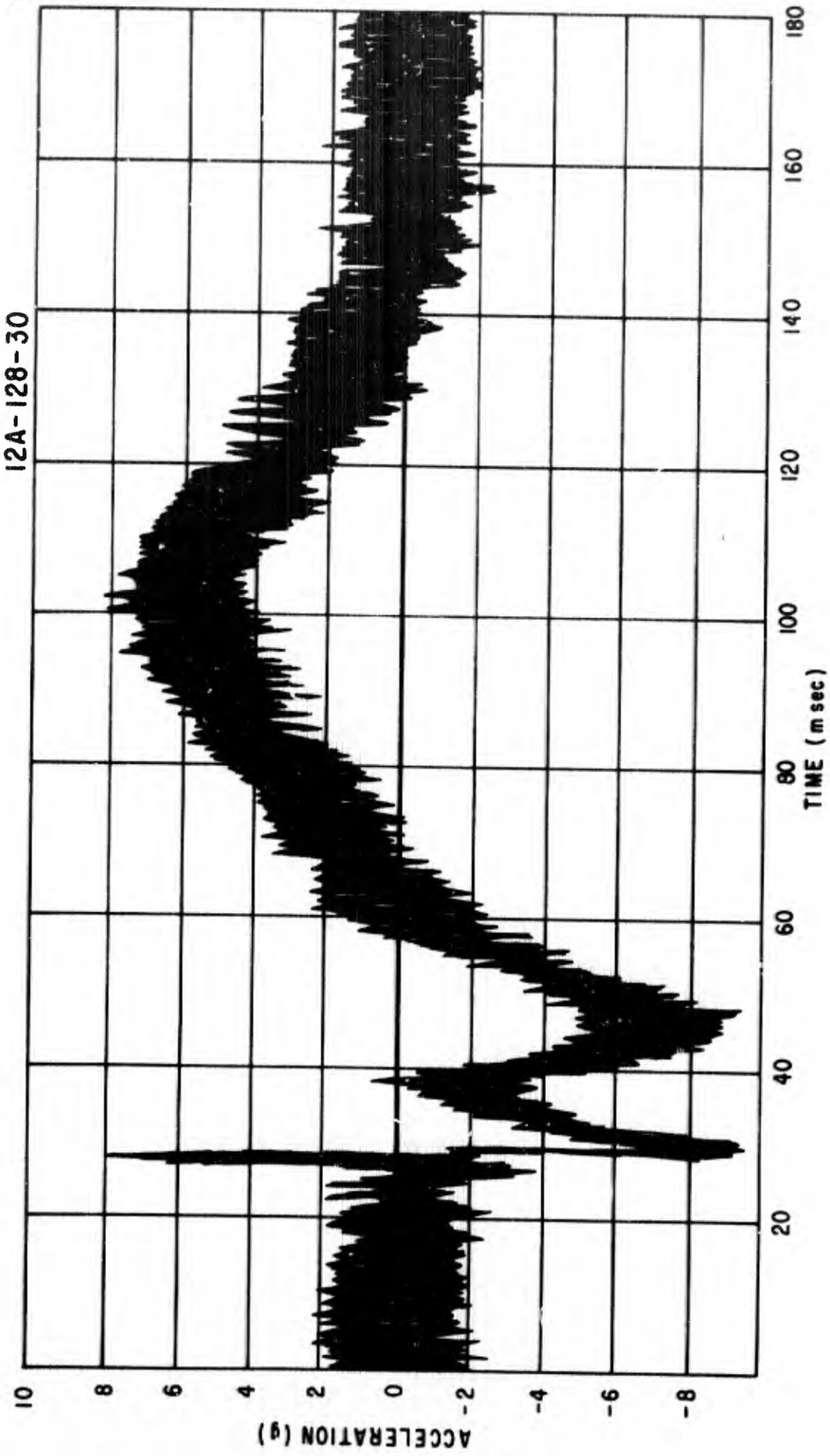

Figure 63. Particle Acceleration-Time Histories

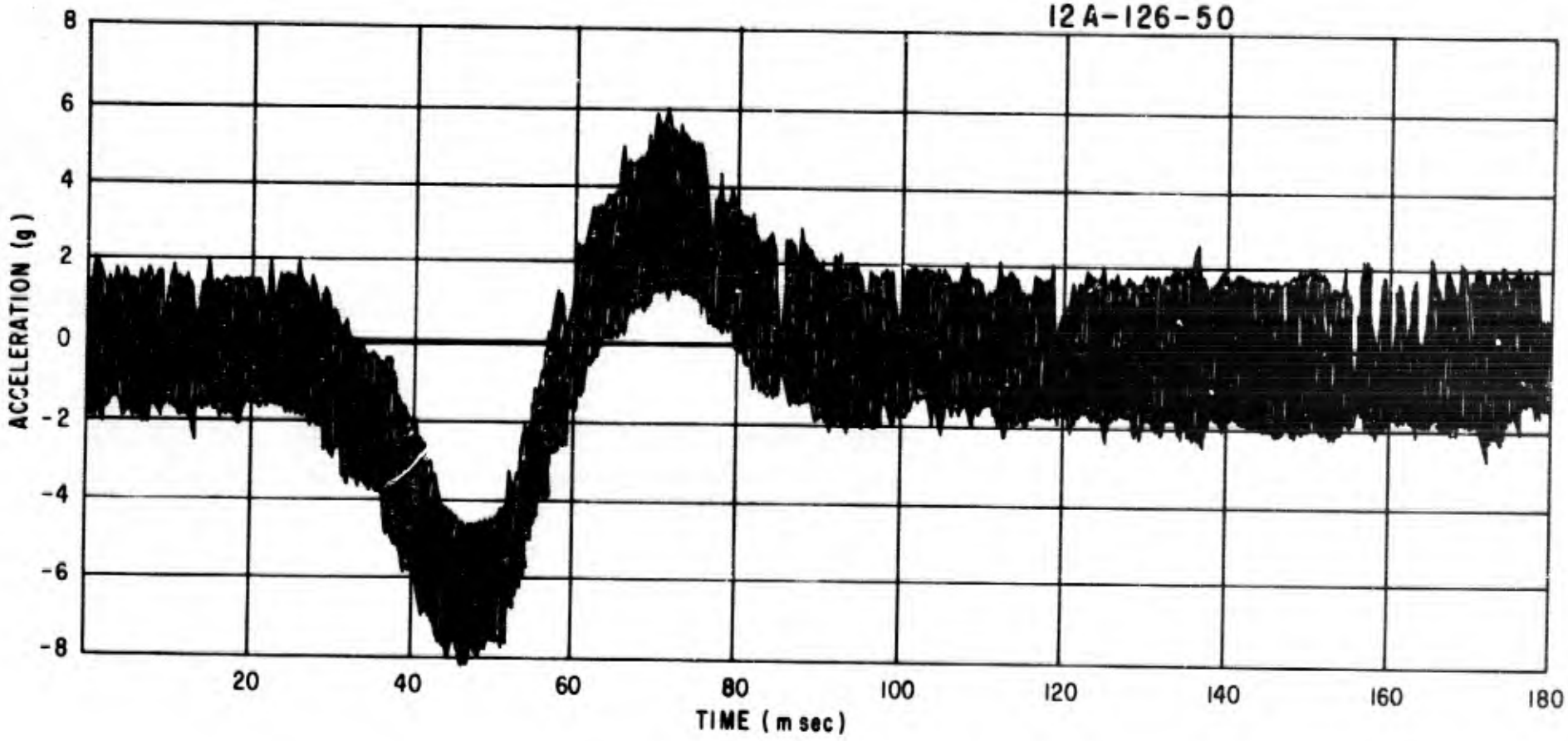

Figure 64. Particle Acceleration-Time Histories

12A-124-70

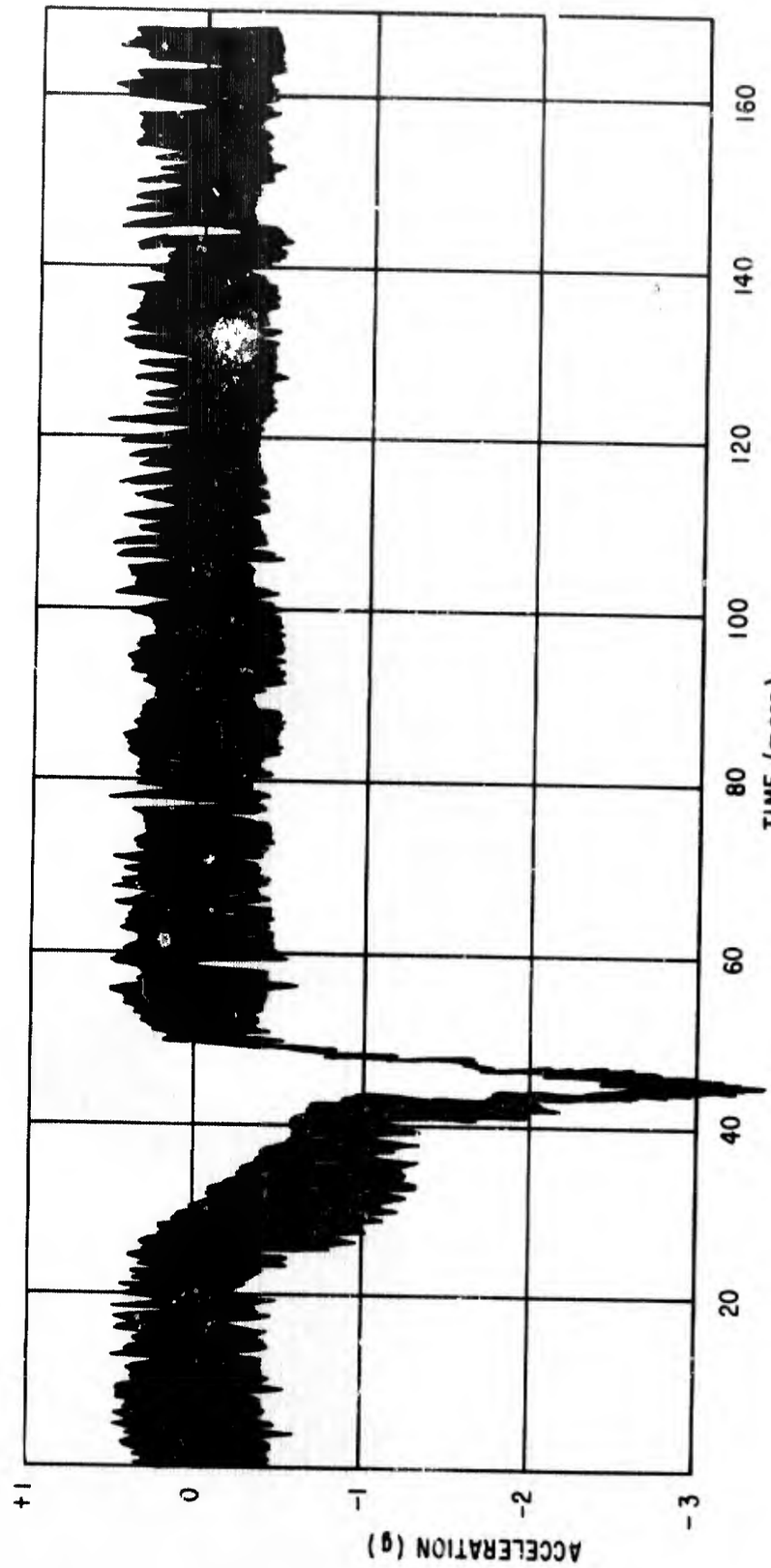

Figure 65. Particle Acceleration-Time Histories

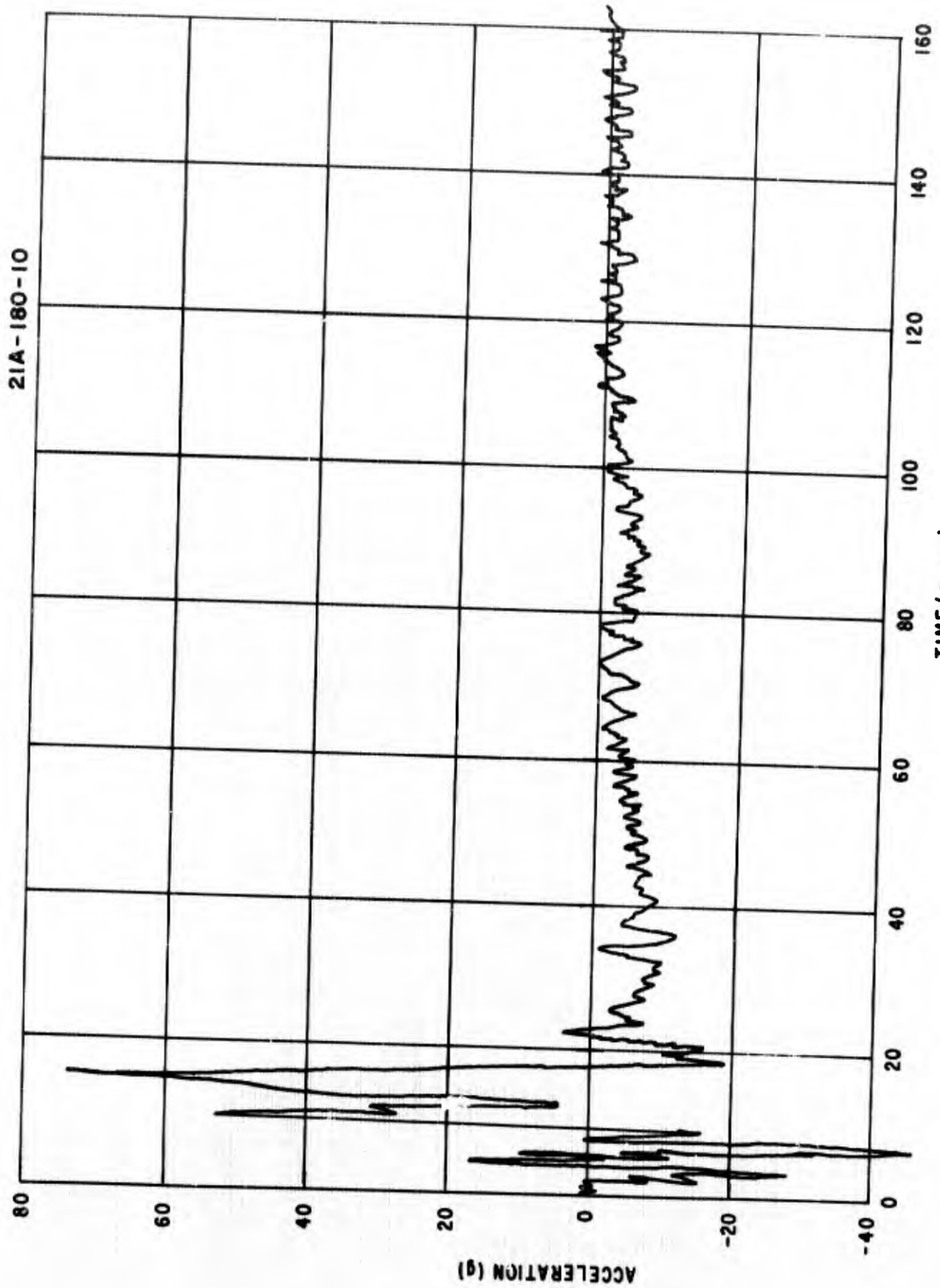

Figure 66. Particle Acceleration-Time Histories

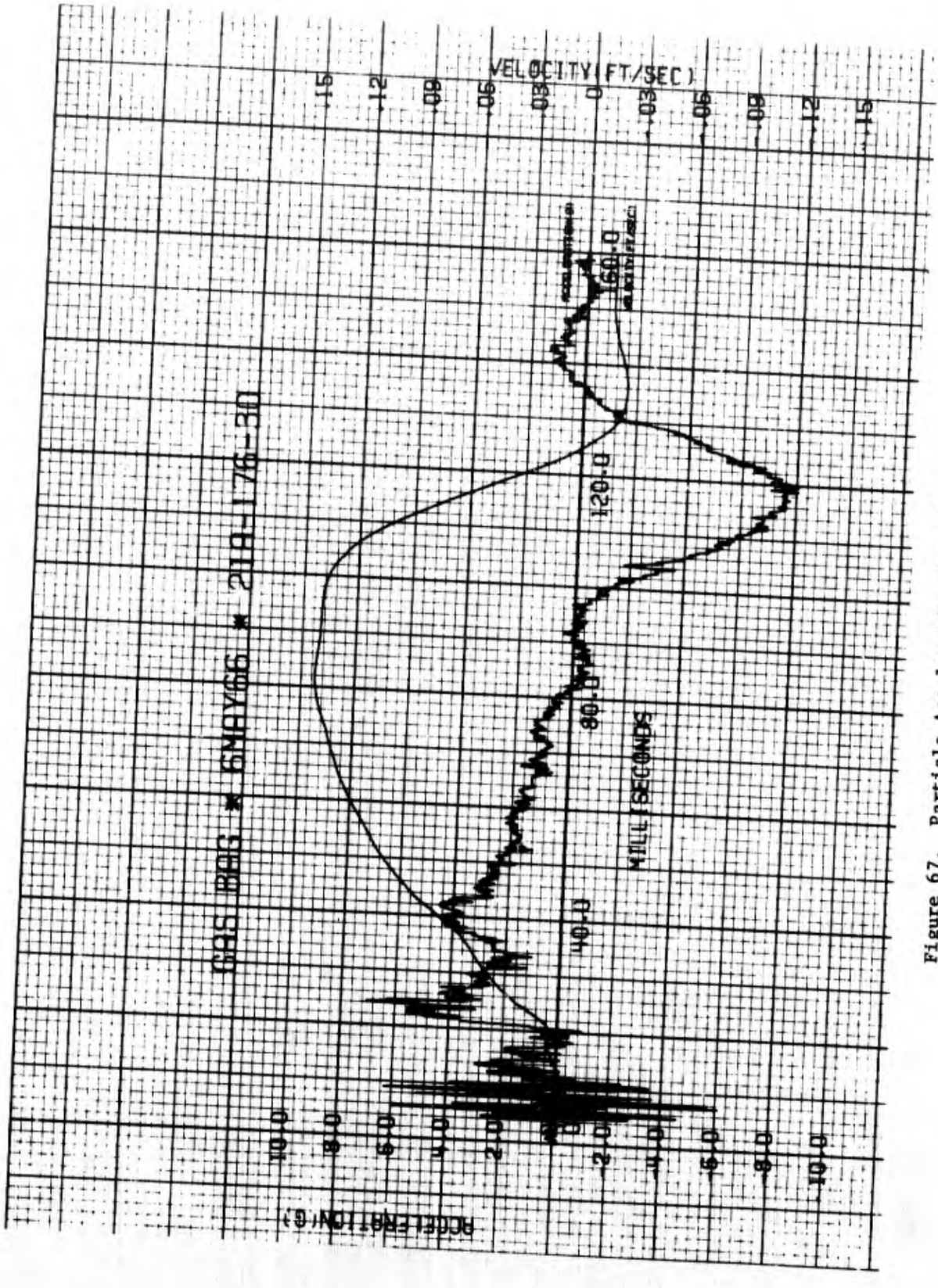

Figure 67. Particle Acceleration-Time Histories

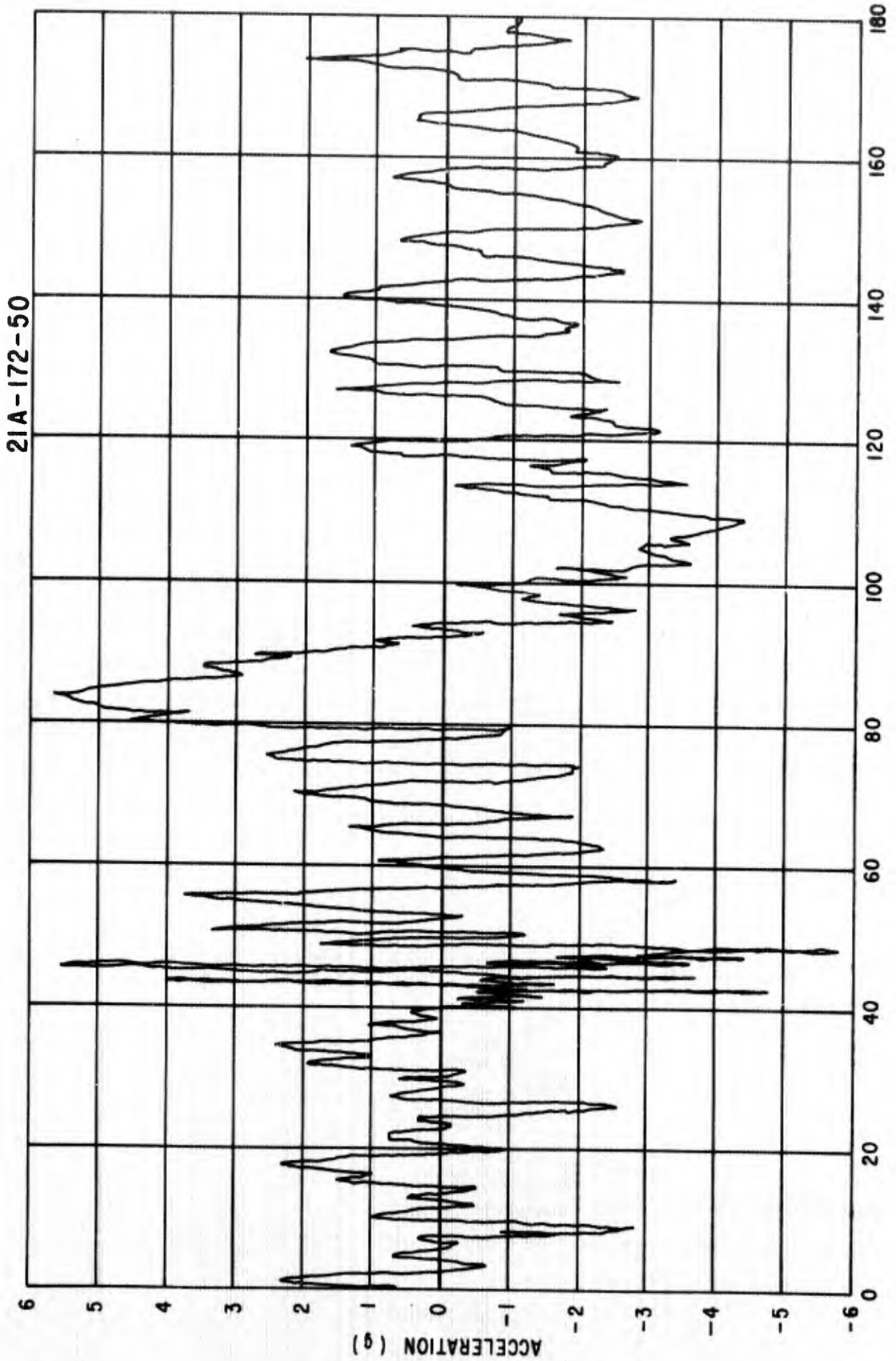

Figure 68. Particle Acceleration-Time Histories

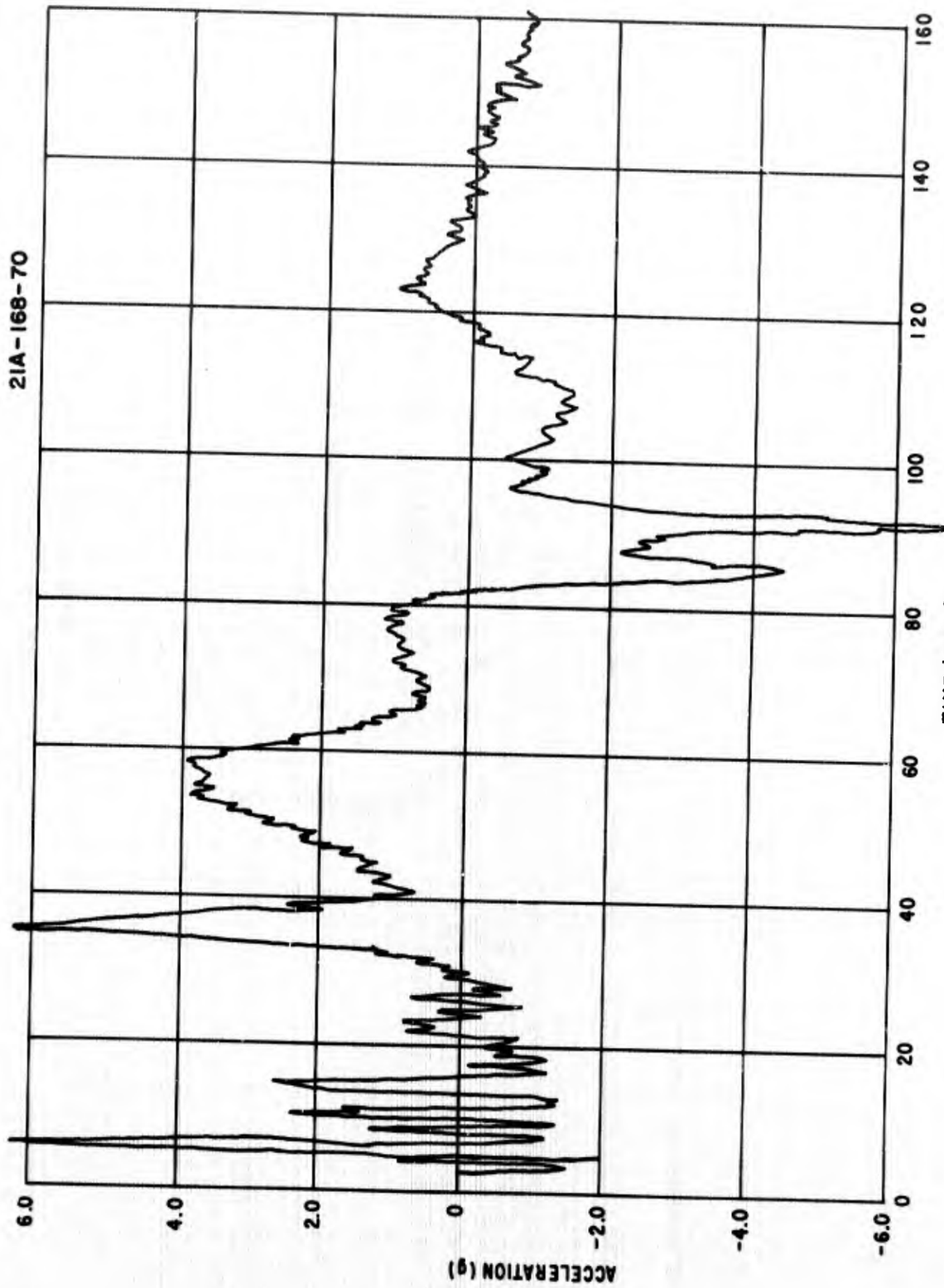

Figure 69. Particle Acceleration-Time Histories

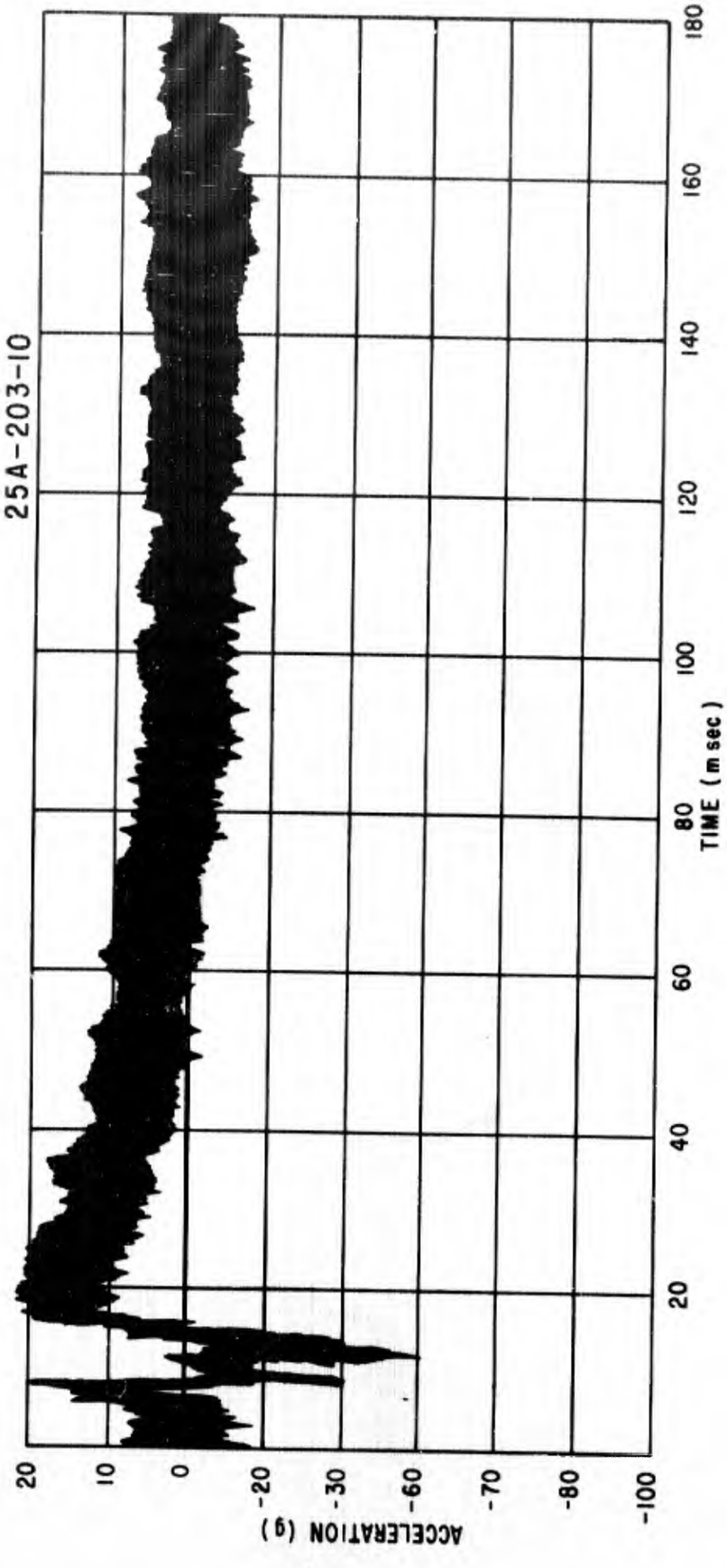

Figure 70. Particle Acceleration-Time Histories

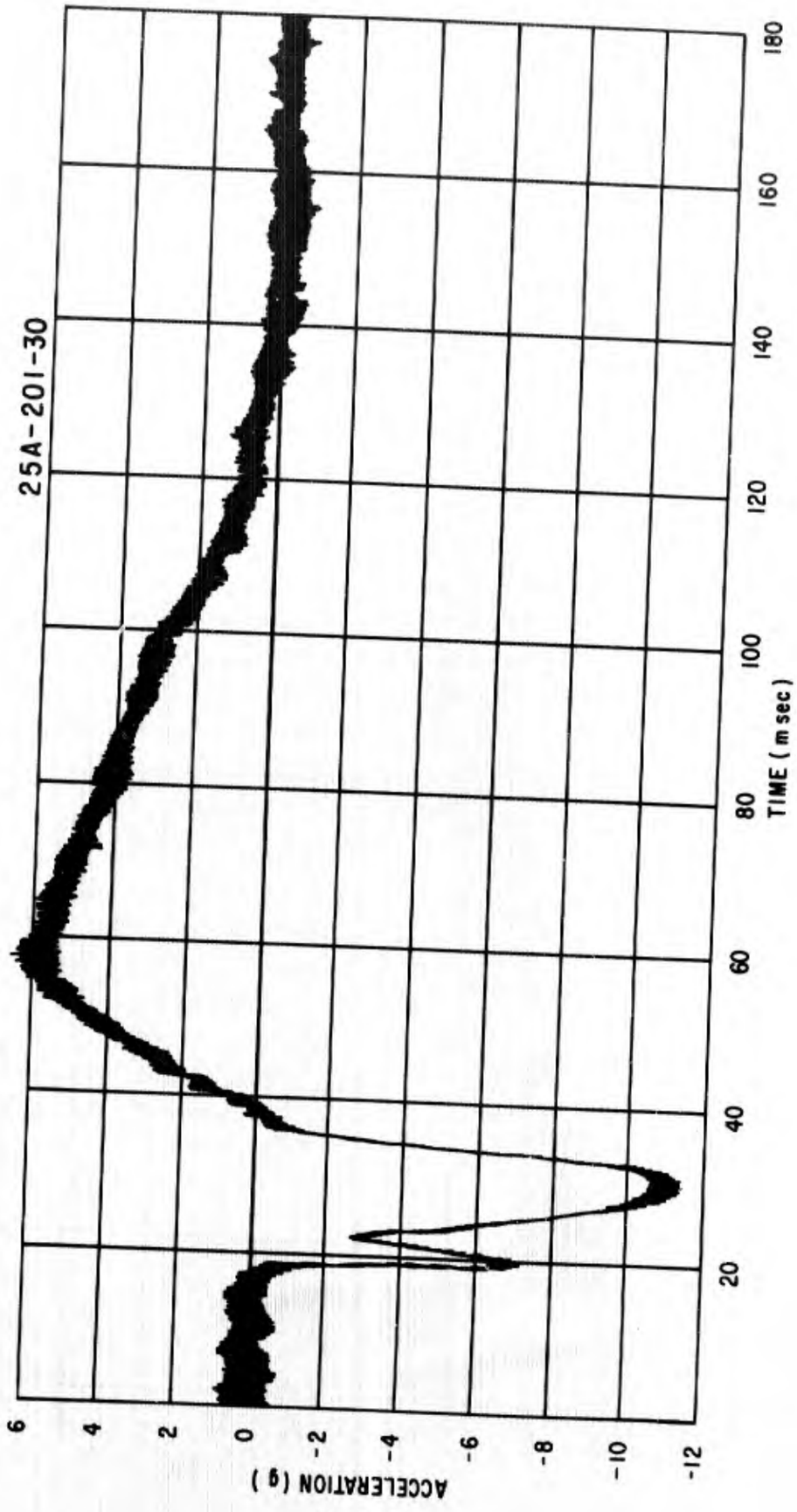

Figure 71. Particle Acceleration-Time Histories

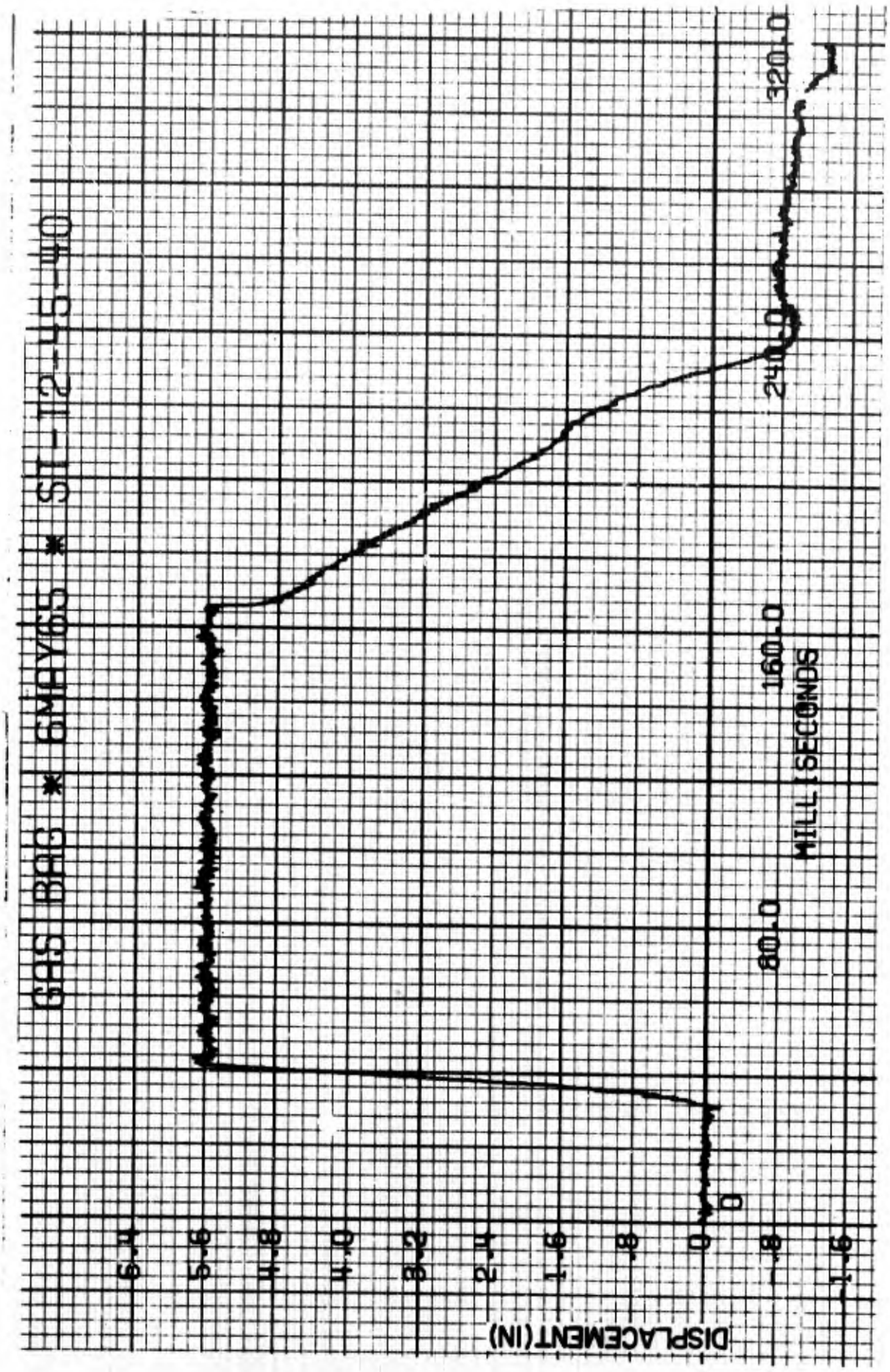

Figure 72. Long Span Displacement

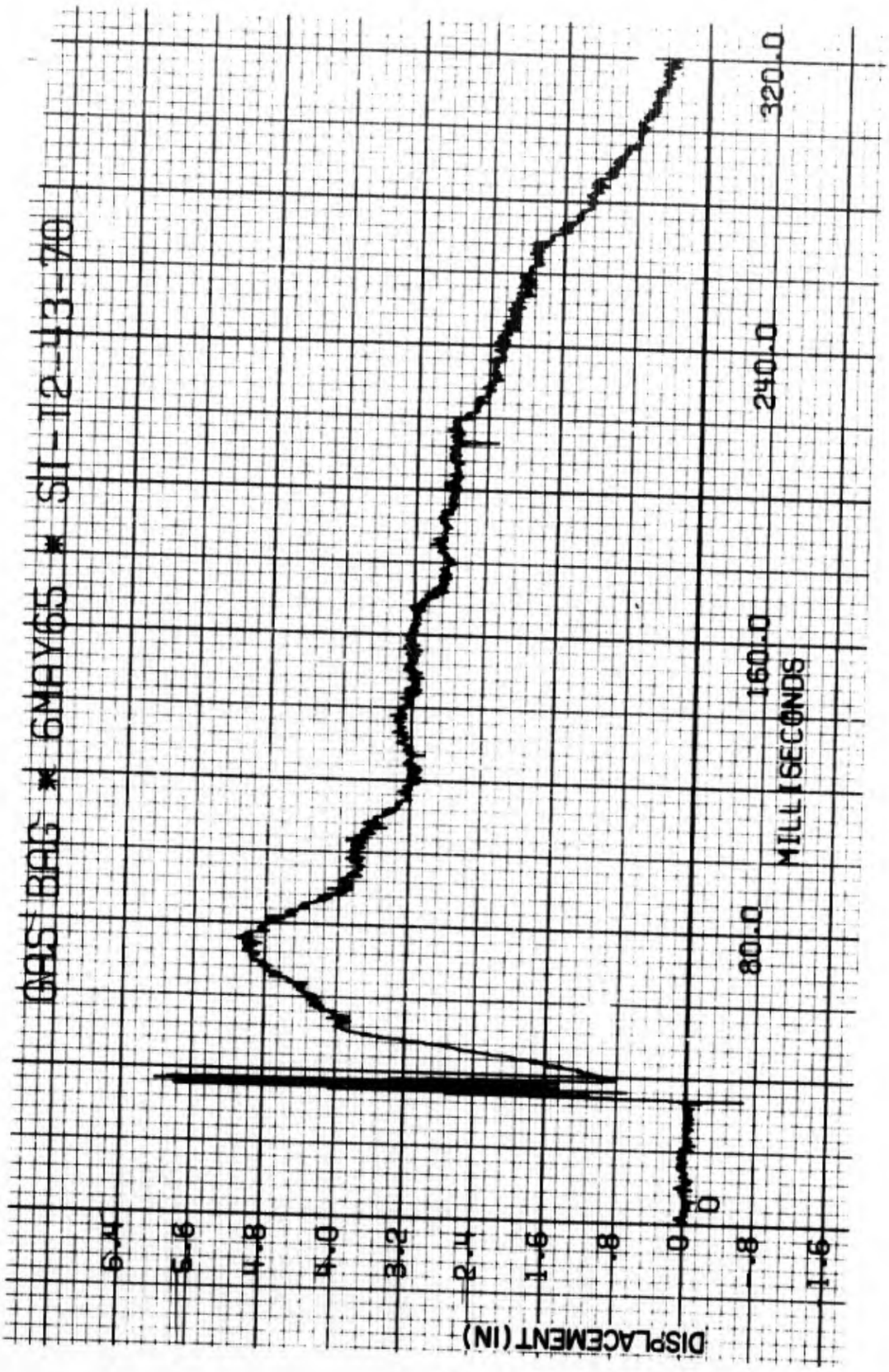

Figure 73. Long Span Displacement

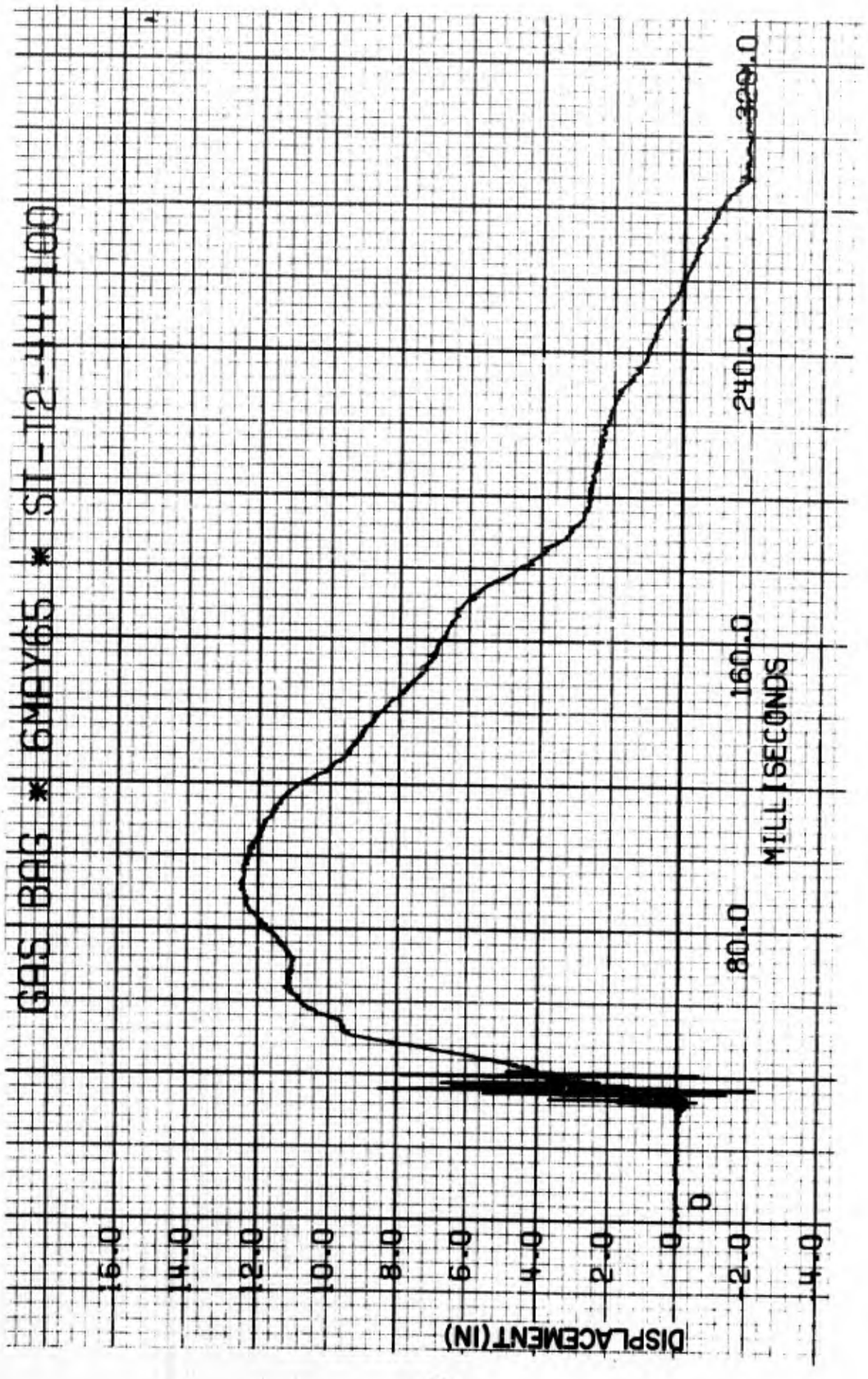

Figure 74. Long Span Displacement

REFERENCES

1. Auld, H. E., D'Arcy, G. P., Leigh, G. G.; Simulation of Air-Blast-Induced Ground Motions (Phase II), AFWL-TR-65-26, Vol I, Air Force Weapons Laboratory, Kirtland AFB, New Mexico, April 1965.

2. Johnson, J. E., Eddings, J. A., Flory, J. F.; Simulation of Air-Blast-Induced Ground Motions (Phase II), AFWL-TR-65-26, Vol II, Air Force Weapons Laboratory, Kirtland AFB, New Mexico, May 1965. (SECRET Report)

3. Auld, H. E., D'Arcy, G. P., Leigh, G. G.; Simulation of Air-Blast-Induced Ground Motions (Phase I), AFWL-TR-65-11, Air Force Weapons Laboratory, Kirtland AFB, New Mexico, April 1965.

4. D'Arcy, G. P., Clark, R. O.; Simulation of Air Shocks with Detonation Waves, AFWL-TR-65-9, Air Force Weapons Laboratory, Kirtland AFB, New Mexico, February 1966.

5. Truesdale, W. B., Schwab, R. B.; Soil Strain Gage Instrumentation, AFWL-TR-65-104, Air Force Weapons Laboratory, Kirtland AFB, New Mexico, April 1965.

UNCLASSIFIED
Security Classification

DOCUMENT CONTROL DATA - R&D

(Security classification of title, body of abstract and indexing annotation must be entered when the overall report is classified)

1. ORIGINATING ACTIVITY (Corporate author)
Air Force Weapons Laboratory (WLDC)
Kirtland Air Force Base, New Mexico 87117

2a. REPORT SECURITY CLASSIFICATION
UNCLASSIFIED

2b. GROUP

3. REPORT TITLE
SIMULATION OF AIRBLAST-INDUCED GROUND MOTIONS (PHASE IIA)

4. DESCRIPTIVE NOTES (Type of report and inclusive dates)
March 1965-July 1966

5. AUTHOR(S) (Last name, first name, initial)
Bratton, Jimmie L., Lt, USAF; Pratt, Howard R., Lt, USAF

6. REPORT DATE	7a. TOTAL NO. OF PAGES	7b. NO. OF REFS
October 1967	110	5

8a. CONTRACT OR GRANT NO.	9a. ORIGINATOR'S REPORT NUMBER(S)
b. PROJECT NO. 5710	AFWL-TR-66-85
c. Subtask No. 13.144	9b. OTHER REPORT NO(S) (Any other numbers that may be assigned this report)
d.	

10. AVAILABILITY/LIMITATION NOTICES This document is subject to special export controls and each transmittal to foreign governments or foreign nationals may be made only with prior approval of AFWL (WLDC), Kirtland AFB, NM, 87117. Distribution is limited because of the technology discussed in the report.

11. SUPPLEMENTARY NOTES

12. SPONSORING MILITARY ACTIVITY
AFWL (WLDC)
Kirtland AFB, NM 87117

13. ABSTRACT
(Distribution Limitation Statement No. 2)

The results of the Phase IIA, High-Explosive Simulation Technique (HEST) experiment are presented in the form of reduced data. A comprehensive analysis is not presented, although irregularities in the data are discussed. The experiment simulated airblast loading from a nuclear burst by detonating a contained Primacord matrix over a plan area 88 feet by 100 feet. The peak overpressure was 598 psi, the total impulse 19.25 psi-sec, the total duration was 172 msec, and the shock front velocity was 5640 feet per second. Measurements of free field stress, strain, particle velocity, particle acceleration, time of arrival of the wave front, and long-span displacement were made. These data are presented as plots of peak values and time histories.

DD FORM 1 JAN 64 1473

UNCLASSIFIED
Security Classification

14. KEY WORDS	LINK A		LINK B		LINK C	
	ROLE	WT	ROLE	WT	ROLE	WT
Free-field ground motions HEST Dynamic field testing of soils Wave propagation						

INSTRUCTIONS

1. ORIGINATING ACTIVITY: Enter the name and address of the contractor, subcontractor, grantee, Department of Defense activity or other organization *(corporate author)* issuing the report.

2*a*. REPORT SECURITY CLASSIFICATION: Enter the overall security classification of the report. Indicate whether "Restricted Data" is included. Marking is to be in accordance with appropriate security regulations.

2*b*. GROUP: Automatic downgrading is specified in DoD Directive 5200.10 and Armed Forces Industrial Manual. Enter the group number. Also, when applicable, show that optional markings have been used for Group 3 and Group 4 as authorized.

3. REPORT TITLE: Enter the complete report title in all capital letters. Titles in all cases should be unclassified. If a meaningful title cannot be selected without classification, show title classification in all capitals in parenthesis immediately following the title.

4. DESCRIPTIVE NOTES: If appropriate, enter the type of report, e.g., interim, progress, summary, annual, or final. Give the inclusive dates when a specific reporting period is covered.

5. AUTHOR(S): Enter the name(s) of author(s) as shown on or in the report. Enter last name, first name, middle initial. If military, show rank and branch of service. The name of the principal author is an absolute minimum requirement.

6. REPORT DATE: Enter the date of the report as day, month, year; or month, year. If more than one date appears on the report, use date of publication.

7*a*. TOTAL NUMBER OF PAGES: The total page count should follow normal pagination procedures, i.e., enter the number of pages containing information.

7*b*. NUMBER OF REFERENCES: Enter the total number of references cited in the report.

8*a*. CONTRACT OR GRANT NUMBER: If appropriate, enter the applicable number of the contract or grant under which the report was written.

8*b*, 8*c*, & 8*d*. PROJECT NUMBER: Enter the appropriate military department identification, such as project number, subproject number, system numbers, task number, etc.

9*a*. ORIGINATOR'S REPORT NUMBER(S): Enter the official report number by which the document will be identified and controlled by the originating activity. This number must be unique to this report.

9*b*. OTHER REPORT NUMBER(S): If the report has been assigned any other report numbers *(either by the originator or by the sponsor)*, also enter this number(s).

10. AVAILABILITY/LIMITATION NOTICES: Enter any limitations on further dissemination of the report, other than those imposed by security classification, using standard statements such as:

(1) "Qualified requesters may obtain copies of this report from DDC."

(2) "Foreign announcement and dissemination of this report by DDC is not authorized."

(3) "U. S. Government agencies may obtain copies of this report directly from DDC. Other qualified DDC users shall request through

_____."

(4) "U. S. military agencies may obtain copies of this report directly from DDC. Other qualified users shall request through

_____."

(5) "All distribution of this report is controlled. Qualified DDC users shall request through

_____."

If the report has been furnished to the Office of Technical Services, Department of Commerce, for sale to the public, indicate this fact and enter the price, if known.

11. SUPPLEMENTARY NOTES: Use for additional explanatory notes.

12. SPONSORING MILITARY ACTIVITY: Enter the name of the departmental project office or laboratory sponsoring *(paying for)* the research and development. Include address.

13. ABSTRACT: Enter an abstract giving a brief and factual summary of the document indicative of the report, even though it may also appear elsewhere in the body of the technical report. If additional space is required, a continuation sheet shall be attached.

It is highly desirable that the abstract of classified reports be unclassified. Each paragraph of the abstract shall end with an indication of the military security classification of the information in the paragraph, represented as *(TS)*, *(S)*, *(C)*, or *(U)*.

There is no limitation on the length of the abstract. However, the suggested length is from 150 to 225 words.

14. KEY WORDS: Key words are technically meaningful terms or short phrases that characterize a report and may be used as index entries for cataloging the report. Key words must be selected so that no security classification is required. Identifiers, such as equipment model designation, trade name, military project code name, geographic location, may be used as key words but will be followed by an indication of technical context. The assignment of links, rules, and weights is optional.